

**EXTRACTION OF AROMATICS USING GREEN
SOLVENTS BASED ON IONIC LIQUIDS**

BY

Kazi Zamshad Sumon

A Thesis Presented to the
DEANSHIP OF GRADUATE STUDIES

KING FAHD UNIVERSITY OF PETROLEUM & MINERALS

DHAHRAN, SAUDI ARABIA

In Partial Fulfillment of the
Requirements for the Degree of

MASTER OF SCIENCE

In

Chemical Engineering

December 2005

KING FAHD UNIVERSITY OF PETROLEUM & MINERALS
DHAHRAN 31261, SAUDI ARABIA

DEANSHIP OF GRADUATE STUDIES

This thesis, written by **KAZI ZAMSHAD SUMON** under the supervision of his thesis advisor and approved by his thesis committee, has been presented to and accepted by the Dean of Graduate Studies, in partial fulfillment of the requirements for the degree of **MASTER OF SCIENCE IN CHEMICAL ENGINEERING.**

Thesis Committee



Prof. Esam Z. Hamad
Thesis Advisor



Dr. Nadhir A. Al-Baghli
Member



Dr. Ian Forristal
Member



Prof. Mohamed B. Amin
Department Chairman



Dr. Mohammad Abdulaziz Al-Ohali
Dean of Graduate Studies

٥٤٤٧/١/١٥

Date: 14-2-2006



*Dedicated to
My grandparents, parents, parents-in-law
& Isnat*

ACKNOWLEDGEMENT

All praises and thanks are first due to Almighty Allah for allowing me to complete this work. Acknowledgement is also due to King Fahd University of Petroleum and Minerals for its support in carrying out this research.

I express my profound gratitude to my thesis supervisor Dr. Esam Z Hamad for his guidance, suggestions, excellent ideas, valuable time, and cooperation. I am also indebted to my thesis committee members Dr. Nadhir A. Al-Baghli and Dr. Ian Forristal for their constructive suggestions and generous cooperation. I am deeply indebted to Dr. Asrof Ali, for his invaluable contribution to the experimental part of this research.

I am thankful to the chairman, Dr. Mohamed B. Amin, all faculty and staff members of the Department of Chemical Engineering, whose integrated effort made the department a congenial place to perform research. I would like to thank Mr. Arab, Mr. Mariano, and Mr. Kamal for assisting me to run my experiments smoothly.

I am grateful to my fellow graduate students and to all members of Bangladeshi community at KFUPM whose wonderful company was really inspiring during my staying here. Very Special thanks go to Saidu M Waziri, Md. Ehsanul Kabir, and A T M Jahiruddin. The following persons also deserve my thanks: Saad Bin-Mansoor, Md Rafiqul Islam, A S M Sayem Mozumder, Md. Hasan Iqbal, Muhammad Muhitur Rahman, Syed Mosiur Rahman, Md. Ashraful Islam, Sheikh Abdur Razzak, Md. Badrul

Islam Chowdhury, Md. Abdullah Al Kafi, Shahed Akond, Md Shamsul Islam, Muhammad Reaz Uddin Chowdhury and Dr. M A Nasser Khondaker. I am also thankful to my friends Hasan, Gazi, Isam, Awwal and Bello.

Finally, I am very grateful to my parents, brother Shabooj, sisters Munni and Roni, wife Mitu, parents-in-law and all other well wishers for their prayers, inspiration, mental support and sacrifice that helped me to accomplish this research.

TABLE OF CONTENTS

LIST OF FIGURES	xi
LIST OF TABLES	xvii
ABSTRACT	xviii
ملخص	xix
CHAPTER 1	1
INTRODUCTION	1
1.1 THE USE OF AROMATICS	1
1.2 MARKET SCENARIO OF BTEX.....	2
1.3 SOURCES OF AROMATICS.....	2
1.4 AROMATICS EXTRACTION PROCESSES	6
1.4.1 Membrane Permeation.....	6
1.4.2 Adsorption.....	6
1.4.3 Extraction and Extractive Distillation.....	7
1.5 LIQUID-LIQUID EXTRACTION	7
1.6 THERMODYNAMICS OF LLE.....	8
1.7 GREEN SOLVENTS.....	12
CHAPTER 2	14
LITERATURE REVIEW	14
2.1 PRESENT INDUSTRIAL SOLVENTS & PROCESSES.....	14
2.2 IONIC LIQUIDS- A REVIEW.....	15
2.2.1 Introduction.....	15
2.2.2 Background.....	16

2.2.3 Attractiveness as New Generation Solvent.....	17
2.2.4 Solvent Properties of ILs	18
2.2.5 IL Polarity in the Presence of Other ‘Solvents’	27
2.2.6 Challenges Posed for Separation Technologies by ILs.....	27
2.3 IONIC LIQUIDS IN CHEMICAL SEPARATIONS	29
2.4 ILS FOR AROMATIC EXTRACTION.....	30
2.5 MODELING SOLUTIONS CONTAINING ILS.....	34
2.5.1 Models for Electrolyte Solutions	34
2.5.2 Models for Ionic Liquids	35
2.5.3 Simulation of Ionic Liquids	36
CHAPTER 3.....	38
RESEARCH OBJECTIVES.....	38
CHAPTER 4.....	40
COMPUTATIONAL SCREENING OF POTENTIAL SOLVENTS.....	40
4.1 COMPUTATIONAL SCREENING.....	40
4.2 SCREENING METHOD- THE COSMO-RS	40
4.3 THEORY	41
4.4 COMPARISON OF COSMO CALCULATION WITH EXPERIMENTAL DATA	45
4.5 COMPUTATIONAL DETAILS	50
4.6 THE IL DATABASE AND NOMENCLATURE OF ILS.....	52
4.7 COMPUTATIONAL RESULTS AND DISCUSSION	53
4.7.1 General Presentation of S & C of the ILs and Comparison with Sulfolane	53

4.7.2 Selectivity (S) & Capacity(C) of Different Cation Based ILs and Effect of Alkyl Chain Length of Cation on S & C.....	59
4.7.2.1 Imidazolium Based ILs.....	59
4.7.2.2 Pyridinium Based ILs.....	65
4.7.2.3 Pyrrolidinium Based ILs.....	71
4.7.2.4 Other Cation Based ILs.....	74
4.7.3 Computationally Recommended ILs.....	81
4.7.4 Effect of Volume of Anions on Capacity and Selectivity.....	88
4.7.5 Effect of Volume of Cations on Capacity and Selectivity.....	90
4.7.6 Effect of Temperature on Capacity and Selectivity.....	91
CHAPTER 5.....	95
EXPERIMENT.....	95
5.1 INTRODUCTION.....	95
5.2 COMPUTATIONAL PREDICTION OF SYNERGISTIC BEHAVIOR OF BINARY IL MIXTURES.....	97
5.3 EXPERIMENTAL VERIFICATION OF SYNERGISTIC BEHAVIOR OF BINARY ILS MIXTURE.....	100
5.3.1 Materials.....	100
5.3.2 Phase Equilibrium Equipment.....	102
5.3.3 Procedures.....	104
5.3.4 Analysis.....	104
5.3.5 Experimental Results and Discussions.....	105
5.3.5.1 Binary Solvent, [dmi] [ms] + [omi] [tfb].....	105

5.3.5.2 Binary Solvent, [mbpy][tfb]+ [omi][tfb]	109
CHAPTER 6.....	114
MODELING IONIC LIQUIDS SOLUTIONS.....	114
6.1 INTRODUCTION	114
6.2 NPT ENSEMBLE.....	114
6.3 MODELING IL SOLUTIONS IN NPT ENSEMBLE	115
6.4 ASSUMPTIONS.....	116
6.5 APPROACH.....	116
6.6 THE RPM ELECTROLYTE MODEL IN NVT ENSEMBLE	117
6.7 PROPOSED MODEL.....	118
6.7.1 Proposed Model for RPM Electrolytes.....	118
6.7.1.1 Short Range Repulsive Forces in NPT	118
6.7.1.2 Ionic Interactions in NPT.....	122
6.7.2 Proposed Model for Multicomponent System Containing Ionic Liquids.....	123
6.7.3 Excess Molar Gibbs Energy.....	127
6.8 RESULTS AND DISCUSSIONS.....	128
6.8.1 Application to RPM electrolyte	128
6.8.2 Application to Real Solution: [bmpy] [tfb] +Toluene+Heptane System.....	131
CHAPTER 7.....	135
CONCLUSIONS & RECOMMENDATIONS.....	135
7.1 CONCLUSIONS	135
7.2 SUGGESTIONS FOR FUTURE WORK.....	136
APPENDIX A: Identification Number and Full Name of Cations & Anions	138

APPENDIX B: Chemical Formula/Structure of Some Anions	142
APPENDIX C: Calculated Infinite Dilution Capacity and Selectivity of the ILs..	144
APPENDIX D: Experimental Data	160
APPENDIX E: Sample NMR Spectra	163
NOMENCLATURE.....	168
REFERENCES.....	170
VITAE.....	178

LIST OF FIGURES

Figure 1.1: Process roots for aromatics.....	5
Figure 1.2: Principle of liquid-liquid extraction	9
Figure 2.1: Examples of some common cations	15
Figure 4.1: Calculated and Experimental values of logarithmic infinite dilution activity coefficient for alkanes (▪) and alkyl benzenes (•) in 4-methyl-N-butylpyridinium tetrafluoroborate.....	47
Figure 4.2: Calculated and Experimental values of logarithmic infinite dilution activity coefficient for alkanes (▪) and alkylbenzenes (•) in 1, 2-dimethyl-3-ethylimidazolium bis(trifluoromethyl)sulfonyl-imide	48
Figure 4.3: Calculated and Experimental values of logarithmic infinite dilution activity coefficient for alkanes (▪) and alkylbenzenes (•) in 1-methyl-3-ethylimidazolium bis (trifluoromethyl) sulfonyl)-imide.....	49
Figure 4.4: Selectivity and Capacity of all the solvents investigated	54
Figure 4.5: Selectivity and Capacity of solvents investigated in a smaller scale	55
Figure 4.6: The selectivity-capacity plane is divided into four quadrant based on sulfolane, the benchmark solvent.....	57
Figure 4.7: ILs with higher capacity and selectivity than sulfolane	58
Figure 4.8: Capacity at infinite dilution of ILs consisting of imidazolium based cations with increasing alkyl chain length and 26 different anions	60
Figure 4.9: Selectivity at infinite dilution of ILs consisting of imidazolium based cations with increasing alkyl chain length and 26 different anions	61

Figure 4.10: Capacity at infinite dilution of imidazolium ILs consisting of cations with increasing alkyl chain length (ordered).....	63
Figure 4.11: Selectivity at infinite dilution of imidazodinium based ILs consisting of cations with increasing alkyl chain length (ordered)	64
Figure 4.12: Capacity at infinite dilution of pyridinium ILs consisting of cations with increasing alkyl chain length	66
Figure 4.13: Selectivity at infinite dilution of pyridinium ILs consisting of cations with increasing alkyl chain length	67
Figure 4.14: Capacity at infinite dilution of pyridinium ILs consisting of cations with increasing alkyl chain length (ordered).....	69
Figure 4.15: Selectivity at infinite dilution of pyridinium ILs consisting of cations with increasing alkyl chain length (ordered).....	70
Figure 4.16: Capacity at infinite dilution of pyrrolidinium ILs consisting of cations with increasing alkyl chain length	72
Figure 4.17: Selectivity at infinite dilution of pyrrolidinium ILs consisting of cations with increasing alkyl chain length	73
Figure 4.18: Capacity at infinite dilution of phosphonium ILs consisting of cations with increasing alkyl chain length	75
Figure 4.19: Selectivity at infinite dilution of phosphonium ILs consisting of cations with increasing alkyl chain length	76
Figure 4.20: Capacity at infinite dilution of ammonium ILs consisting of cations with increasing alkyl chain length	77

Figure 4.21: Selectivity at infinite dilution of ammonium ILs consisting of cations with increasing alkyl chain length	78
Figure 4.22: Capacity at infinite dilution of guanidinium, uranium and quinilinium based ILs	79
Figure 4.23: Selectivity at infinite dilution of guanidinium, uranium and quinilinium based ILs	80
Figure 4.24: Trend of Capacity and Selectivity of a typical butyl-methyl-pyrrolidinium cation with different anions	83
Figure 4.25: Trend of Capacity and Selectivity of a typical butyl-methyl-imidazolium cation with different anions	84
Figure 4.26: Trend of Capacity and Selectivity of a typical 1-butyl-pyridinium cation with different anions	85
Figure 4.27: Trend of Capacity and Selectivity of a typical phosphonium cation with different anions	86
Figure 4.28: Trend of Capacity and Selectivity of a typical ammonium cation with different anions	87
Figure 4.29: Capacity of 1-butyl-3-methyl- imidazolium with anions of increasing volume.....	89
Figure 4.30: Selectivity of 1-butyl-3-methyl- imidazolium with anions of increasing volume.....	90
Figure 4.31: Trend of selectivity and capacity of ILs consisting tetrafluoroborate anion and pyridinium-based cations with increasing volume.	92

Figure 4.32: Effect of temperature on the infinite dilution selectivity and capacity of 1-butyl-3-methyl-imidazolium tetrafluoroborate	93
Figure 4.33: Effect of temperature on the infinite dilution selectivity and capacity of N-butyl-4-methyl-pyridinium tetrafluoroborate.....	94
Figure 5.1: Physical Properties expected in synergized solvents	96
Figure 5.2: Selectivity & Capacity of the mixed solvent [bmi] [tcb] & [bmi] [tnbtp] for toluene and heptane mole fraction 0.01 and 0.09 in the IL-phase	98
Figure 5.3: Selectivity & Capacity of the mixed solvent [bmi][os] & [bmi][cl] for toluene and heptane mole fractions 0.02 and 0.08 in the IL-phase	99
Figure 5.4: Chemical structure of components of synergized solvents	101
Figure 5.5: Typical feed and solvent mixtures (a) Toluene+heptane (b) [omi][tfb] + [dmi][ms] + toluene+heptane, (c) [omi][tfb] + [mbpy][tfb] + toluene+heptane.	103
Figure 5.6: Experimental capacity for the system [dmi][ms] + [omi][tfb] at 40° C, 0.1 Mpa, for the feed composition of toluene 0.1 gm, heptane 0.9 gm and total solvent ([dmi][ms] + [omi][tfb]) 1 gm.	106
Figure 5.7: Experimental selectivity for the system [dmi][ms] + [omi][tfb] at 40° C, 0.1 Mpa, for the feed composition of toluene 0.1 gm, heptane 0.9 gm and total solvent ([dmi][ms] + [omi][tfb]) 1 gm.	107
Figure 5.8: Calculated C & S for the system [dmi][ms] + [omi][tfb] at 40° C, 0.1 Mpa, for the IL-Phase composition (MF): 0.95 IL, 0.049 T, 0.01 H.....	108
Figure 5.9: Experimental capacity for the solvent [omi][tfb] + [bmpy][tfb] at 40° C & 1 atm, for the feed composition of toluene 0.1 gm, heptane 0.9 gm and total solvent 1 gm.	110

Figure 5.10: Experimental selectivity for the solvent [omi][tfb]+[bmpy][tfb] at 40° C & 1atm for the feed composition of toluele 0.1 gm, heptane 0.9 gm and total solvent 1 gm.	111
Figure 5.11: Calculated C & S for the system [bmpy][tfb]+[omi][tfb] at 40° C,0.1 Mpa.	112
Figure 6.1: The hard-sphere potential.....	120
Figure 6.2: Square well potential.....	125
Figure 6.3: Comparison of compressibility factor of restricted primitive model electrolyte between MC simulation results and the ones calculated with the model proposed.130	
Figure 6.4: Predicted phase diagram of [bmpy] [tfb] + toluene+ heptane system at 1 atm and 40°C by the model developed.....	133
Figure 6.5: Comparison of phase diagram of ionic liquid ([bmpy] [tfb]) +toluene+heptane system at 1 atm and 40°C (—, prediction; ---, experimental).....	134
Figure E.1: NMR spectra of the organic phase of the mixture 1-butyl- 4-methyl pyridinium tetrafluroborate+1-methyl-3-octylimidazolium tetrafluroborate + toluene + heptane at 1 atm and 40°C. 1-methyl-3-octylimidazolium is 10 mol% of the solvent.....	164
Figure E.2: NMR spectra of the IL-phase of the mixture 1-butyl- 4-methyl pyridinium tetrafluroborate+1-methyl-3-octylimidazolium tetrafluroborate + toluene + heptane at 1 atm and 40°C. 1-methyl-3-octylimidazolium is 10 mol% of the solvent.....	165
Figure E.3: NMR spectra of the organic phase of the mixture 1-butyl- 4-methyl pyridinium tetrafluroborate+1-methyl-3-octylimidazolium tetrafluroborate + toluene	

+ heptane at 1 atm and 40°C. 1-methyl-3-octylimidazolium is 30 mol% of the solvent.

..... 166

Figure E.4: NMR spectra of the IL phase of the mixture 1-butyl- 4-methyl pyridinium tetrafluroborate+1-methyl-3-octylimidazolium tetrafluroborate + toluene + heptane at 1 atm and 40°C. 1-methyl-3-octylimidazolium is 30 mol% of the solvent..... 167

LIST OF TABLES

Table 1.1: Potential Organic Solvents for Aromatic Extraction	12
Table 2.1: Density, viscosity, conductivity and refractive index for various ILs	26
Table 2.2: Overview of measured distribution coefficients and selectivities for aromatic/aliphatic separations.....	31
Table 4.1: Computationally recommended anions for typical cations	82
Table 5.1: Solvents tailored from [omi][tfb] and [dmi][ms] for experiments	101
Table 5.2: Solvents tailored from [omi][tfb] & [mbpy][tfb] for experiment.....	102
Table 6.1: Comparison of compressibility factor for MSA in RPM.....	129

ABSTRACT

FULL NAME: KAZI ZAMSHAD SUMON
TITLE OF STUDY: EXTRACTION OF AROMATICS USING GREEN SOLVENTS
BASED ON IONIC LIQUIDS
MAJOR FIELD: CHEMICAL ENGINEERING
DATE OF DEGREE: DECEMBER, 2005

Ionic Liquids have been identified as one of the new classes of solvents that offer opportunities to transform traditional chemical processes into clean, green technologies. Capacity and selectivity at infinite dilution activity coefficients of 1508 ILs have been computed by *COSMOtherm* for the extraction of toluene from toluene-heptane mixture at 1 atm and 40°C. Some potential ILs are screened computationally for the whole composition range. A good number of ionic liquids are found that display considerably higher capacity and higher selectivity than those of sulfolane which is the most popular solvent in aromatic extraction. A general trend is found in the qualitative relationship between capacity and selectivity- when one is high, the other is low and vice versa. To obtain a good compromise between capacity and selectivity, an attempt is made to tailor new IL based solvents by mixing two suitable ILs in specific proportion. *COSMOtherm* predicts the behavior of binary IL solvents as ideal, synergistic and anti-synergistic. The synergistic behavior of binary ILs is verified experimentally. The binary mixture of N-butyl-pyridinium and 1-methyl-3-octyl-imidazolium is found to behave synergistically. An excess Gibbs energy model for solutions containing ionic liquids is also proposed in NPT ensemble. The prediction of compressibility factor of restrictive primitive electrolyte by the model is very close to Monte Carlo simulation data. The model also predicts phase diagram of real systems containing ionic liquid solutions reasonably well.

MASTER OF SCIENCE DEGREE
KING FAHD UNIVERSITY OF PETROLEUM & MINERALS
DHAHRAN, SAUDI ARABIA

ملخص

الإسم: غازي زمشاد سومون.

عنوان الرسالة: إستخلاص المواد العطرية بإستخدام مذيبات مبنية على السوائل الأيونية.

التخصص: هندسة كيميائية.

تاريخ التخرج: ديسمبر 2005م.

السوائل الأيونية هي أهم المذيبات الجديدة التي توفر إمكانية تحويل الصناعات الكيميائية المعتادة إلى تكنولوجيا نظيفة لا تضر بالبيئة. وقد تم في هذه الدراسة حساب السعة والاختيارية لـ 1508 سائل أيوني عند درجة تخفيف عالية لمخلوط التولين مع الهبتان عند درجة حرارة 40 درجة مئوية. كما تمت الحسابات لبعض السوائل الأيونية عند جميع درجات التخفيف. وقد تم تحديد عدد من السوائل الأيونية التي أظهرت سعة وإختيارية أعلى من السلفولان الذي هو أكثر المذيبات إستخداماً لإستخلاص العطوريات.

وتم تحديد إتجاه عام للعلاقة بين السعة والاختيارية: عندما تزيد أحدها تنقص الأخرى ولتصميم افضل السوائل الأيونية تم تحديد العوامل الجزيئية التي تزيد السعة والاختيارية. وتمت محاولة تحسين السعة والاختيارية للسوائل الأيونية النقية بخلطها مع سوائل أخرى. وقد تم تجريباً اثبات زيادة سعة كبيرة لمخلوط: بيوتل بيريدينيوم مع ميثيل اوكتل إيمدازوليوم وتم كذلك تطوير نموذج الدالة جيس للمحاليل الأيونية عند درجة حرارة وضغط معينين. والنبأ بمعامل الإنضغاط لنموذج الأيونات البسيطة قريب جداً من الحسابات المبنية على طريقة مونتي كارلو. كما أن التنبأ بشكل الأطوار للمحاليل الحقيقية جيد جداً.

درجة الماجستير في العلوم
جامعة الملك فهد للبترول والمعادن
الظهران، المملكة العربية السعودية

CHAPTER 1

INTRODUCTION

1.1 THE USE OF AROMATICS

Aromatics are key chemicals in the petrochemical and chemical industries. They are significant raw materials for many intermediates of commodity petrochemicals and valuable fine chemicals, such as monomers for polyesters and intermediates for detergents. Among all aromatics, benzene, toluene, ethyl benzene and xylenes (BTEX) are the four most important ones.

As a gasoline additive, benzene increases the octane rating and reduces knocking. By far the largest use of benzene is an intermediate to make other chemicals. The most widely produced derivatives of benzene are styrene, phenol and cyclohexane. Styrene is used to make polymers and plastics, phenol is used to produce resins and adhesives (via cumene), and cyclohexane is used in nylon manufacture. Smaller amounts of benzene are used to make some types of rubbers, lubricants, dyes, drugs, explosives and pesticides.

Toluene is used as an octane booster in fuel, as a solvent in paints, paint thinners, chemical reactions, rubber, printing, adhesives, lacquers, leather tanning, disinfectants, and to produce phenol and TNT. It is also used as a raw material for toluene diisocyanate, which is used in the manufacture of polyurethane foams.

Xylene is used as a solvent and in the printing, rubber, and leather industries. P-xylene is used as a feedstock in the production of terephthalic acid, which in turn is a monomer used in the production of polymers. It is also used as a cleaning agent, a

pesticide, a thinner for paint, and in paints and varnishes. It is found in small amounts in airplane fuel and gasoline.

1.2 MARKET SCENARIO OF BTEX

The steadily increasing demands of p-xylene made it the main product in the processing of BTEX. The yearly growth of the consumption of p-xylene, is determined mainly by the polyester fibers, between 1984 and 2000 the growth rate was 6.5-8.8%/year. World production in 2000 was 16.4 million tons. Moreover, it is expected that the worldwide production of p-xylene will increase by 5% by 2010. Since the demand for toluene is less than its content in the produced BTX, dealkylation and disproportionation processes were developed for converting it in more valuable products. The demand for m-xylene determines its isomerization to more valuable isomers. The world consumption of styrene increases by about 4.5% per year. The demand for benzene is mainly determined by its consumption in the chemical industry, which increases by about 4.9%/year (Raseev). Therefore, there is a high demand of BTEX in the chemical and petrochemical industries.

1.3 SOURCES OF AROMATICS

BTEX chemicals are used on a large scale as petrochemical feedstock. Because they are often produced together in the same process, they can be considered as a group. However, BTEX as such is not an article of commerce. The BTX aromatics are derived from the gasoline fraction of petroleum products produced by the catalytic reforming of naphtha. Catalytic Reforming is a platinum-catalyzed, high-temperature, vapor-phase

processes that converts a relatively nonaromatic C₆-C₁₂ HC mixture (naphtha) to an aromatic reformat. The octane rating of reformat is directly related to its aromatic content, which is high when the reformer is operated at high severity (high temperatures, low space velocity). Some cracking to light products also occurs, and this increases at high severity. A typical reformat contains BTX in the proportions 19:49:32, respectively, although these proportions can be varied somewhat by tailoring the feed composition and operating conditions (Kirk et al., 1997).

Aromatics are extracted from many hydrocarbon feed stocks which are mainly a mixture of aromatic and non-aromatic hydrocarbons. Catalytic reformat is the main source of aromatics in most of the world. Catalytic reforming is used to prepare high-octane blending stocks for gasoline production and for producing aromatics as separate chemicals. The reforming process accounts for about 45% of all benzene produces in the United States.

Pyrolysis gasoline is produced as a by-product of olefin production by the steam cracking of naphtha or gas oil feedstock. Pyrolysis gasoline contains a high proportion of aromatics, primarily benzene and toluene and a smaller amount of mixed xylenes. In Western Europe pyrolysis gasoline is a significant source of total aromatics (47%).

Coal tar is another source of getting aromatics. Aromatics are present in these major sources with aliphatics. The proportion of aromatics vary in pyrolysis gasoline and reformat according to processing conditions applied during their production. In the past they could be added back to gasoline to raise the octane number. However, there are now

limits on the amount of benzene allowed in gasoline (1%), and it cannot be considered as an octane enhancer.

Reformate, the product of catalytic reforming, has a high octane rating, mostly because of the BTX components. Any BTX needed for chemical use or intended for sale to other refineries as an octane enhancer, is separated from the reformate stream before it is blended into the gasoline pool. On the whole, perhaps only 15% of the BTX produced in refinery reformate streams is separated and sold or used separately.

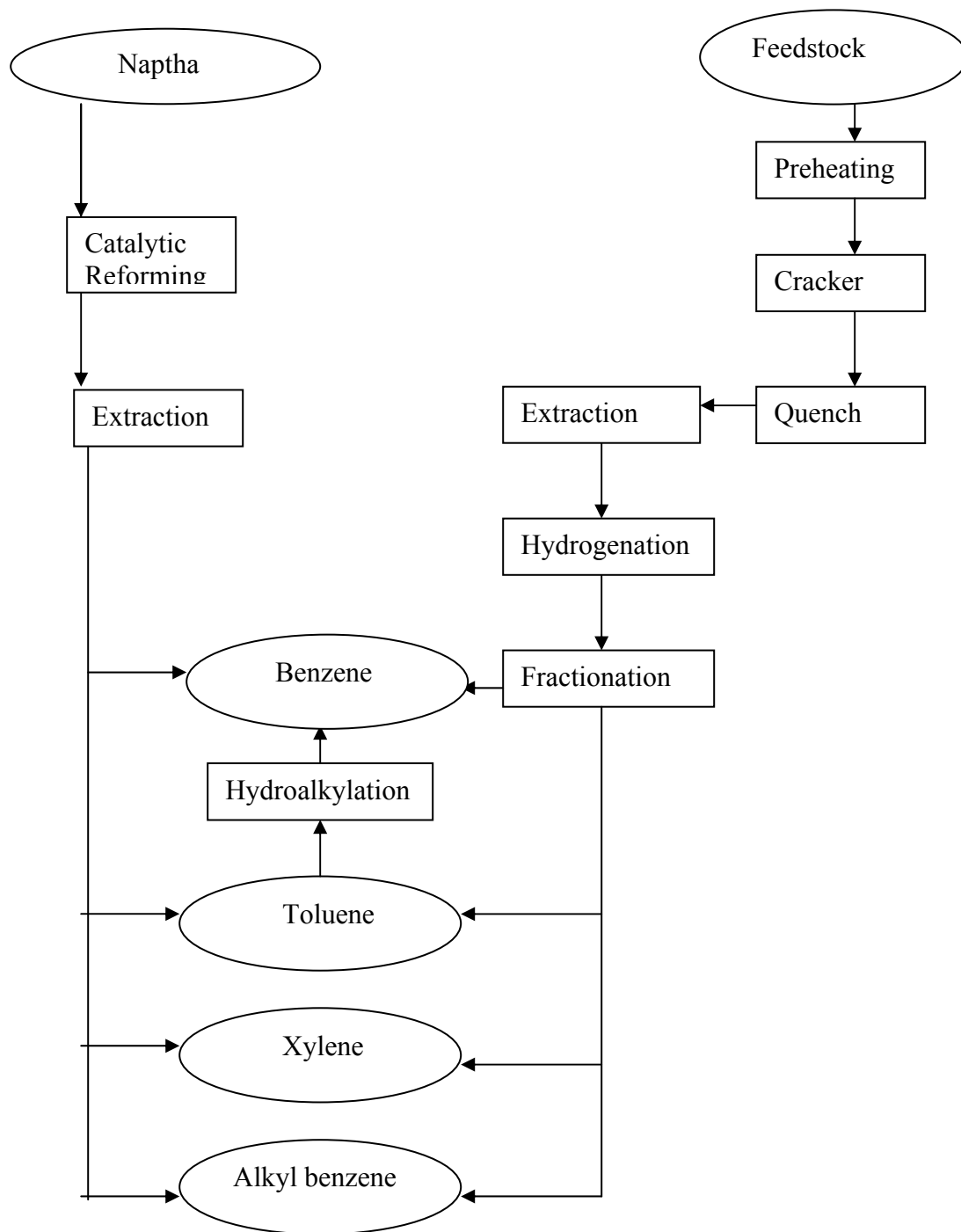


Figure 1.1: Process roots for aromatics

1.4 AROMATICS EXTRACTION PROCESSES

1.4.1 Membrane Permeation

For membrane separation of aromatic and aliphatic hydrocarbon, a large number of literature articles deal with the development of polymeric membranes for the separations of benzene and cyclohexane or toluene and n-octane (Yoshikawa et al.,1997). In recent years, pervaporation separation and vapor permeation have emerged as relatively simple alternatives to many water/organic and organic/water separation application. Pervaporation and vapor permeation are especially attractive in azeotropic and close-boiling point separation applications, since these processes are not based on the relative volatilities of components, but on the difference in sorption and diffusion properties of these substances as well as the permselectivity of the membrane. On the other hand, application of pervaporation or vapor permeation in organic/organic separation with organic membranes is still very limited because of their low selectivity and/or low flux rates.

1.4.2 Adsorption

A suitable adsorbent for the separation of aromatic and aliphatic hydrocarbons from a process stream such as naphtha, which contains 10-25% aromatics, must absorb the aromatic hydrocarbons. Most zeolites, because of the presence of the exchangeable cations are polar adsorbents. Molecules such as water or ammonia (high dipole), CO₂, N₂ (quadrupolar) or aromatic hydrocarbons (Pi-layer interaction) are therefore adsorbed more strongly than non-polar species of comparable molecular weight (Ruthven,1988). However, since aromatic hydrocarbons are strongly adsorbed on zeolites, desorption is a

difficult step. Therefore adsorption is also not an attractive technique for the separation of aromatics from aliphatics.

1.4.3 Extraction and Extractive Distillation

The separation of aromatics hydrocarbons (benzene, toluene, ethyl benzene and xylenes) from C₄-C₁₀ aliphatic hydrocarbon mixtures is challenging since these hydrocarbons have boiling points in a close range and several combinations form azeotropes. The conventional processes for the separation of these aromatic and aliphatic hydrocarbon mixtures are liquid-liquid extraction(LLE), suitable for the range 20-65 wt% aromatic content, extractive distillation(ED) for the range of 65-90 wt% aromatics and azeotropic distillation for high aromatic content, >90 wt% (Ali et al.,2003).

1.5 LIQUID-LIQUID EXTRACTION

Liquid-liquid extraction or solvent extraction involves the distribution of a solute between two immiscible liquid phases in contact with each other. Scientists and engineers are concerned with the extent and dynamics of the distribution and its use scientifically and industrially for separation of solution mixture. Solvent extraction is used in numerous chemical industries to produce pure chemical compounds, ranging from pharmaceuticals and biomedical to heavy organics and metals, in analytical chemistry, in environmental waste purification, as well as in research. This is the most important commercial process for aromatic extraction.

The principle is illustrated in fig 2-2. Solvents that form a separate liquid phase are used in this process. Aromatics are considerably more soluble than nonaromatics in the solvents employed. As a result, the solutes prefer the solvent phase to remain in than

the organic phase. It is necessary that the solvent form a non-ideal solution with the mixture to be separated. The solvents used have a purely physical interaction with the hydrocarbon phase. The hydrocarbons are repelled by the polar solvent to a greater or lesser extent, depending on the type of hydrocarbon.

1.6 THERMODYNAMICS OF LLE

Many pairs of chemical species, were they to mix to form a single liquid phase in a certain composition range, would not satisfy the thermodynamic stability criterion. Such system therefore split in this composition range into two liquid phases of different compositions. If the phases are at thermal equilibrium, the phenomenon is an example of Liquid/liquid equilibrium (LLE). LLE operations are generally conducted at atmospheric pressure, and the gas phase is irrelevant to them. The system involves two phases and at least three components: a mixture of two components (such as toluene and heptane) including the distribuends (toluene) and a solvent (such as sulfolane). A phase is defined as a region of space that has uniform properties throughout. The phase rule of Gibbs tells us what the variance of such a system is, i.e., how many intensive variables can be chosen at will in order for the equilibrium state of the system to be defined. In our cases, there are two phases each comprising three components resulting into three degrees of freedom. Now, if the temperature and the concentrations of the any two components in

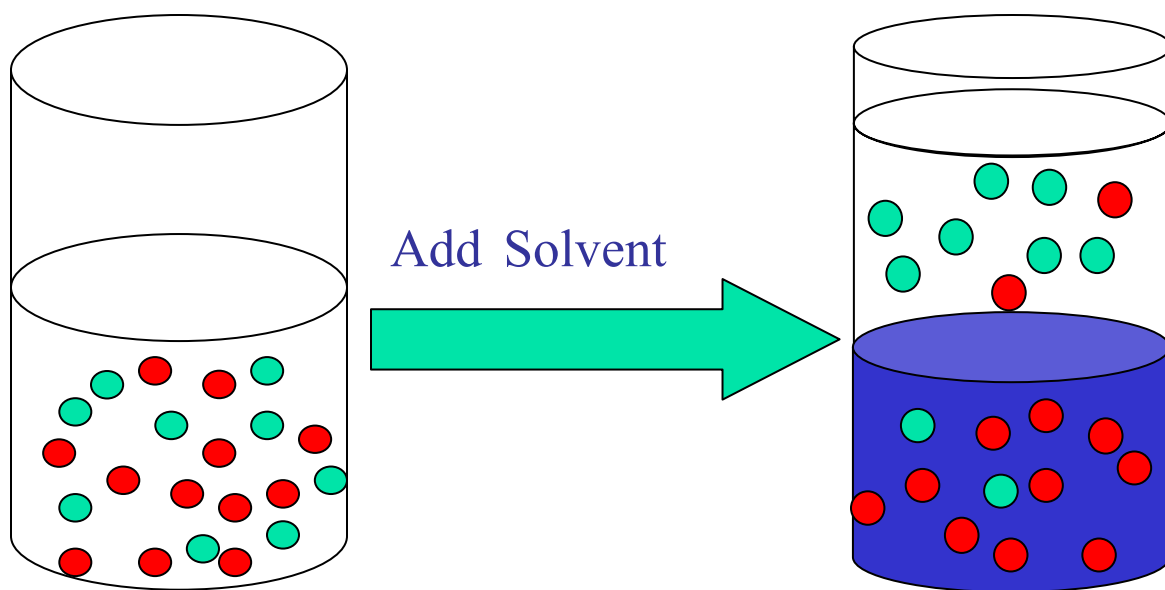


Figure 1.2: Principle of liquid-liquid extraction

one of the phase is arbitrarily fixed, thereby all degrees of freedom is exhausted and the concentrations in other phase will be fixed by equilibrium condition.

The driving force of mass transfer in LLE is termed the chemical potential of the distribuends, and as long as this is larger in one phase than in the other, the distribuends will transfer from the former to the latter. The transfer causes changes in the chemical potentials in the direction of their equalization, and the transfer will cease when the chemical potentials are the same in the two phases. This is the condition for distribution equilibrium.

At equilibrium, for a component i ,

$$x_i^I \gamma_i^I = x_i^{II} \gamma_i^{II}$$

where, x_i^I = mol fraction of component i in phase I

x_i^{II} = mol fraction of component i in phase II

γ_i^I = activity coefficient of component i in phase I

γ_i^{II} = activity coefficient of component i in phase II

Activity coefficient is a measure of the non-ideality of a phase and can be calculated from thermodynamic models such as excess Gibbs energy models. One can also calculate mol fractions and thereby generate phase diagrams from excess Gibbs energy model.

Numerous factors contribute to the success of an aromatics extraction process. However, the solvent characteristics have the most effect on the process economics. The solvent selectivity and capacity are the most important properties of the solvent. The selectivity of a solvent for aromatics may be defined as the ratio of the activity coefficient or composition of a particular aliphatic component in the solvent to that of a desired aromatic. Capacity measures the quantity of the material to be separated that can be contained in the solvent phase. These quantities are defined as:

$$D_{arom} = \frac{x_{arom}^{solvent}}{x_{arom}^{org}} \quad (2-1)$$

$$D_{alip} = \frac{x_{alip}^{solvent}}{x_{alip}^{org}} \quad (2-2)$$

$$Capacity = D_{arom} \quad (2-3)$$

$$Selectivity = D_{arom} / D_{alip} \quad (2-4)$$

The ideal solvent should have sufficient capacity to ensure good aromatics recovery without excessive solvent circulation rates. Other important properties of the solvent include: aromatics range, density, viscosity, boiling and solidification points, thermal stability, corrosiveness, toxicity, and price. Table 2-1 shows a number of potential solvents that can be used in aromatic extraction.

Table 1.1: Potential Organic Solvents for Aromatic Extraction

1. SULFOLANE	12. TETRAETHYLENE GLYCOL
2. FORMYLMORPHOLINE	13. PROPYLENE CARBONATE
3. THIODIPROPIONITRILE	14. ETHYLENE DIAMINE
4. OXIDIPROPIONITRILE	15. METHYLCARBAMATE
5. ETHYLENE GLYCOL	16. FURFURAL
6. ETHYLENE CARBONATE	17. DIETHYLENE GLYCOL METHYLETHER
7. DIETHYLENE GLYCOL	18. TRIETHYLENE TETRAMINE
8. NITROMETHANE	19. PROPYLENE GLYCOL
9. DIMETHYLSULFOXIDE	20. N-METHYLPYRROLIDONE
10. METHYLFORMAMIDE	21. DIPROPYLENE GLYCOL
11. TRIETHYLENE GLYCOL	

1.7 GREEN SOLVENTS

The green chemistry movement which encompasses the designing of chemical processes and products that reduce or eliminate the use and generation of hazardous substances has become a new paradigm in many aspects of pure and applied chemistry. One aspect of the Green Chemistry movement involves the development and use of benign solvents to replace volatile organic compounds (VOCs). VOCs, required for dissolving, mixing, and separation in chemical processes and supporting media in

electrolyte processes, represent the bulk of hazardous substances lost to atmosphere, by incineration or disposal, from chemical industries. Strategies to reduce or eliminate solvent waste from chemical industries include solvent-free synthesis and the use of more benign solvents, such as water, supercritical fluids, *ionic liquids* [ILs]. Exploration of the latter strategy, ionic liquids as solvent replacements, has been the focus of much research in recent years. A wide range of solvent applications have been investigated and in many cases the ionic liquid media are now studied for reasons of specific advantages in rate, specificity, and yield rather than simple VOC replacement (Stewart et al., 2004).

CHAPTER 2

LITERATURE REVIEW

2.1 PRESENT INDUSTRIAL SOLVENTS & PROCESSES

Commercial processes have been based on solvents such as Sulfolane, N-methyl pyrrolidine, and Dimethylsulfoxide. These solvents have a number of common characteristics which are worth noting. They all have densities & boiling points which are higher than the material to be extracted and all are to a greater or lesser extent polar molecules or water soluble. Each of these properties has a definite influence on the type of equipment employed & the process flow sheet (McKetta, 1984).

The most important of all industrial processes is the Sulfolane process. As of 1999, UOP has licensed a total of 130 Sulfolane units throughout the world. The Sulfolane process takes its name from the solvent used: tetrahydrothiophene 1, 1-dioxide. This process was developed in 1960s and is still the most efficient solvent available for the recovery of aromatics. The Sulfolane process combines liquid-liquid extraction with extractive distillation to recover high purity aromatics from hydrocarbon mixtures. The recovery of benzene exceeds 99.9 wt%, and recovery of toluene is typically 99.8 wt%. Other important industrial processes include Tetra process by Udex, Carom process by UOP, Morphylane process by Uhde and the Arosolvan process.

2.2 IONIC LIQUIDS- A REVIEW

2.2.1 Introduction

ILs have been identified as one of the new classes of solvents that offer opportunities to move away from traditional chemical processes to new, clean, Green technologies in which waste streams are minimized with the goals of atom-efficiency and resulting environmental and cost benefits. ILs typically comprise of large asymmetric organic cations and inorganic or organic anions (Figure 4.1), and have (by definition) low melting points ($<150^{\circ}\text{C}$) induced largely by packing frustration of the usually asymmetric Cations.

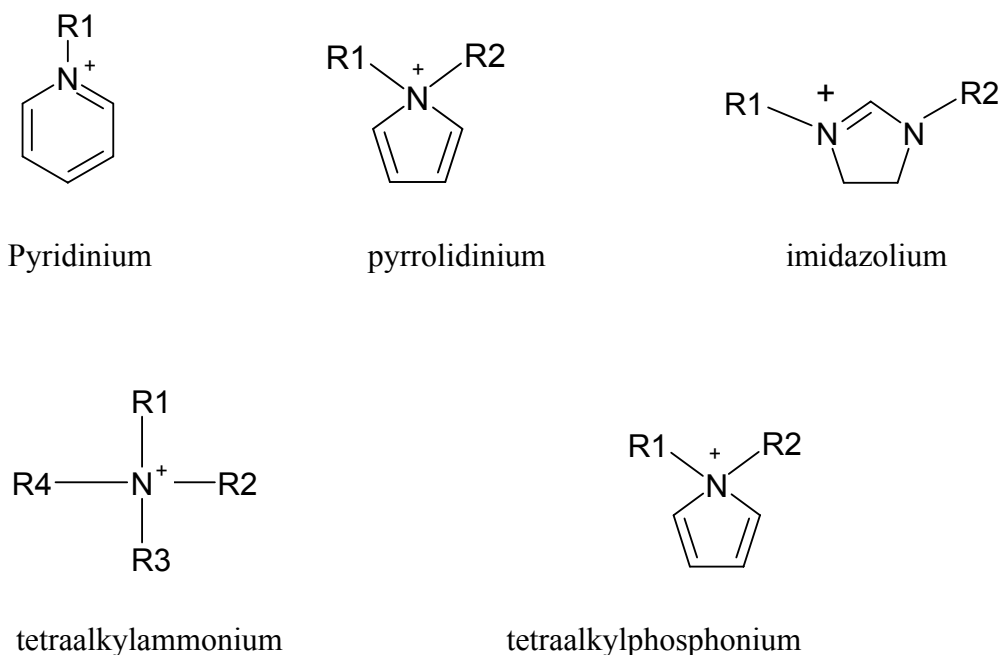


Figure 2.1: Examples of some common cations

The cations are based on methylimidazolium [Rmim], N-butylpyridinium, [R-N-bupy] quaternary ammonium or phosphonium ions and others, and anions such as hexafluorophosphate, tetrafluoroborate, alkylsulfates, alkylsulfonates, chloride, bromide, nitrate, sulfate, aluminium chloride, triflate (CF_3SO_3^-), bis (triflyl)imide ($((\text{CF}_3\text{SO}_2)_2\text{N}^- = \text{TfN})$), etc. (Brennecke,2001). The R group of the cation is variable (e.g. methyl, ethyl, butyl, etc.). The variability of the anion and R groups in the imidazolium, pyridinium, ammonium or phosphonium cations may be used to adjust the properties of the ionic liquids (Meindersma et al.,2005).

2.2.2 Background

The first low melting salt, ethyl ammonium nitrate, with low melting point of 12°C was synthesized by Walden (1914) and Hurley et al. (1951) developed low melting salts with chloroaluminate ions for low-temperature electroplating of aluminium. During the 1970s and 1980s, these liquids were studied mainly for electrochemical applications. In the mid 1980s, low melting point ionic liquids were proposed as solvents for organic synthesis by Fry et al. (1986) and Boon et al. (1986). In the 1990s, an understanding that molten salts having melting point below 100°C created a new unique media for chemical reactions became widespread and the term “room temperature ionic liquids (RTILs)” was assigned to them. However, electrochemists still prefer the term “room-temperature molten salts” or RTMS. At the present time the number of RTILs synthesized exceeds 500 and research in this area is expanding rapidly. There is virtually no limit in the number of salts with low melting points. Earle et al. (2004) have estimated this number to be of the order of 1 billion.

2.2.3 Attractiveness as New Generation Solvent

Compared to conventional organic solvents, the use of ionic liquids for synthesis and extraction has a number of advantages determined by the unique combinations of their properties. Ionic liquids involving fully quarternized nitrogen cations have negligible vapor pressure and non-flammable. These properties are significant when addressing the health and safety concerns associated with many solvent applications. Negligible vapor pressure solvent evaporation is eliminated, reducing the need for respiratory protection and exhaust systems (Huang et al., 2001 ; Stewart et al., 2004). They have liquid range more than 400K. While many solvents will freeze or boil across such a large temperature range, ionic liquids maintain their volume and fluidity. This wide range of thermal stability allows for tremendous kinetic control of chemical processes. The wide temperature range is also helpful in temperature dependent separation processes as extraction. Ionic liquids are little denser than water and miscible with substances having very wide range of polarities and can simultaneously dissolve organic and inorganic substances. These features of RTILs offer numerous opportunities for modifications of existing and for the development of new extraction processes. In such cases, such processes would be impossible with conventional solvents because of their limited liquid range or miscibility. The novel feature of RTILs as solvents is the possibility to design one with the necessary properties for a specific application, hence the term “designer solvents”.

The choice of base cation and anion creates the major properties of a particular RTIL. The fine tuning of properties is possible by the variation of the length and branching of the alkyl groups incorporated into the cation. For example, for 1-alkyl-3-

alkylimidazolium cation, replacing the (PF_6^-) anion with (BF_4^-) dramatically increases the solubility of the ionic liquid in water while replacement with (Tf_2N^-). Regeneration of ionic liquids is comparatively easy.

2.2.4 Solvent Properties of ILs

In this section, some macroscopic properties of ILs, such as melting-point, viscosity and density will be examined. Before discussing the physical properties of ILs, it must be remembered that they can be dramatically altered by the presence of impurities. Purification of the ILs is essential not only to avoid possible interactions between reactants and impurities, but also because they can change the nature of these solvents. The main contaminants are halide anions and organic bases, arising from unreacted starting material, and water (Seddon et al., 2004).

Melting-point and crystal structure

Unfortunately, the melting-points of many ILs are very uncertain because they undergo considerable supercooling; the temperature of the phase change can differ considerably depending on whether the sample is heated or cooled. However, by examining the properties of a series of imidazolium cation-based ILs, it has been established (Huddleston et al., 2001) that the melting-point decreases when the size and asymmetry of the cation increase. Further, an increase in the branching on the alkyl chain increases the melting-point. The anion effect is more difficult to rationalize. For imidazolium ILs containing structurally similar anions, such as triflate ($[\text{TfO}]^-$) and bis(triflyl)imide ($[\text{Tf}_2\text{N}]^-$), the lower melting-points of the latter have been attributed to

the electron delocalization and the relative inability of this anion to undergo hydrogen bonding with the proton(s) of the cation (Pringle et al., 2003)

Moreover, it has been shown (Kolle et al., 2004) that the contribution of the hydrogen bonds to lattice energies, and therefore to melting-points, can be correlated with the acceptor strength of the anion. It has been proposed that the thermodynamic properties of ILs are strongly dependent on the mutual fit of the cation and anion, in terms of size, geometry and charge distribution although, within a similar class of salts, small changes in the shape of uncharged, covalent regions of the ions may have an important influence. For example, in the case of 1-butyl-3-methyl imidazolium ILs, having as counter anions substituted tetraphenylborates, the increasing bulk and orientational flexibility of the substituents on the aromatic rings of the anion depresses the melting-point of these salts (van de Broeke et al., 2003). Strictly related to the melting-points are the crystal structures of the ILs. Although the structural organization is much lower in a liquid than in a crystal, the structural organization of the crystal lattice may provide a reasonable starting point for understanding structural features in the liquid phase.

Thermal stability

Most ILs exhibit high thermal stability; the decomposition temperatures reported in the literature are generally >300 °C, with minimal vapor pressure below their decomposition temperatures. The onset of thermal decomposition is furthermore similar for the different cations but appears to decrease as the anion hydrophilicity increases. It has been suggested that the stability dependence on the anion is $[\text{PF}_6]^- > [\text{Tf}_2\text{N}]^- \sim [\text{BF}_4]^- >$

halides. (Ngo et al., 2000) An increase in cation size, at least from 1-butyl to 1-octyl, [bmim]⁺ to [omim]⁺, does not appear to have a large effect.

The thermal stability of ILs has, however, been revised recently, (Kosmulski et al., 2004) showing that high decomposition temperatures, calculated from fast thermogravimetric analysis (TGA) scans under a protective atmosphere, do not imply long-term thermal stability below these temperatures. After 10 h, even at temperatures as low as 200 °C, 1-alkyl-3-methylimidazolium hexafluorophosphates and 1-decyl-3-methylimidazolium triflate show an appreciable mass loss. On the other hand, 1-butyl-3-methylimidazolium triflate is stable under the same conditions, in the absence of silica. Carbonization generally occurs irrespective of the nature of the anion (hexafluorophosphate, triflate) but not for the salts with a shorter side-chain; the color of these ILs does not change after conditioning for 10 h at 200 °C in air.

Viscosity

One of the largest barriers to the application of ILs arises from their high viscosity. A high viscosity may produce a reduction in the rate of many reactions. Current research for new and more versatile ILs is driven, in part, by the need for materials with low viscosity. The viscosity of ILs is normally higher than that of water, similar to those of oils, and decreases with increasing temperature. Generally, viscosity follows a non-Arrhenius behavior but, sometimes, it can be fitted with the Vogel–Tammann–Fulcher (VFT) equation. Furthermore, viscosity remains constant with increasing shear rate and ILs can

be classified in terms of Newtonian fluids, although non-Newtonian behaviors have been observed (Okoturo et al., 2004).

Examining various anion–cation combinations, the increase in viscosity observed on changing selectively the anion or cation has been primarily attributed (Xu et al., 2003) to an increase in the van der Waals forces. In agreement with this statement, in the 3-alkyl-1-methylimidazolium hexa- fluorophosphate and bis (triflyl) imide series ([Rmim][PF₆] and [Rmim][Tf₂N]), viscosity increases as n, the number of carbon atoms in the linear alkyl group, is increased. The trends are, however, different; a linear dependence has been found for the [Tf₂N]⁻ salts whereas a more complex behavior characterized the [PF₆]⁻ salts. Branching of the alkyl chain in 1-alkyl-3-methylimidazolium salts always reduces viscosity. Finally, also the low viscosity of ILs bearing polyfluorinated anions has been attributed to a reduction in van der Waals interactions.

Hydrogen bonding between counter anions is, however, another factor considered to affect viscosity. The large increase in viscosity recently found on changing the anion of several ILs (imidazolium, pyrrolidinium and ammonium salts) from [Tf₂N]⁻ to [Ms₂N]⁻ has been attributed to the combination of the decreased anion size, less diffuse charge and large increase in hydrogen bonding. Finally, the symmetry of the inorganic anion has sometimes been considered as an additional parameter; viscosity decreases in the order Cl⁻ > [PF₆]⁻ > [BF₄]⁻ > [NTf₂]⁻.

Density

Density is one of the most often measured properties of ILs, probably because nearly every application requires knowledge of the density. In general, ionic liquids are denser than water. The molar mass of the anion significantly affects the overall density of ILs. The $[\text{Ms}_2\text{N}]^-$ species have lower densities than the $[\text{Tf}_2\text{N}]^-$ salts, in agreement with the fact that the molecular volume of the anion is similar but the mass of the fluorine is greater. In the case of orthoborates, with the exception of bis(salicylato)borate, the densities of the examined ILs having the $[\text{bmim}]^+$ cation decrease with increase in anion volume and this order is followed also when the densities of other salts, such as those having $[\text{Tf}_2\text{N}]^-$, $[\text{TfO}]^-$ or $[\text{BF}_4]^-$ as anion, have been included. This behavior has been attributed to the fact that packing may become more compact as the alternating positive and negative species become more even in size.

Ionic diffusion coefficients and conductivity

The transport properties are crucial when we consider the reaction kinetics in a synthetic process or ion transport in an electrochemical device. Despite this, the correlation between IL chemical structure and transport properties is still not completely understood. Probably, since ILs are concentrated electrolyte solutions, the interpretation of their transport properties is very complicated. Through pulse-gradient spin-echo NMR measurements, carried out on two 1-ethyl-3-methylimidazolium and two 1-butylpyridium ILs, in particular $[\text{emim}][\text{BF}_4]$, $[\text{emim}][\text{Tf}_2\text{N}]$, $[\text{bpy}][\text{BF}_4]$ and $[\text{bpy}][\text{Tf}_2\text{N}]$, it has been shown (Noda et al., 2001) that the two cations diffuse at almost the same rate as $[\text{BF}_4]^-$ but faster than $[\text{Tf}_2\text{N}]^-$. The sum of cationic and anionic diffusion

coefficients for each IL follows the order [emim][Tf₂N]⁺> [emim][BF₄]⁺>[bpy][Tf₂N]⁺> [bpy][BF₄].

Surface tension

Surface tension may be an important property in multiphase processes. ILs are widely used in catalyzed reactions, carried out under multiphase homogeneous conditions, that are believed to occur at the interface between the IL and the overlying organic phase. These reactions should therefore be dependent on the access of the catalyst to the surface and on the transfer of the material across the interface, i.e. the rate of these processes depends on surface tension.

In general, liquid/air surface tension values for ILs are somewhat higher than those for conventional solvents [(3.3–5.7)×10⁻⁴Ncm⁻¹], although not as high as for water, and span an unusually wide range. Surface tension values vary with temperature and both the surface excess entropy and energy are affected by the alkyl chain length, decreasing with increasing length. For a fixed cation, in general, the compound with the larger anion has the higher surface tension. However, alkyimidazolium [PF₆]⁻ salts have higher surface tensions than the corresponding [Tf₂N]⁻ salts (Law et al.,2001).

Refractive index

This parameter is related to polarizability/dipolarity of the medium and is used in the least-squares energy relationship of Abraham as a predictor of solute distribution. The

values found for [bmim][X] salts are comparable to those for organic solvents. The above properties for various ILs are summarized in Table 3-1.

Solubility in water

The hydrophilic/hydrophobic behavior is important for the solvation properties of ILs as it is necessary to dissolve reactants, but it is also relevant for the recovery of products by solvent extraction. Furthermore, the water content of ILs can affect the rates and selectivity of reactions. The solubility of water in ILs is, moreover, an important factor for the industrial application of these solvents. One potential problem with ILs is the possible pathway into the environment through wastewater.

Extensive data are available on the miscibility of alkyimidazolium ILs with water. The solubility of these ILs in water depends on the nature of the anion, temperature and the length of the alkyl chain on the imidazolium cation. For the [bmim]⁺ cation the [BF₄]⁻, [CF₃CO₂]⁻, [NO₃]⁻, [NMs₂]⁻ and halide salts display complete miscibility with water at 25°C. However, upon cooling the [bmim][BF₄]-water solution to 4°C, a water rich-phase separates. In a similar way, 1-hexyl-3-methylimidazolium hexafluorophosphate, [hmim][PF₆], shows a low solubility in water even at 25°C. [PF₆]⁻, [SbF₆]⁻, [NTf₂]⁻, [BF₄]⁻ salts are characterized by very low solubilities in water, but 1,3-dimethylimidazolium hexa-fluorophosphate is water soluble. Also, the ILs which are not water soluble tend to adsorb water from the atmosphere. On the basis of IR studies it has been established (Cammarata et al.,2001) that water molecules absorbed from the air are mostly present in the 'free' state, bonded via H-bonding with [PF₆]⁻, [BF₄]⁻, [SbF₆]⁻,

$[\text{ClO}_4]^-$, $[\text{CF}_3\text{SO}_3]^-$ and $[\text{Tf}_2\text{N}]^-$ with a concentration of the dissolved water in the range 0.2–1.0 mol dm⁻³. The strength of H-bonding between anion and water increases in the order $[\text{PF}_6]^- < [\text{SbF}_6]^- < [\text{BF}_4]^- < [\text{Tf}_2\text{N}]^- < [\text{ClO}_4]^- < [\text{NO}_3]^- < [\text{CF}_3\text{CO}_2]^-$.

Polarity

The key features of a liquid that is to be used as solvent are those which determine how it will interact with potential solutes. For molecular solvents, this is commonly recorded as the ‘polarity’ of the pure liquid, and is generally expressed by its dielectric constant. ILs can be classified, as all the other solvents, on the basis of their bulk physical constants. At variance with molecular solvents, however, dielectric constants cannot be used in the quantitative characterization of solvent polarity. Actually, this scale is unable to provide adequate correlations with many experimental data also in the case of molecular solvents, and the quantitative characterization of the ‘solvent polarity’ is a problem not completely solved even for molecular solvents.

Table 2.1: Density, viscosity, conductivity and refractive index for various ILs

IL	Density(25°C)(g ml ⁻¹)	Viscosity (cP)	Conductivity (mS cm ⁻¹)	Refractive index
[emim][PF ₆]	Solid			
[bmim][PF ₆]	1.368	450(25°C)		
[hmim][PF ₆]	1.292	585(25 °C)		
[omim][PF ₆]	1.237	682 (25 °C)		1.42
[emim][Tf ₂ N]	1.519	28 (25 °C)	8.8	1.42
[bmim][Tf ₂ N]	1.436	52 (25 °C)		1.43
[hmim][Tf ₂ N]	1.372			
[omim][Tf ₂ N]	1.320			
[emim][NMs ₂]	1.343	787	1.7	
[bmim][BF ₄]	1.12	233 (25 °C)		1.43
[bmim][Cl]		Solid	Solid	Solid
[hmim][Cl]	1.03	716 (25 °C)		1.52
[omim][Cl]	1.00	337 (25 °C)		1.51
[bmim][I]	1.44	1110 (25°C)		1.57
[bmim][TfO]	1.29	90 (25 °C)	3.7	1.44
[bmim][CF ₃ CO ₂ H]	1.21	73 (25 °C)	3.2	1.45
[em ₂ im][Tf ₂ N]	1.51	88 (20 °C)	3.2	1.43

[bmpy][Tf ₂ N]	1.41	85(25 °C)	2.2	
[bmpy][NMs ₂]	1.28	1680 (20 °C)		

2.2.5 IL Polarity in the Presence of Other ‘Solvents’

The use of ILs as solvents implies also the knowledge of their behavior in the presence of other compounds, in particular water, other organic solvents and supercritical CO₂, the last often being used for product extraction. Furthermore, to increase the efficiency of the processes (syntheses, extractions, separations) carried out in ILs, sometimes co solvents are added and these affect the physical properties of ILs.

Water is often present in ILs as an unwanted impurity, as a consequence of their hygroscopic nature, and the presence of even small amounts of water can modify not only the physical properties of ILs (viscosity, density, etc.) but also the polarity. The recently reported determination of the polarity of [bmim][PF₆] and [hmim][PF₆] (1-hexyl-3-methylimidazolium hexafluorophosphate) through the partition coefficients between water and the investigated ILs may be considered a determination of the polarity of these ILs in the presence of water (Abraham et al.,2003) Both ILs have practically the same dipolarity/polarizability as that of water and they are less basic than water (about the same as a typical ester).

2.2.6 Challenges Posed for Separation Technologies by ILs

A significant amount of research on ionic liquid-based separations processes has been done at the laboratory scale. Only one industrial process has been made widely

known to date. Implementation of additional processes will require cost-benefit, economic (including waste) and life-cycle analyses of processes. Several important questions remain regarding potential limitations of the applicability of many ILs, particularly in large-scale separations.

Loss

Dissolution of ionic liquids in aqueous phase could present significant cost and waste-treatment challenges (Anthony et al.,2001) Loss of ionic liquids to the aqueous phase was measured during metal extraction in liquid-liquid systems. (Dietz et al., 2001; Jensen et al.,2002). Progress with approaches such as supercritical phase splitting (Scurto et al.,2003) and water-structuring salts (Gutowski et al.,2003) may reduce IL losses in aqueous streams.

Toxicity

There is significant uncertainty regarding the toxicity and potential environmental impact of ionic liquids. Structural similarities between certain types of ionic liquids and either herbicides or plant growth regulators have been noted (Jastroff et al.,2003) Significant efforts are ongoing, both in obtaining toxicological data –PEG-5 cocomonium methosulfate is first IL for which full toxicological data is available and to develop RTILs based on biomolecules (e.g., L-alanine ethyl ester hydrochloride) for reduced toxicity and increased biodegradability (Davis et al.,2003).

Instability & Regenerability

Swatloski et al. (2003) reported the instability of ionic liquids incorporating the widely used hexafluorophosphate anion (the decomposition of which is likely to yield

HF). For practical process development, additional means are needed to recover nonvolatile solutes in IL, particularly salts.

2.3 IONIC LIQUIDS IN CHEMICAL SEPARATIONS

The use of ionic liquids in separations is presently mostly in the extraction of metal ions with [bmim]PF₆, [hmim]PF₆ and other PF₆⁻ based ILs [(Visser et al.,2001); (Visser et al.,2002), (Wei et al.,2003)], alcohols using [bmim]PF₆, [omim]PF₆ and [Rmim]PF₆ (Fadeev et al.,2001; Heintz et al.,2003 ;Wu et al.,2001), separation of alcohols and alkanes or alkenes with [omim]Cl, [hmim]BF₄ or [hmim]PF₆ (Letcher et al.,2003 ; Letcher et al.,2004) desulphurization of oILs with [emim]AlCl₄, [bmim]AlCl₄, [bmim]BF₄, [bmim]PF₆, trimethylamine hydrochloride/AlCl₃, [emim] ethyl sulfate and [bmim] octylsulfate (Bosmann et al.,2001; Zhang et al.,2002 ; Zhang et al.,2004), ethers from ethanol with [omim]Cl and [bmim] trifluoromethanesulfonate(Arce et al.,2004). It is also possible to separate compounds from each other by selective transport by using supported liquid membranes based on ionic liquids, such as [bmim]PF₆ (Branco et al.,2002; Matsumoto et al.,2005). Environmental pollutants, such as aromatic and polycyclic aromatic hydrocarbons, can be extracted from aqueous solutions with ionic liquids [bmim]PF₆ and [omim]PF₆ (Liu et al.,2005). There are only a few publications concerning extraction of aromatic hydrocarbons from mixtures of aromatic and aliphatic hydrocarbons, notably with [emim]I₃, [bmim]I₃, [emim](CF₃SO₂)₂N, [omim]Cl, [hmim]BF₄ and [hmim]PF₆ (Letcher et al.,2005). Recent efforts by a number of investigators have focused on the application of ionic liquids in separations, typically as replacements for the organic diluents employed in traditional liquid-liquid extraction or in membrane-based separations of organic solutes, metal ions, and gases.

2.4 ILS FOR AROMATIC EXTRACTION

Aromatic hydrocarbons are reported to have low activity coefficients at infinite dilution in several ionic liquids, while aliphatic hydrocarbons show high activity coefficients in the same ionic liquids (Arlt et al., 2002). In Table 2, aromatic distribution coefficients and aromatic/aliphatic selectivities for toluene/heptane and some other aromatic/aliphatic systems, determined by either extraction (Selvan et al., 2001), solubility (Blanchard et al., 2001) or by activity coefficients at infinite dilution (David et al., 2003) are shown. This suggests that these ionic liquids can be used as extractants for the separation of aromatic hydrocarbons from aliphatic hydrocarbons. Extraction of aromatics from mixed aromatic/aliphatic streams with ionic liquids is expected to require less process steps and less energy consumption than extraction with conventional solvents because ionic liquids have a negligible vapor pressure.

Table 2.2: Overview of measured distribution coefficients and selectivities for aromatic/aliphatic separations

Solvent	Separation	T (°C)	D _{arom}	S _{arom/alip}	Ref
Sulfolane	Toluene/heptane	40	0.31	30.9	(Meindersma et al.,2005)
[emim]I ₃	Toluene/heptane	45	0.84	48.6	(Selvan et al.,2005)
[bmim]I ₃	Toluene/heptane	35	2.3	30.1	(Selvan et al.,2005)
[omim]Cl	Benzene/heptane	25	0.58	6.1	(Letcher et al.,2003)
	Benzene/heptane	25	0.50	10.7	(David et al.,2003)
	Benzene/heptane	40	0.63	11.3	(Mutelet et al.,2005)
	Toluene/heptane	35	0.38	8	(David et al.,2003)
	Toluene/heptane	40	0.43	7.7	(Mutelet et al.,2005)
[mmim][Tf ₂ N]	Toluene/heptane	40	0.49	29.8	(Krummen et al.,2002)
[emim][Tf ₂ N]	Benzene/cyclohexane	24.5		17.7	(Gmehling et al.,2003)

[emim][Tf ₂ N]	Benzene/cyclohexane	30	0.84	13.2	(Gmehling et al.,2003)
	Toluene/heptane	40	0.55	22.2	(Krummen et al.,2002)
	Toluene/heptane	40	0.58	22.1	(Heintz et al.,2002)
	Toluene/heptane	40	0.56	16.5	(Mutelet et al.,2005)
[bmim][Tf ₂ N]	Toluene/heptane	40	0.81	16.7	(Krummen et al.,2005)
[emim][Tf ₂ N]	Toluene/heptane	40	0.61	22.7	(Heintz et al.,2002)
[bmim][PF ₆]	Benzene/cyclohexane	22	0.66	3.1	(Blanchard et al.,2005)
	Toluene/heptane	68	0.43	9.7	(Domanska et al.,2003)
	Toluene/heptane	40	0.34	21.3	(Mutelet et al.,2005)
	Toluene/heptane	60	0.30	18.3	(Mutelet et al.,2005)
	Benzene/heptane	25	0.70	8.2	(Letcher et al.,2005)

[bmim][PF ₆]	Benzene/heptane	25	0.97	29.7	(Letcher et al.,2005)
	Benzene/heptane	25	0.81	8.4	(Letcher et al.,2005)
	Toluene/heptane	40	0.38	32.8	(Heintz et al.,2001)
	Toluene/octane	40	0.14	48	(Kato et al.,2004)
[bmim][PF ₆]	Toluene/heptane	40	0.06	16.4	(Kato et al.,2004)
	Toluene/heptane	40	0.19	43	(Krummen et al.,2005)

2.5 MODELING SOLUTIONS CONTAINING ILS

2.5.1 Models for Electrolyte Solutions

Electrolyte solutions historically set themselves apart from ordinary solutions in the study of mixtures because of the difficulty in treating electrically charged species which interact through long-range Columbic forces. It was not until 1960s and 1970s when liquid state theories had well developed that a common approach to electrolyte and nonelectrolytes solutions became possible. The common basis is the molecular distribution functions. One of the statistical mechanical models of electrolyte solutions is charged hard spheres which represents an important advance in the study of concentrated electrolyte solutions (Loyd, 1988).

In 1923, Debye and Huckel (DH) introduced a model for electrolyte solutions where the ions are treated as point electric charges (i.e., charges have no excluded volume) obeying classical electrostatic principles. The charge density is given by an exponential distribution law (Boltzman distribution). It is successful in describing dilute solution properties. As such, the DH theory was considered a milestone in electrolyte theories. However for concentrated solutions, the point charge model is no longer valid. Large deviations in osmotic and mean activity coefficients are observed. Thus DH is not quantitative at high ionic strengths.

Modeling behavior at higher concentrations presents a great challenge for researchers. Countless investigators have wrestled with the problem of developing a

suitable model to extend Debye-Huckel theory to finite concentrations. In the intervening years, progress was made due to efforts by MacInnes, Harned, Scatchard in the 1930s and 40s and by Bjerrum (1949), Mayer (1950) and Guggenheim (1955) and others (Jefferson et al., 1997).

In the 1970s, an integral equation theory, the mean spherical model (MSA), was solved for charged hard spheres with finite size. This success represents another step forward in modeling ionic solutions, because it takes the sizes of the ions into account. The solution given by MSA reveals an intricate interplay between ion size and charge strength. Further developments along the liquid distribution function approach produced the Percus-Yevick (PY) and hypernetted chain (HNC) version for electrolyte solution. Meanwhile, Monte Carlo simulations were performed for the so-called primitive model of ionic solutions. These developments are instrumental for the development of a quantitative theory.

2.5.2 Models for Ionic Liquids

Belve et al. (2004) applied a conventional electrolyte model, the electrolyte nonrandom two-liquid (NRTL) model proposed by Chen et al. (1982) to model activity coefficients of quaternary ammonium salts in water. This model requires two parameters per salt that must be fit to the experimental data. Particular attention is paid to computing these binary parameters using a reliable parameter estimation technique, which is based on interval analysis. Indeed, this technique allows us to find deterministically the global minimum and, if desired, all local minima in the parameter estimation problem within a

given interval. Results indicate that this model is able to capture the nonideal phase behavior of these salts in aqueous solutions up to relatively high concentrations. Limitations of this simple model appear at higher concentrations and for highly branched compounds, most likely due to effects of incomplete dissociation and micelle formation that are not taken into account in the model.

Breure et al. (2005) proposed an equation of state approach is used for the modeling of the phase behavior of binary systems of ionic liquids and CO₂. The Group Contribution Equation of State (GC-EOS) developed by Skjold-Jorgensen is used to predict the phase behavior of binary systems consisting of CO₂ and ionic liquids of the homologous family 1-alkyl-3-methylimidazolium hexafluorophosphate. The agreements between experimental and predicted bubble point data for the ionic liquids [emim][PF₆], [bmim][PF₆] and [hmim][PF₆] are excellent for pressures up to 10 MPa and even for pressures up to about 100 MPa the agreements are good. These results show the capability of the GC-EOS model to describe the phase behavior of binary systems of ionic liquids and CO₂ and its potential for modeling supercritical processes involving ionic liquids.

2.5.3 Simulation of Ionic Liquids

Shah et al. (2002) reported results from the first molecular simulation study of 1-*n*-butyl-3-methylimidazolium hexafluorophosphate [bmim][PF₆], a widely studied ionic liquid. Monte Carlo simulations are carried out in the isothermal–isobaric (NPT) ensemble to calculate the molar volume, cohesive energy density, isothermal

compressibility, cubic expansion coefficient and liquid structure as a function of temperature and pressure. A united atom force field is developed using a combination of *ab initio* calculations and literature parameter values. Calculated molar volumes are within 5% of experimental values, and a reasonable agreement is obtained between calculated and experimental values of the isothermal compressibility and cubic expansion coefficient. PF6 anions are found to preferentially cluster in two favorable regions near the cation.

Cadena et al. (2005) presented the results of extensive molecular dynamics simulations of ionic liquids based on the pyridinium and triazolium cations. Classical force fields for both types of ionic liquids are developed and used to simulate both the crystalline and liquid phases. Computed liquid phase volumetric properties agree well with experiment, as do the crystal structures of the salts. Self-diffusivities of the liquid pyridinium-based materials were obtained through pulsed field gradient NMR measurements. Computed self-diffusivities were lower than experiment, possibly due to the neglect of polarization effects. It was also found that the liquids exhibit strong dynamic heterogeneity at room temperature; even though this is above the solidification temperature. This finding suggests that to properly compute the dynamics of these systems, extraordinarily long simulations are required.

CHAPTER 3

RESEARCH OBJECTIVES

According to Weissermel et al. (2003), no feasible processes are available for the extraction of aromatic and aliphatic hydrocarbons in the range below 20 wt% aromatics in the feed mixture. For example there is no viable process for separation of aromatics from the feed streams of naphtha crackers, which may contain up to 25 wt% aromatics. Preliminary calculation based on the information from UOP, showed that extraction with conventional solvents is not an option since additional separations are required to purify the raffinate, extract and solvent streams, which would induce high investment and energy cost. The cost of regeneration of sulfolane are high, since the sulfolane, which has a boiling point of 287.3°C, is in the current process taken overhead from the regenerator and returned to the bottom of the aromatic stripper as a vapor (David et al., 2003). The application of ionic liquids for extraction processes is promising because of their non-volatile nature (Domanska et al., 2003).

Brennecke et al. (2003) reported that until that date hardly any chemical engineer was involved in the design and development of ionic liquids for practical applications. Considering the low number of relevant publications on extractions and other separations, this is still true today. The goal of present thesis is to identify potential ILs for extraction of aromatics and their further development in this regard. Specific objectives include:

1. Computationally screen some ionic liquids for extraction of aromatics using COSMO-RS.
2. Investigate the synergy of binary mixture of ILs.
3. Propose an excess Gibbs energy model for solutions containing ionic liquids based on statistical thermodynamics in the NPT ensemble to use in design.

CHAPTER 4

COMPUTATIONAL SCREENING OF POTENTIAL SOLVENTS

4.1 COMPUTATIONAL SCREENING

Ionic liquids are salts composed of a cation and an anion. Their physical and chemical properties can be tailored by the proper selection of anion and cation. Therefore, it is possible to generate a huge number of different ionic liquids, each with specific properties. In fact, Earle et al. (2000) have estimated this number to be the order of 1 billion.

Despite much interest, accurate thermodynamic data of ionic liquids and their mixtures are still rare. To exploit the potential of these new substances, it would be of great value to have prediction methods that can reliably predict the thermodynamic properties of ionic liquids and their mixtures. This would help to scan the growing set of already known ILs in order to find suitable candidates for a certain task or to design new ILs for special applications.

4.2 SCREENING METHOD- THE COSMO-RS

At present, structure-interpolating group contribution methods (GCMs) are the most reliable and most widely accepted ways of predicting activity coefficients and other thermophysical data of compounds in liquid multicomponent mixtures without explicit use of experimental mixture data.

However, group contribution methods are not applicable to ILs because group parameters are not available at present. Moreover, the group contribution concept is not suitable to handle the long-range interactions in ionic compounds. Monte Carlo simulations and molecular dynamics need appropriate force-fields for the treatment of ionic liquids, which have to be developed. The development of force-fields together with simulation-derived thermodynamic properties of imidazolium IL solutions has been reported recently (Hurley et al., 1951).

COSMO-RS or ‘Conductor-like Screening Model for Real Solvents’ is another novel and efficient method for the prediction of thermophysical data of liquids. COSMO-RS does not make such extensive use of experimental data as do GCMs but yields a rigorous and physically meaningful description of the interactions of molecules in solution from quantum chemical calculations on the chemical compounds (Klamt et al., 1995). Recently, it was shown, by the thesis of Clausen (1999) that COSMO-RS is a valuable tool for the handling of chemical engineering problems regarding activity coefficients and other thermophysical data of compounds in the fluid phase.

Therefore, COSMORS is chosen in this work to calculate activity coefficients of heptane and toluene at infinite dilution in potential ionic liquids based solvents.

4.3 THEORY

COSMO-RS use a statistical thermodynamics approach based on the results of quantum chemical calculations. The underlying quantum chemical model, the so-called ‘Conductor-like Screening Model’ (COSMO), (Klamt et al., 1993) is an efficient variant

of dielectric continuum solvation methods. In these calculations, the solute molecules will be calculated in a virtual conductor environment. In such an environment, the solute molecule induces a polarization charge density, σ , on the interface between the molecule and the conductor, that is, on the molecular surface. These charges act back on the solute and generate a more polarized electron density than in a vacuum. During the quantum chemical self-consistency algorithm SCF, the solute molecule is thus converged to its energetically optimal state in a conductor with respect to electron density. The molecular geometry can be optimized using conventional methods for calculations in a vacuum. The quantum chemical calculation has to be performed once for each molecule of interest.

In the second step, the polarization charge density of the COSMO calculation, which is a good local descriptor of the molecular surface polarity, is used to extend the model toward the “Real Solvents” (COSMO-RS) (Klamt et al., 1998; Eckert et al., 2002). The 3D polarization density distribution on the surface of each molecule X is converted into a distribution function, the so-called σ -profile $P^{X_i}(\sigma)$, which gives the relative amount of surface with polarity σ on the surface of the molecule. The σ -profile for the entire solvent of interest S , which might be a mixture of several compounds, $P_S(\sigma)$, can be built by adding the $P^{X_i}(\sigma)$, values of the components weighted by their mole fractions X_i in the mixture.

$$P_S(\sigma) = \sum_{i \in S} X_i P^{X_i}(\sigma) \quad (4-1)$$

The most important molecular interaction energy modes, that is, electrostatics (E_{misfit}) and hydrogen bonding (E_{HB}), are described as functions of the polarization charges of two interacting surface segments σ and σ' or $\sigma_{acceptor}$ and σ_{donor} , if the segments are located on a hydrogen bond donor or acceptor atom. The less specific van der Waals (E_{vdw}) interactions are taken into account in a slightly more approximate way.

$$E_{misfit}(\sigma, \sigma') = a_{eff} \frac{\alpha'}{2} (\sigma + \sigma')^2 \quad (4-2)$$

$$E_{HB} = a_{eff} c_{HB} \min(0; \min(0; \sigma_{donor} + \sigma_{HB}) \max(0; \sigma_{acceptor} - \sigma_{HB})) \quad (4-3)$$

$$E_{vdw} = a_{eff} (\tau_{vdw} + \tau'_{vdw}) \quad (4-4)$$

Equations (4-2) to (4-4) contain five adjustable parameters such as an interaction parameter α' , the effective contact area a_{eff} , the hydrogen bond strength c_{HB} , the threshold for hydrogen bonding σ_{HB} , and the element-specific vdW interaction parameter τ_{vdw} . To take into account the temperature dependence of E_{HB} and E_{vdw} , temperature-dependent factors are applied, each with one adjustable parameter as defined in ref (Klamt et al., 2000). Thus, the molecular interactions in the solvent are fully described by $P_s(\sigma)$, and the chemical potential of the surface segments can be calculated by solving a coupled set of nonlinear equations.

$$\mu_s(\sigma) = -\frac{RT}{a_{eff}} \ln \left[\int P_s(\sigma') \exp\left(\frac{a_{eff}}{RT} (\mu_s(\sigma') - E_{misfit}(\sigma, \sigma') - E_{HB}(\sigma, \sigma'))\right) d\sigma' \right] \quad (4-5)$$

The distribution function $\mu_s(\sigma)$ is a measure for the affinity of the system S to a surface of polarity σ . The vdW energy, which does not appear in eq (4-5), is added to the reference energy in solution (energy of the COSMO calculation). The chemical potential of compound X_i in the system S (the solvent) can now be calculated by integration of $\mu_s(\sigma)$, over the surface of the compound.

$$\mu_s^{X_i} = \mu_{C,S}^{X_i} + \int P^{X_i}(\sigma)\mu_s(\sigma)d\sigma \quad (4-6)$$

To take into account size and shape differences of the molecules in the system, an additional combinatorial term, which depends on the area and volume of all the compounds in the mixture and three adjustable parameters $\mu_{C,S}^{X_i}$, is added. The combinatorial contribution $\mu_{C,S}^{X_i}$ to the chemical potential of compound i is

$$\mu_{C,S}^{X_i} = RT \left[\lambda_0 \ln r_i + \lambda_1 \left(1 - \frac{r_i}{\bar{r}} - \ln \bar{r} \right) + \lambda_2 \left(1 - \frac{q_i}{\bar{q}} - \ln \bar{q} \right) \right]$$

In the above equation, r_i is the molecular volume and q_i is the molecular area of compound i . The total volume and area of all compounds in the mixture are defined as:

$$\bar{r} = \sum_i x_i r_i$$

$$\bar{q} = \sum_i x_i q_i$$

The chemical potential of compound X_i can now be used to calculate a wide variety of thermodynamic properties, for example, the activity coefficient:

$$\gamma_S^{X_i} = \exp\left\{\frac{\mu_S^{X_i} - \mu_{X_i}^{X_i}}{RT}\right\} \quad (4-7)$$

where ,

$\mu_S^{X_i}$ =chemical potential of compound X_i in the solvent

$\mu_{X_i}^{X_i}$ =chemical potential of the pure component

4.4 COMPARISON OF COSMO CALCULATION WITH EXPERIMENTAL DATA

COSMO-RS is used for the calculation of activity coefficients at infinite dilution for 38 compounds in the ionic liquids 1-methyl-3-ethylimidazolium bis((trifluoromethyl)sulfonyl)imide, 1,2-dimethyl-3-ethylimidazolium is((trifluoromethyl)sulfonyl)imide, and 4-methyl-*N*-butylpyridinium tetrafluoroborate. Calculated values for (314 and 344) K are presented and compared with experimental data. It was found that COSMO-RS predicts the activity coefficients at infinite dilution in various ionic liquids with the same accuracy that is observed for normal organic solvents, without any adjustment of the theory or the use of specific parameters. Thus COSMO-RS and its implementation in the program *COSMOtherm* are capable of giving a priori predictions of the thermodynamics of ionic liquids, which may be of considerable value for the exploration of suitable ILs for practical applications (Diedenhofen et al., 2003).

Figure 4.1 shows calculated and experimental values of logarithmic infinite dilution activity coefficient for alkanes and alkyl benzenes in 4-methyl-N-butylpyridinium tetrafluoroborate. The calculated values for [bmpy] [BF₄] show some deviations from the experimental data for the examined ILs. This is mainly due to the underestimation of the activity coefficients of alkanes. Figures 4.2 and 4.3 shows that logarithmic infinite dilution activity coefficient for alkanes and alkyl benzenes in other ILs are close to experimental values. However in all the three ILs, the ranking of solutes in terms of the ascending order of the experimental or calculated values of logarithmic infinite dilution activity coefficients will be similar.

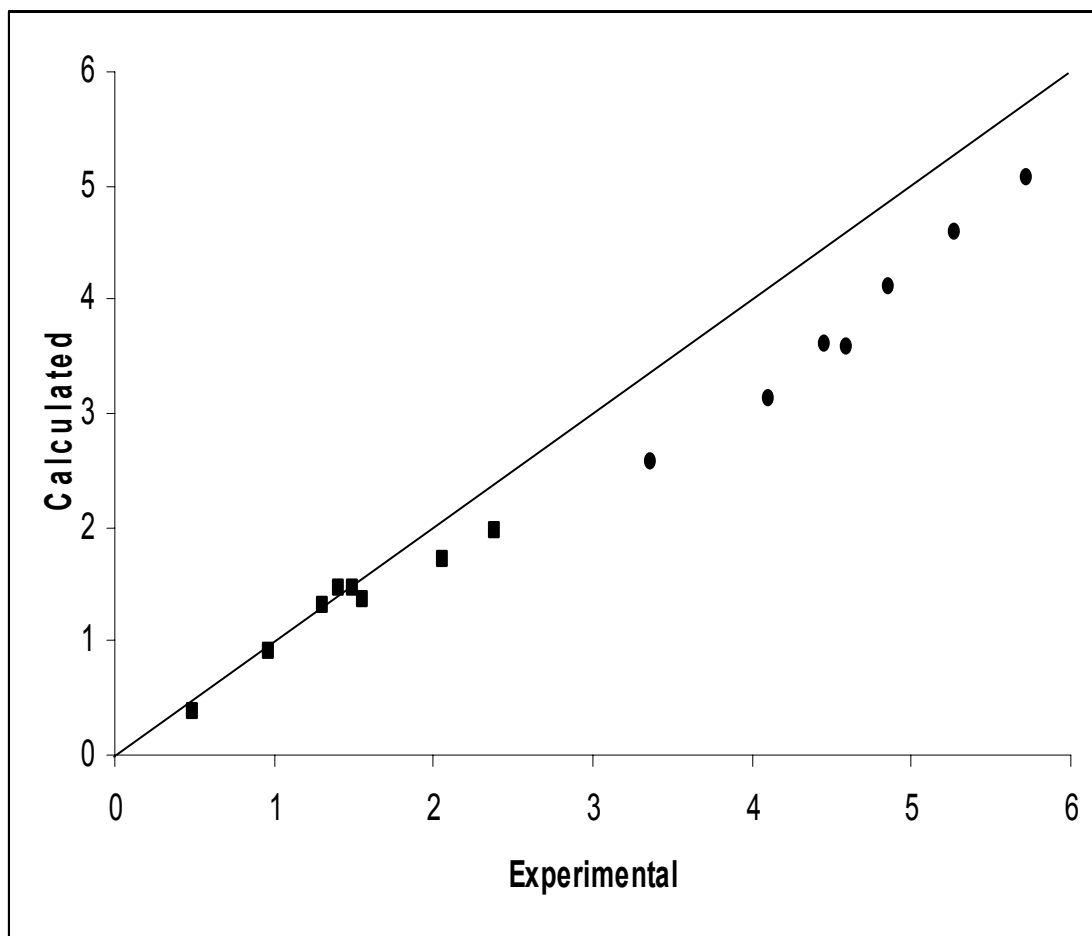


Figure 4.1: Calculated and Experimental values of logarithmic infinite dilution activity coefficient for alkanes (▪) and alkyl benzenes (•) in 4-methyl-N-butylpyridinium tetrafluoroborate

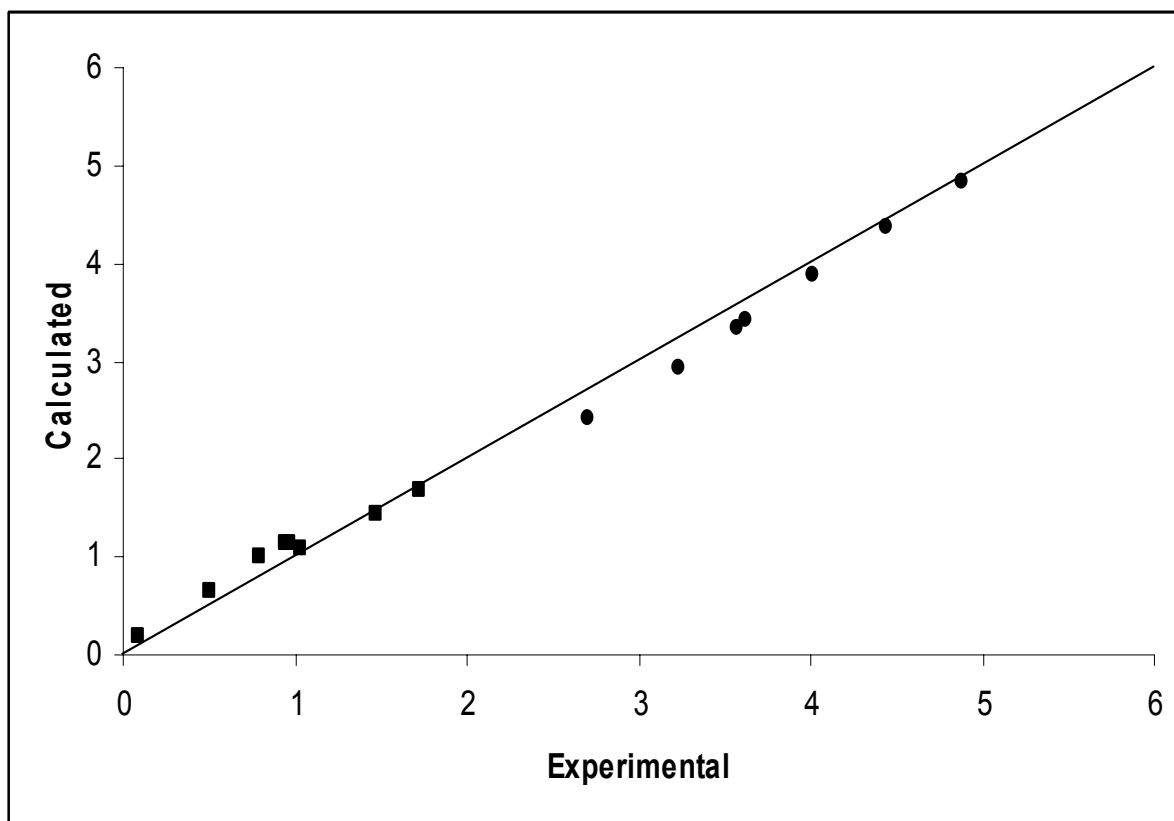


Figure 4.2: Calculated and Experimental values of logarithmic infinite dilution activity coefficient for alkanes (■) and alkylbenzenes (●) in 1, 2-dimethyl-3-ethylimidazolium bis(trifluoromethyl)sulfonyl-imide

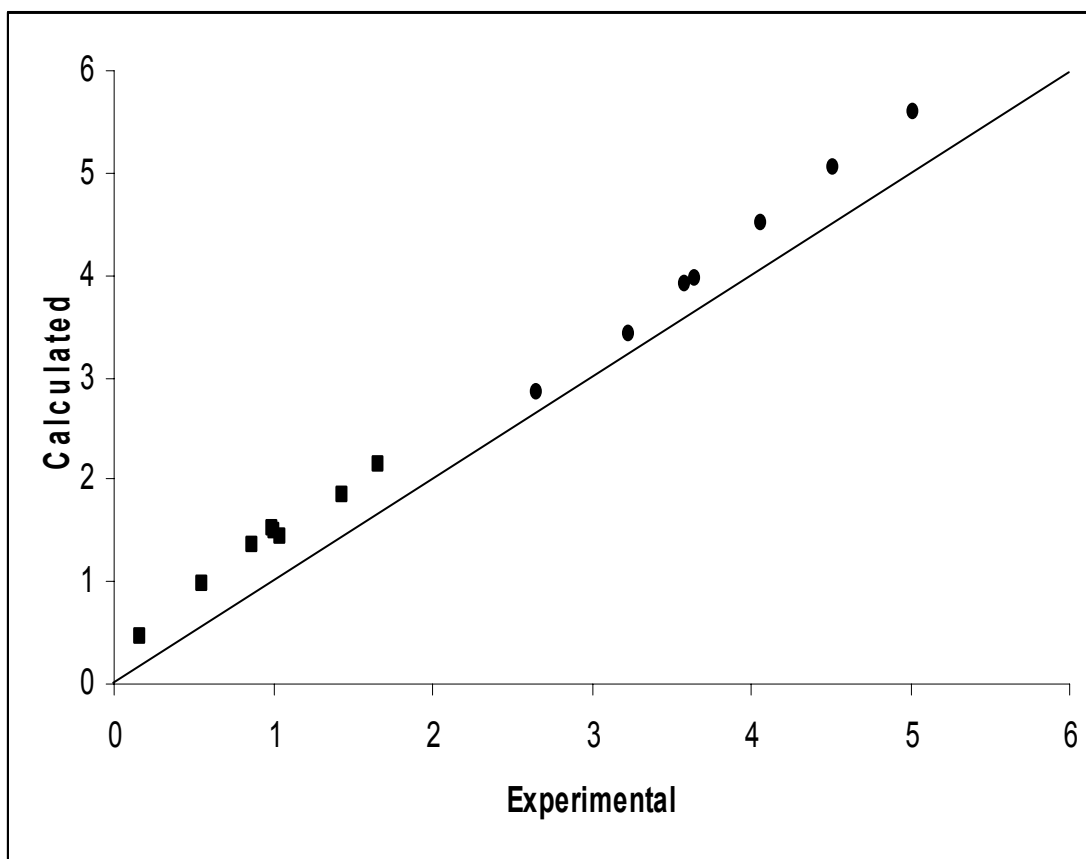


Figure 4.3: Calculated and Experimental values of logarithmic infinite dilution activity coefficient for alkanes (■) and alkylbenzenes (●) in 1-methyl-3-ethylimidazolium bis (trifluoromethyl) sulfonyl-imide

4.5 COMPUTATIONAL DETAILS

The COSMO calculations have been performed with the TURBOMOLE (Ahlich et al., 1989) program package on the density functional theory (DFT) level, utilizing the BP functional (Perdew et al., 1986) with a triple- ζ valence polarized basis set (TZVP) (Schafer et al., 1989). All COSMORS calculations are performed using the COSMOtherm program, which provides an efficient and flexible implementation of the COSMO-RS method. The latest parameterization BP_TZVP_C12_0402 is used. In such parameterization, the very few global parameters (~ 15) of the COSMO-RS method are optimized based on a set of about 1000 thermodynamic data, mostly partition coefficients and vapor pressures, in combination with DFT/COSMO calculations of a certain quantum chemical method. The temperature dependence of E_{HB} and E_{misfit} is fitted to pure compound vapor pressures and hence does not contain information about the special systems under consideration. It is important to mention that ionic compounds are not included in the optimization data set. The parameter set used in this study is a general one and is not fitted for ionic liquids.

The activity coefficients have been calculated using eq (4-7). The ILs have been described by an equimolar mixture of two distinct ions; that is, the cation and the anion contribute to $P_s(\sigma)$ as two different compounds. The mole fraction of IL solutions can be defined with respect to distinct ions or with respect to an ion pair (cation plus anion as one compound). Therefore, the COSMOtherm infinite dilution activity coefficient calculation is based on a ternary mixture: cation, anion and solute I with the boundary

condition that the molar amount of anion equals the molar amount of cation in the mixture.

$$x_i^{ternary} = \frac{n_i}{n_i + 2n_{ion}} \quad (4-8)$$

On the other hand, experimental determination of IL thermodynamic properties is based on the assumption of a binary system consisting of the IL and the solute.

$$x_i^{binary} = \frac{n_i}{n_i + 2n_{IL}} \quad (4-9)$$

These two definitions may lead to different values of activity coefficient if the mol fraction is used explicitly for the determination of experimental data. The activity coefficient that is defined as binary system experimentally but calculated as a ternary system in COSMOtherm is defined as :

$$x_i^{ternary} \gamma_i^{ternary} = \frac{x_i^{ternary}}{x_i^{ternary} + x_{ion}^{ternary}} \gamma_i^{binary} \quad (4-10)$$

Equation (4-10) leads to the conversion following conversion equation that translates the ternary (COSMOtherm calculated) activity coefficient to binary (experimentally measured) activity coefficient.

$$\gamma_i^{binary} = \gamma_i^{ternary} (x_i^{ternary} + x_{ion}^{ternary}) \quad (4-11)$$

For the calculation of activity coefficient in infinite dilution in an IL this reduces to:

$$\gamma_i^{binary} = \frac{1}{2} \gamma_i^{ternary}$$

The calculated values scaled with the factor 0.5 so that it can reflect experimental data and be compared with experimental data that takes the view of the system as a binary mixture. The capacity and selectivity at infinite dilution is then calculated as

$$C^\infty = \gamma_t^{org,\infty} / \gamma_t^{IL,\infty} \approx 1 / \gamma_t^{IL,\infty} \quad (4-12)$$

$$S^\infty \approx \gamma_h^{IL,\infty} / \gamma_t^{IL,\infty} \quad (4-13)$$

$\gamma_t^{IL,\infty}$ and $\gamma_h^{IL,\infty}$ are activity coefficient of toluene and heptane in IL respectively at infinite dilution.

4.6 THE IL DATABASE AND NOMENCLATURE OF ILS

Total 58 cations and 26 anions were chosen which are listed in Appendix-B. Most of the cations are based on imidazolium, pyridinium, pyrrolidinium, phosphonium, ammonium, uranium and guanidium salts. Alkyl chain length varies from simple methyl group to octadecyl in some cases. Structure and short names of some of the anions are also given.

4.7 COMPUTATIONAL RESULTS AND DISCUSSION

4.7.1 General Presentation of S & C of the ILs and Comparison with Sulfolane

Two most important criteria of a desired solvent is its capacity and selectivity. A higher selectivity means less extraction stages and a higher capacity requires a lower solvent to feed ratio. The selectivity and capacity values at infinite dilution for toluene and heptane in 1508 different ionic liquids and in sulfolane at 40°C are listed in Appendix-A.

Figure 4.4 shows the position of all the pure ionic liquids in selectivity (S) vs. capacity (C) profile. We observe that a high selectivity is accompanied with a lower capacity and vice versa. Even this large pool of solvents does not contain a single solvent with appreciable high capacity and selectivity at the same time. Figure 4.5 shows the same thing but in a reduced scale of both axes.

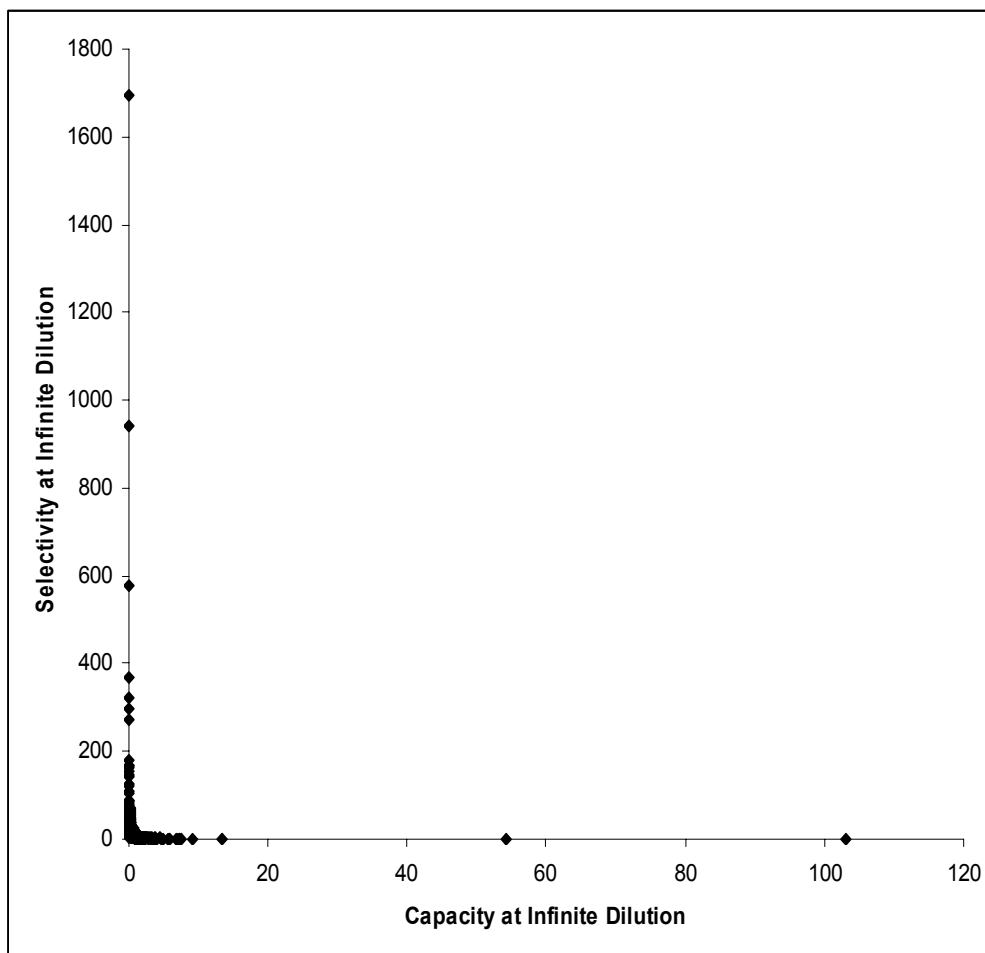


Figure 4.4: Selectivity and Capacity of all the solvents investigated

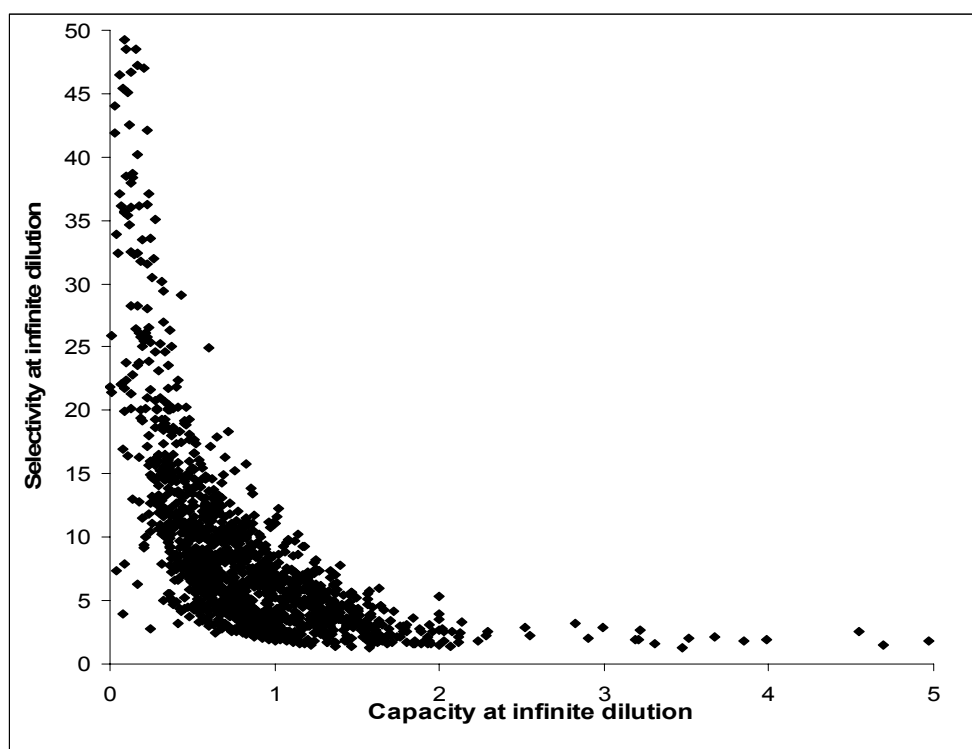


Figure 4.5: Selectivity and Capacity of solvents investigated in a smaller scale

Sulfolane is extensively used for the extraction of aromatics. For the extraction of toluene from heptane, sulfolane has the values, $S^\infty=6.61$ and $C^\infty=0.414$. The S-C plane is divided into four quadrants based on the position of Sulfolane, the benchmark solvent in Figure 4.6. The upper right portion is shown in Fig-4.6 which contains 32% of all the solvents (478 out of 1507). Figure 4.7 includes only those solvents which have both S^∞ and C^∞ values higher than Sulfolane. Mathematically, they satisfy the criteria,

$$C_{IL}^\infty \geq C_{sulfolane}^\infty \text{ and } S_{IL}^\infty \geq S_{sulfolane}^\infty$$

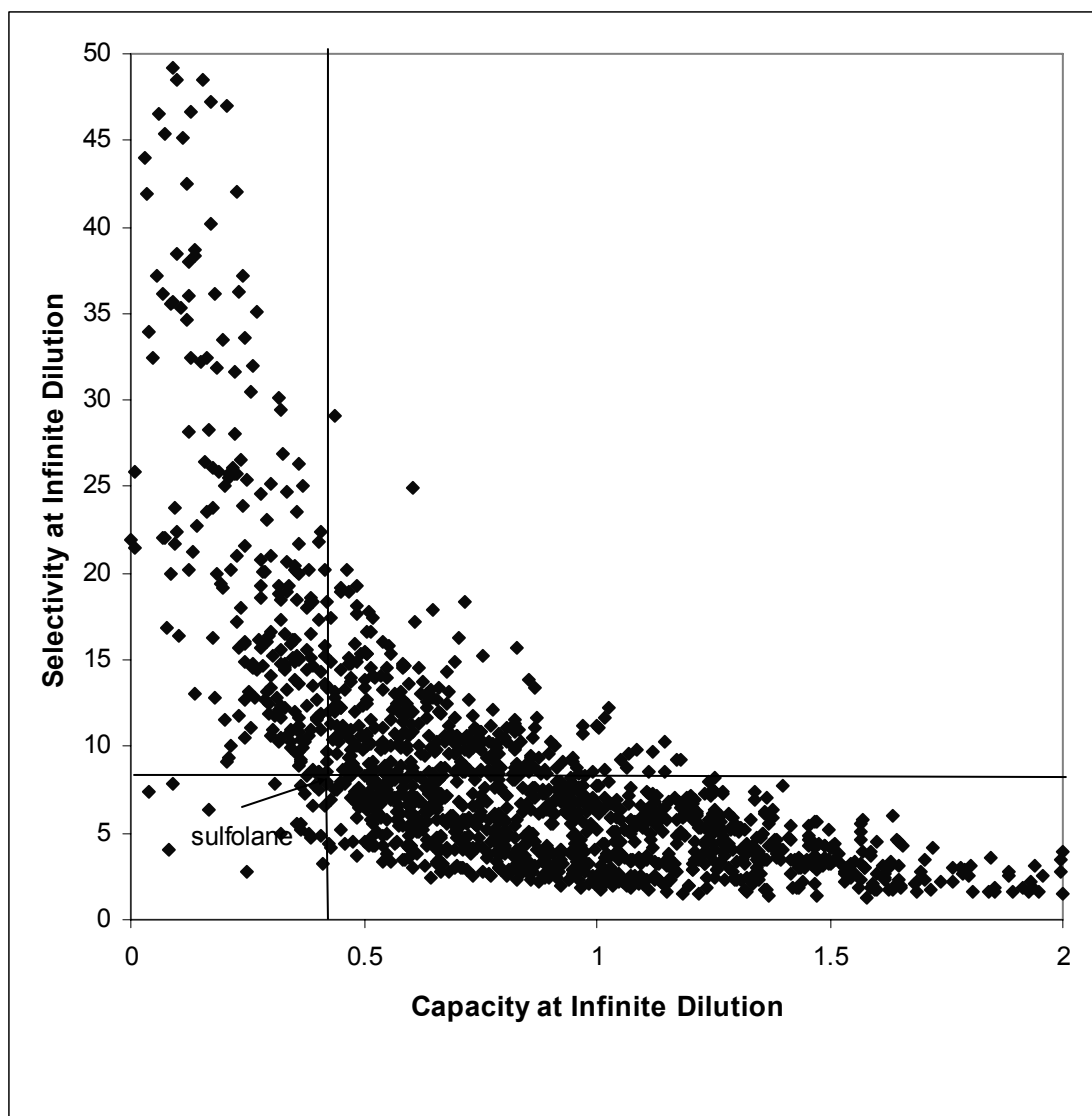


Figure 4.6: The selectivity-capacity plane is divided into four quadrant based on sulfolane, the benchmark solvent

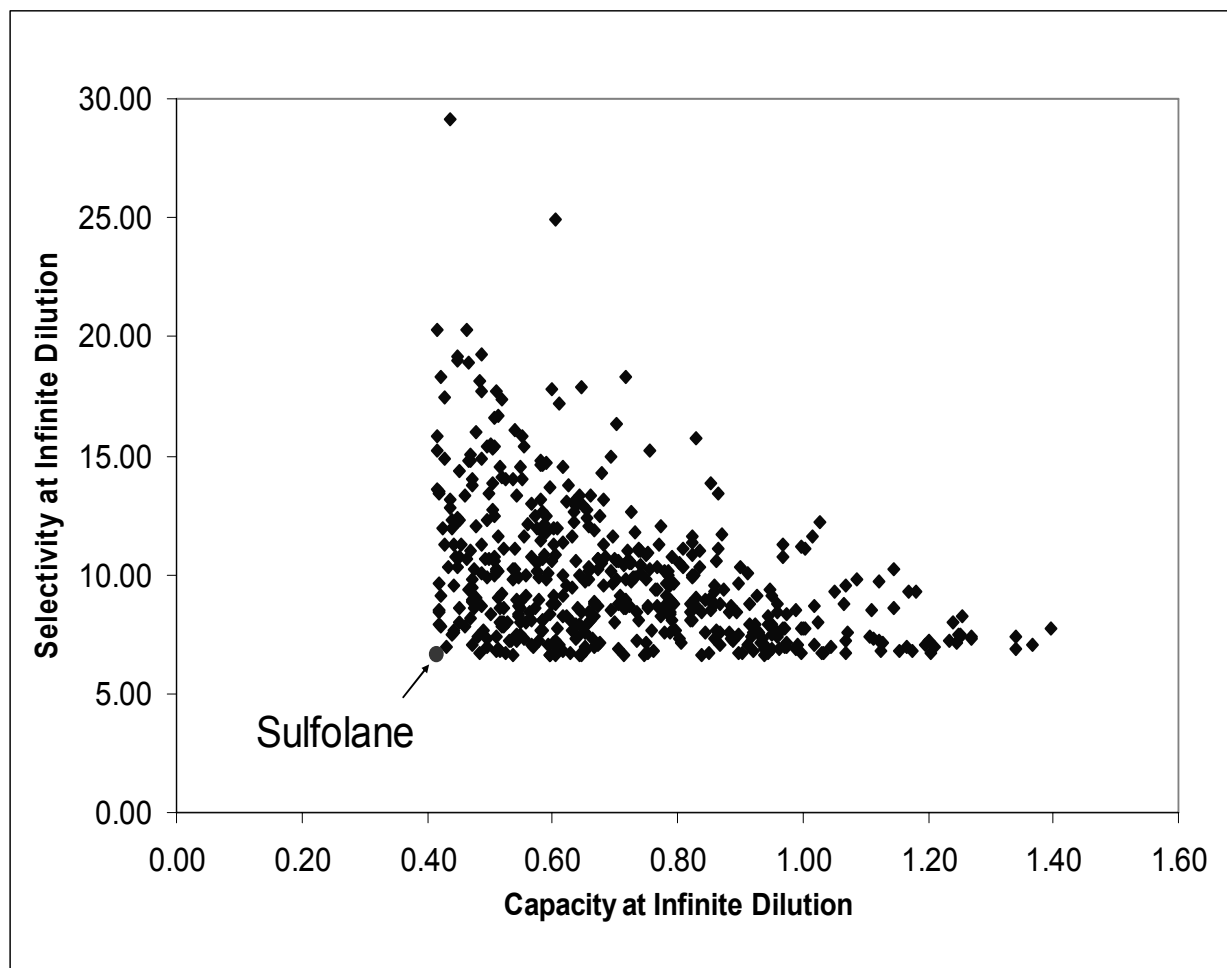


Figure 4.7: ILs with higher capacity and selectivity than sulfolane

4.7.2 Selectivity (S) & Capacity(C) of Different Cation Based ILs and Effect of Alkyl Chain Length of Cation on S & C

4.7.2.1 Imidazolium Based ILs

Imidazolium based ionic liquids are most popular of all and it has attracted most of the attention among other ionic liquids. In our IL-database there are 27 imidazolium based cations and 26 different anions. As a result, there is a total of 702 ILs. Capacity and Selectivity at infinite dilution of all of them are tabulated in appendix. Among them, five representative cations are taken with increasing alkyl chain on the cation to discuss the results. These are butyl imidazolium [bi], butyl-methyl-imidazolium [bmi], hexyl-methyl imidazolium [hmi], octyl-methyl-imidazolium [omi], hexadecyl methyl imidazolium [(hex)mi]. Each of them form 26 ILs by virtually mixing with all the anions one by one.

The capacities at infinite dilution of these ILs are shown in figure 4.8 as capacity at infinite dilution versus the randomly chosen anions and sulfolane. It is observed that for a given anion, the capacity *increases* as the alkyl chain length *increases*. On the other hand, selectivities at infinite dilution of these ILs are shown in figure 4.9 as selectivity at infinite dilution versus the randomly chosen anions. It is further observed that for a given anion, the selectivity *decreases* as the alkyl chain length increases. This is true for all the anions except little discrepancy in case of chloride anion. The capacity and selectivity of sulfolane is also shown in figure 4.8 and 4.9 as comparison. It is observed that there are many imidazolium based ILs who has higher capacity or higher selectivity than the benchmark solvent sulfolane.

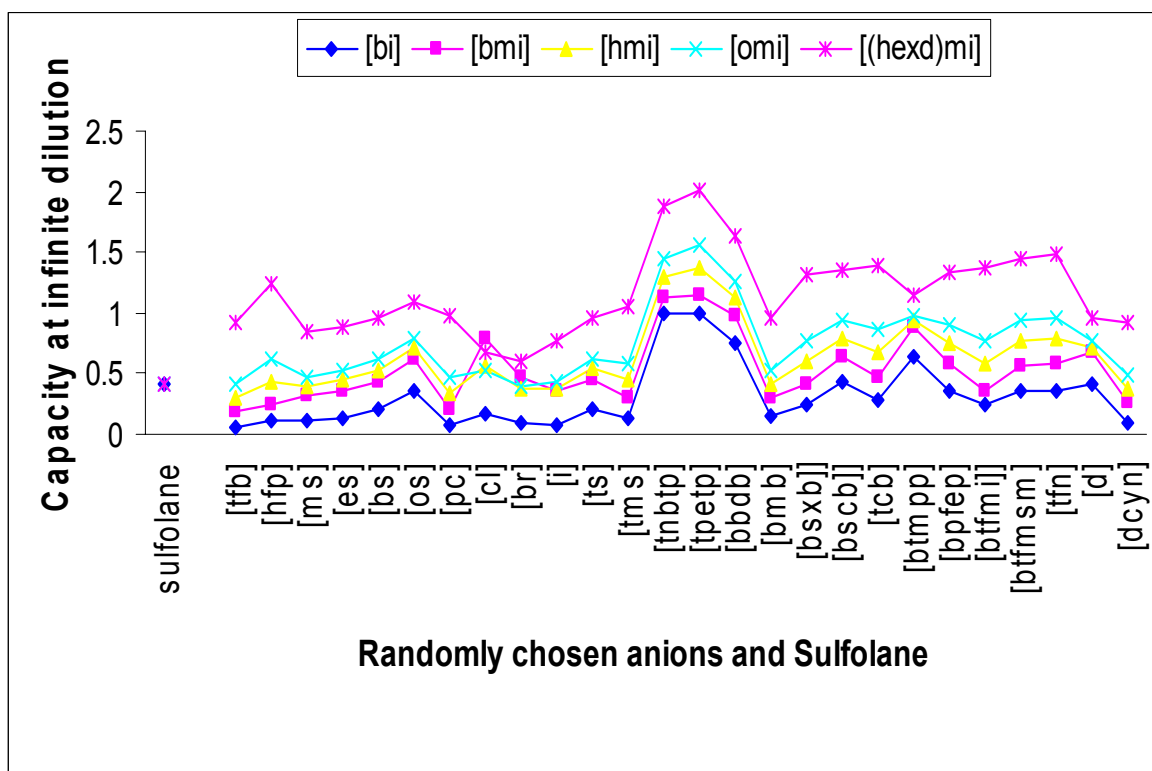


Figure 4.8: Capacity at infinite dilution of ILs consisting of imidazolium based cations with increasing alkyl chain length and 26 different anions

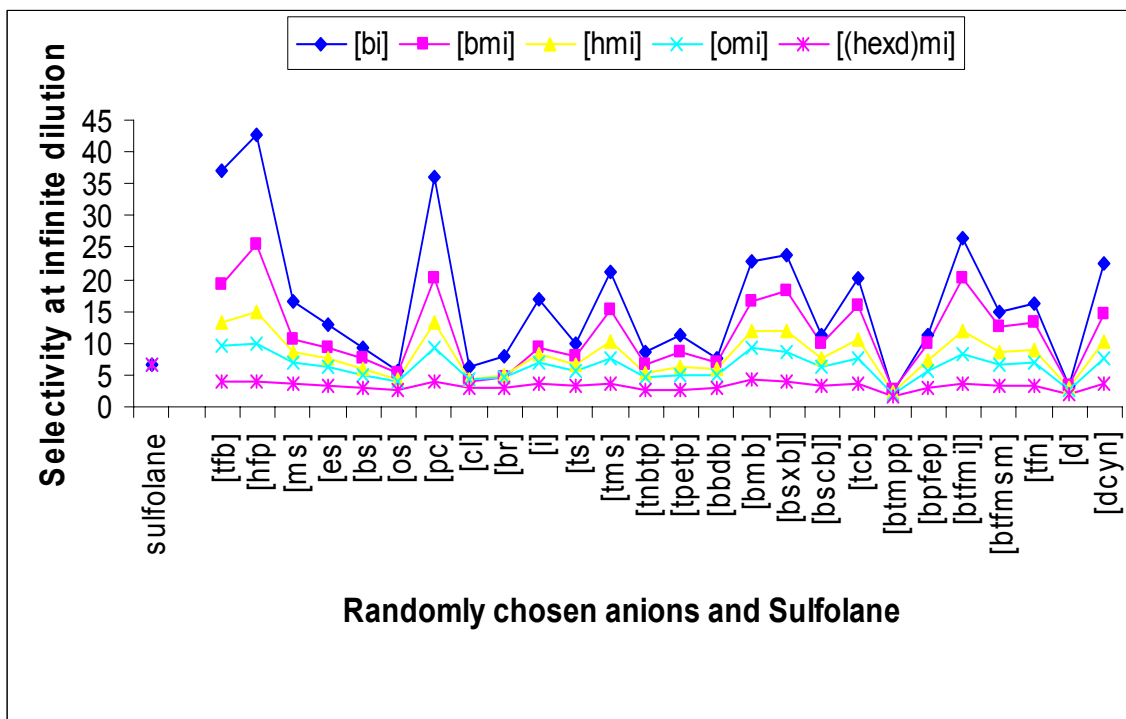


Figure 4.9: Selectivity at infinite dilution of ILs consisting of imidazolium based cations with increasing alkyl chain length and 26 different anions

Figure 4.8 indicates that anions can be ranked in terms of ascending capacity or selectivity. Anions have been rearranged in figure 4.10 in an ascending order of capacity . It is observed that the same ranking is true of imidazolium based ionic liquids even when there is a difference between the alkyl chain lengths of the cation. The ranking in ascending order is [tfb] <[pc] <[i] <[br] <[dcyn] < [ms] <[tms] <[es] <[bmb] <[cl] <[bs] <[ts] < [btfmi] < [bsxb] < [tcb] < [btfmsm] < [tfn] < [bpfep] < [os] < [d] < [bscb] < [btmpp] < [bbdb] < [tnbtp] < [tpetp].

The broken horizontal line represents the capacity of sulfolane at infinite dilution. Imidazolium based ILs with shorter chain on the cation display less capacity than sulfolane with most of the anions. When paired with only a few anions like [bscb], [btmpp], [bbdb], [tnbtp], [tpetp], and these short alkyl chain containing cations display higher capacity than sulfolane. In case of cations having longer alkyl chain give higher capacity than sulfolane when they are paired with most of the anions. Another observation is that, the higher the alkyl chain length, the less is the tendency to follow the above ranking by cations. In fact, if the length is higher than octyl alkyl, the above ranking is not true.

On the other hand, Figure 4.9 indicates that anions can be ranked in terms of ascending selectivity also. Anions have been rearranged in figure 4.11 in an ascending order of selectivity. It is observed that the same ranking is true of imidazolium based ionic liquids even when there is a big difference between the alkyl chain lengths of the corresponding cations. The ranking in ascending order is as follows:

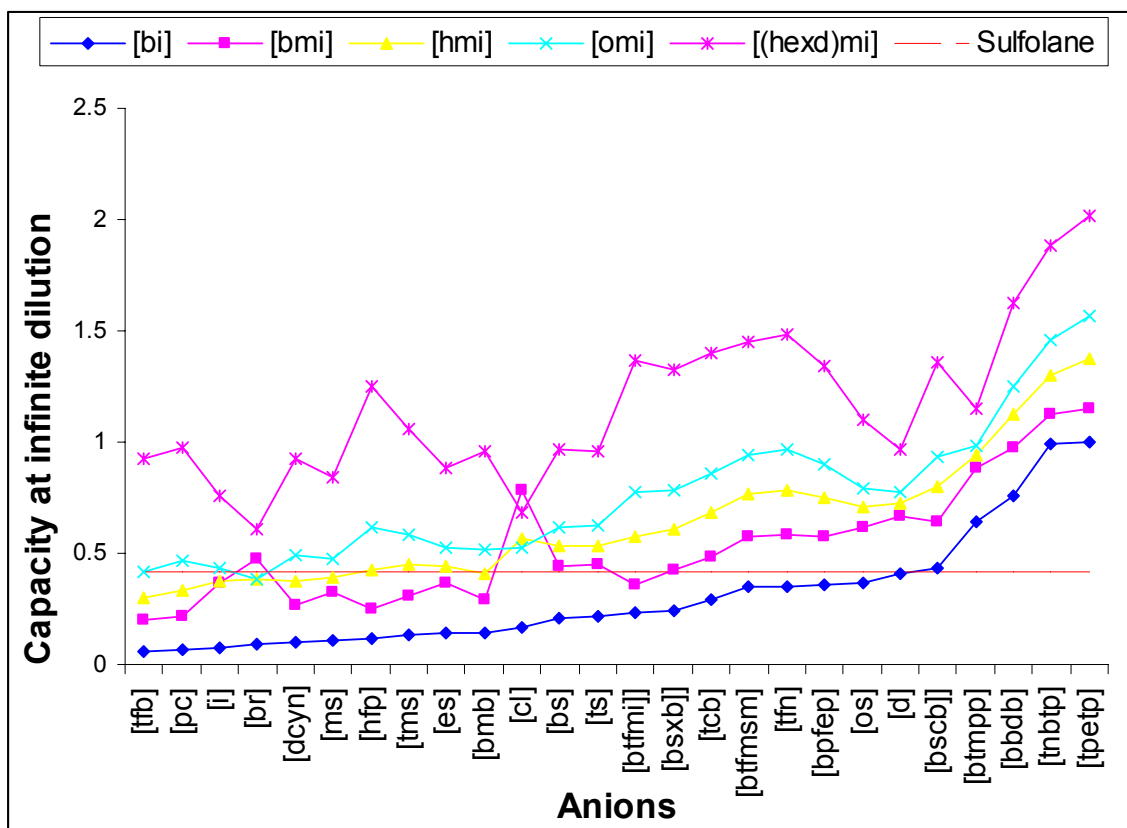


Figure 4.10: Capacity at infinite dilution of imidazolium ILs consisting of cations with increasing alkyl chain length (ordered)

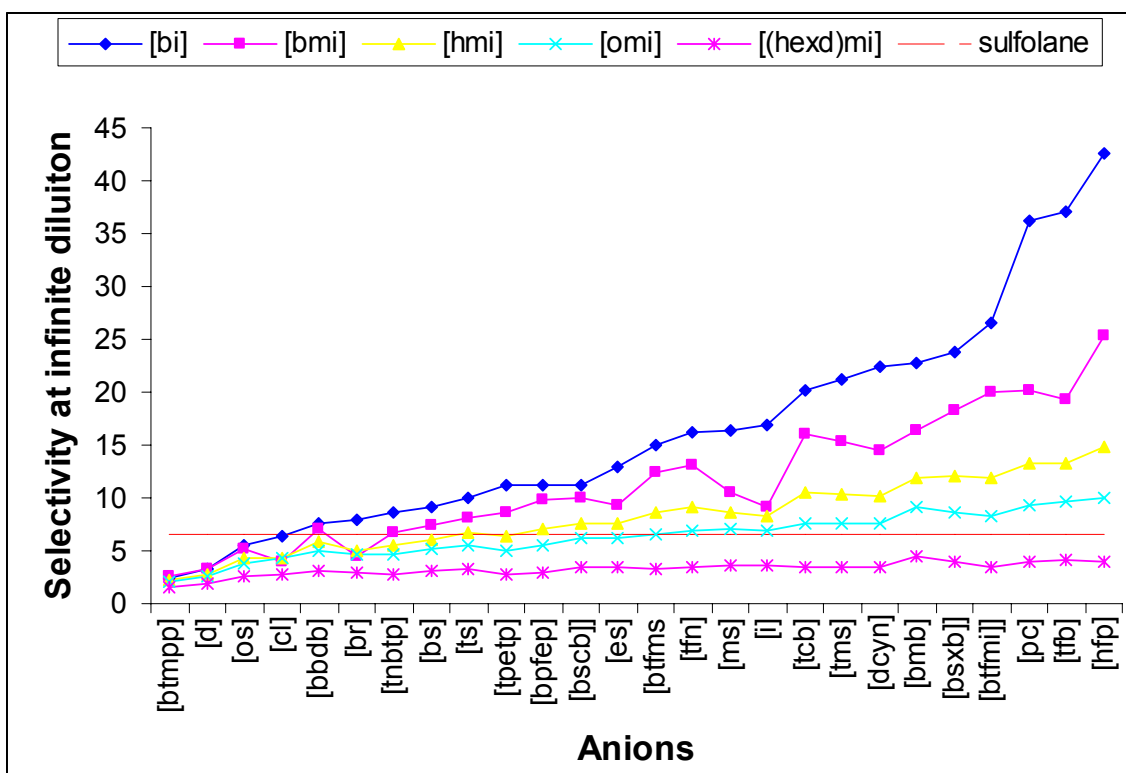


Figure 4.11: Selectivity at infinite dilution of imidazodinium based ILs consisting of cations with increasing alkyl chain length (ordered)

[btmpp]<[d]<[os]< [cl]< [bbdb]< [br]< [tnbtp]< [bs]< [ts]< [tpetp]< [bpfep]< [bscb]< [es]<[btfms]< [tfn]< [ms]< [i]<[tcb] <[tms]< [dcyn]<[bmb]< [bsxb]< [btfmi]< [pc]< [tfb]< [hfp]. This same ranking is observed even for very long alkyl chain.

4.7.2.2 Pyridinium Based ILs

Figure 4.12 shows capacity at infinite dilution for ILs based on pyridinium cations versus the anions chosen randomly. It is observed that for a given anion, the capacity *increases* as the alkyl chain length increases. On the other hand, selectivities at infinite dilution of these ILs are shown in figure 4.13 as selectivity at infinite dilution versus anions chosen randomly. It is further observed that for a given anion, the selectivity *decreases* as the alkyl chain length *increases*. This is true for all the anions except little discrepancy in case of halide anions. The capacity and selectivity of sulfolane is also shown in figure 4.12 and 4.13 for comparison. It is observed that there are many pyridinium based ILs who have higher capacity and higher selectivity than those of the benchmark solvent sulfolane.

Figure 4.12 shows that anions can be ranked in terms of ascending capacity or selectivity. Anions have been rearranged in figure 4.14 in an ascending order of capacity. It is observed that the same ranking is true of imidazolium based ionic liquids even when there is a difference between the alkyl chain lengths of the cation. The ranking in ascending order is as follows:

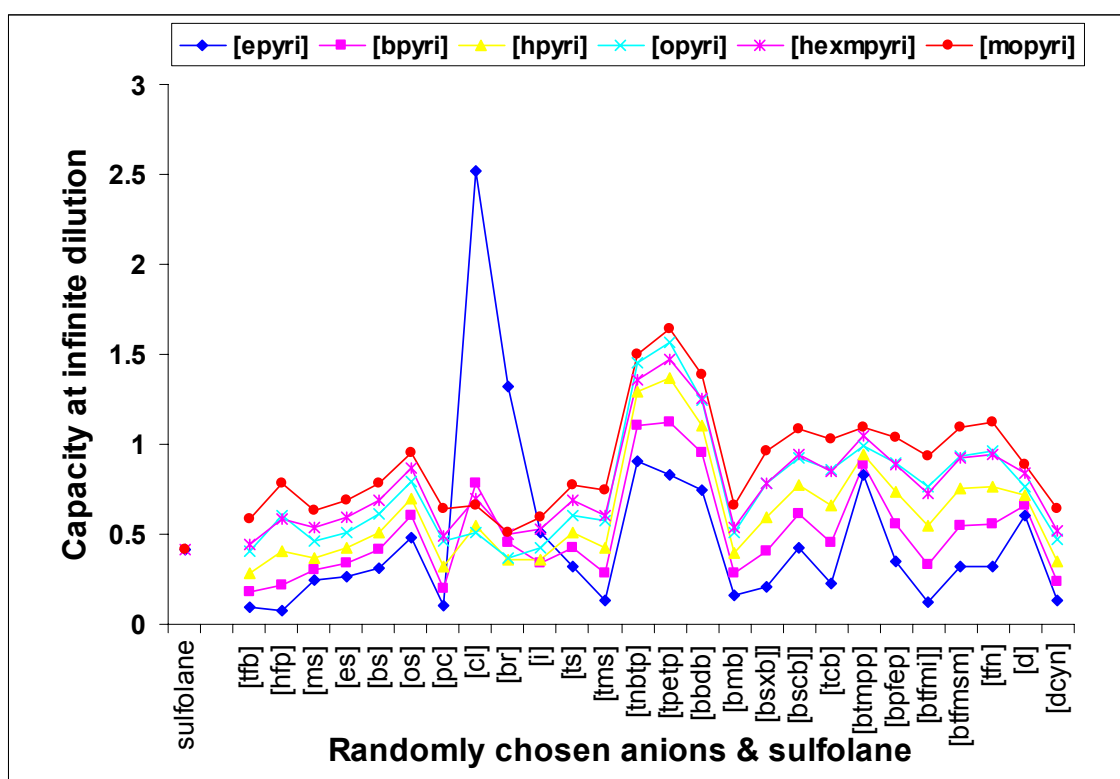


Figure 4.12: Capacity at infinite dilution of pyridinium ILs consisting of cations with increasing alkyl chain length

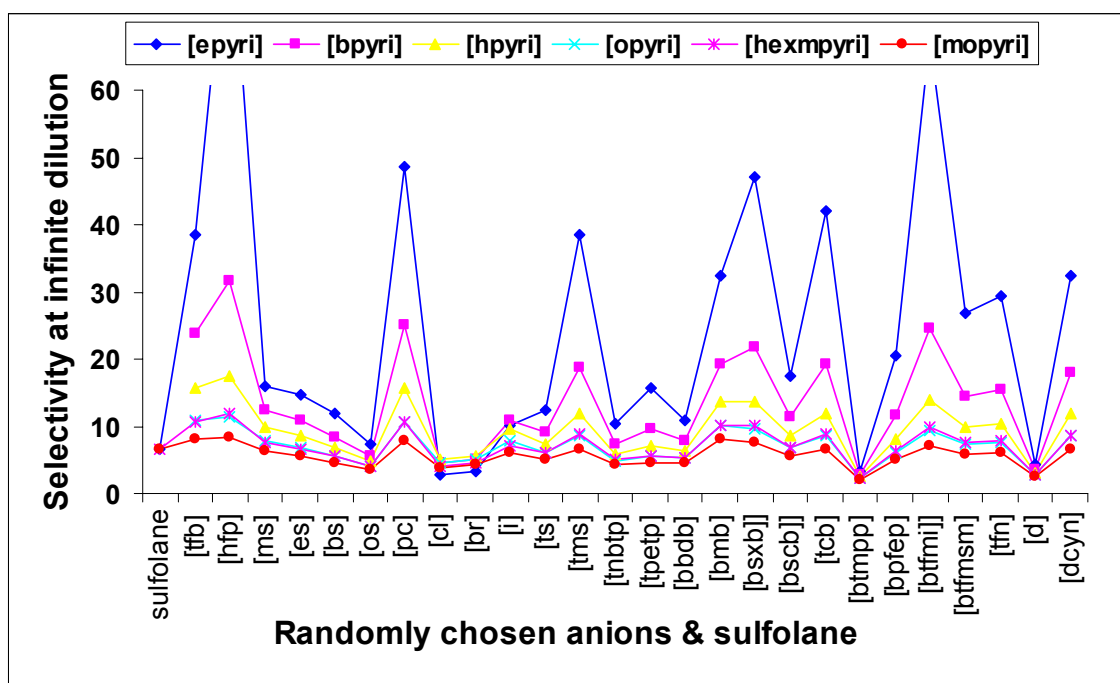


Figure 4.13: Selectivity at infinite dilution of pyridinium ILs consisting of cations with increasing alkyl chain length

[hfp] < [tfb] < [pc] < [btfmi] < [dcyn] < [tms] < [bmb] < [bsxb] < [tcb] < [ms] < [es] < [bs] < [ts] < [tfn] < [btfms] < [bpfep] < [bscb] < [os] < [i] < [d] < [bbdb] < [btmpp] < [tpetp] < [tnbtp] < [br] < [cl]. The broken horizontal line represents the capacity of sulfolane at infinite dilution. Imidazolium based ILs with shorter chain lengths display less capacity than sulfolane with most of the anions. But paired with only a few anions like [d], [bbdb], [bscb], [btmpp], [bbdb], [tnbtp], [tpetp], these short alkyl chain containing cations display higher capacity than sulfolane. In case of cations having longer alkyl chain give higher capacity than sulfolane when paired with most of the anions. Another observation is that, the higher the alkyl chain length, the less is the tendency to follow the above ranking by cations. In fact, if the length is higher than octyl alkyl, the above ranking does not hold true.

On the other hand, Figure 4.13 indicates that anions can be ranked in terms of ascending selectivity also. Anions have been rearranged in figure 4.15 in an ascending order of capacity. It is observed that the same ranking is true of pyridinium based ionic liquids even when there is a big difference between the alkyl chain lengths of the corresponding cations. The ranking in ascending order is as follows: [cl] < [btmpp] < [br] < [d] < [os] < [i] < [tnbtp] < [bbdb] < [bs] < [ts] < [es] < [tpetp] < [ms] < [bscb] < [bpfep] < [btfms] < [tfn] < [bmb] < [dcyn] < [tms] < [tfb] < [tcb] < [bsxb] < [pc] < [btfmi] < [hfp]. This ranking is observed even for very long alkyl chain.

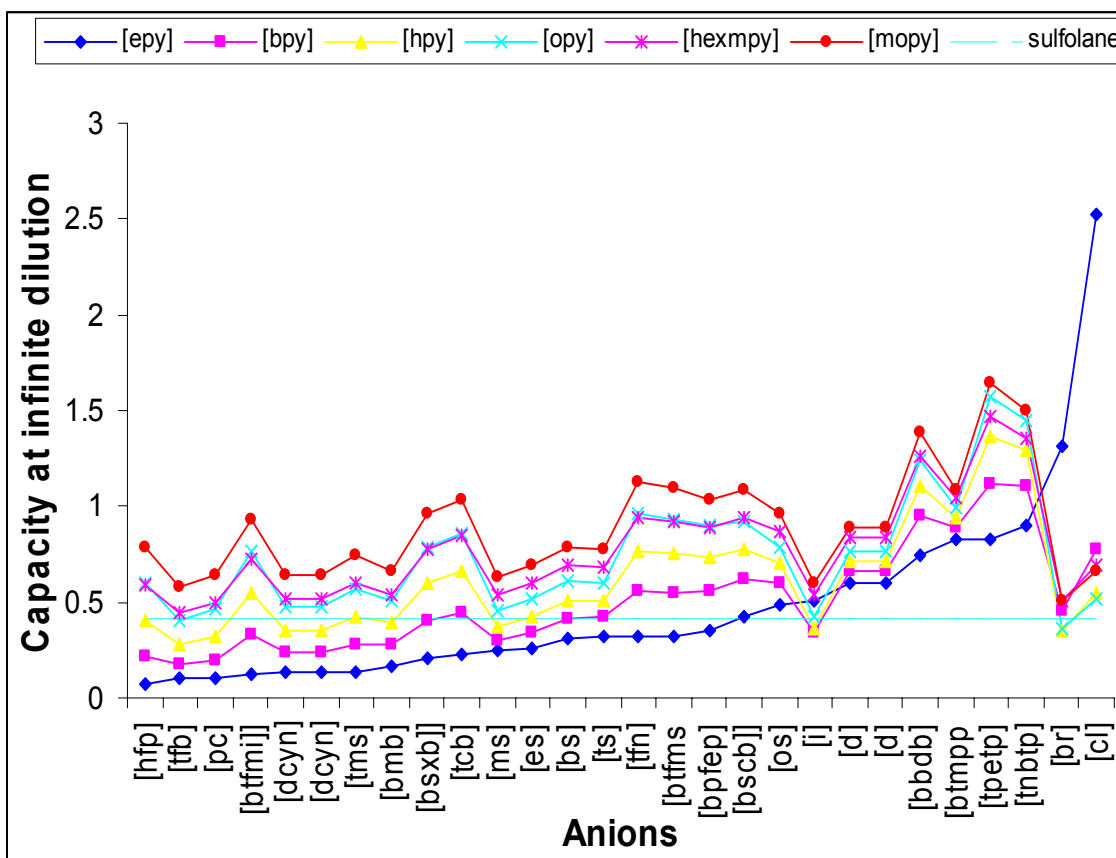


Figure 4.14: Capacity at infinite dilution of pyridinium ILs consisting of cations with increasing alkyl chain length (ordered)

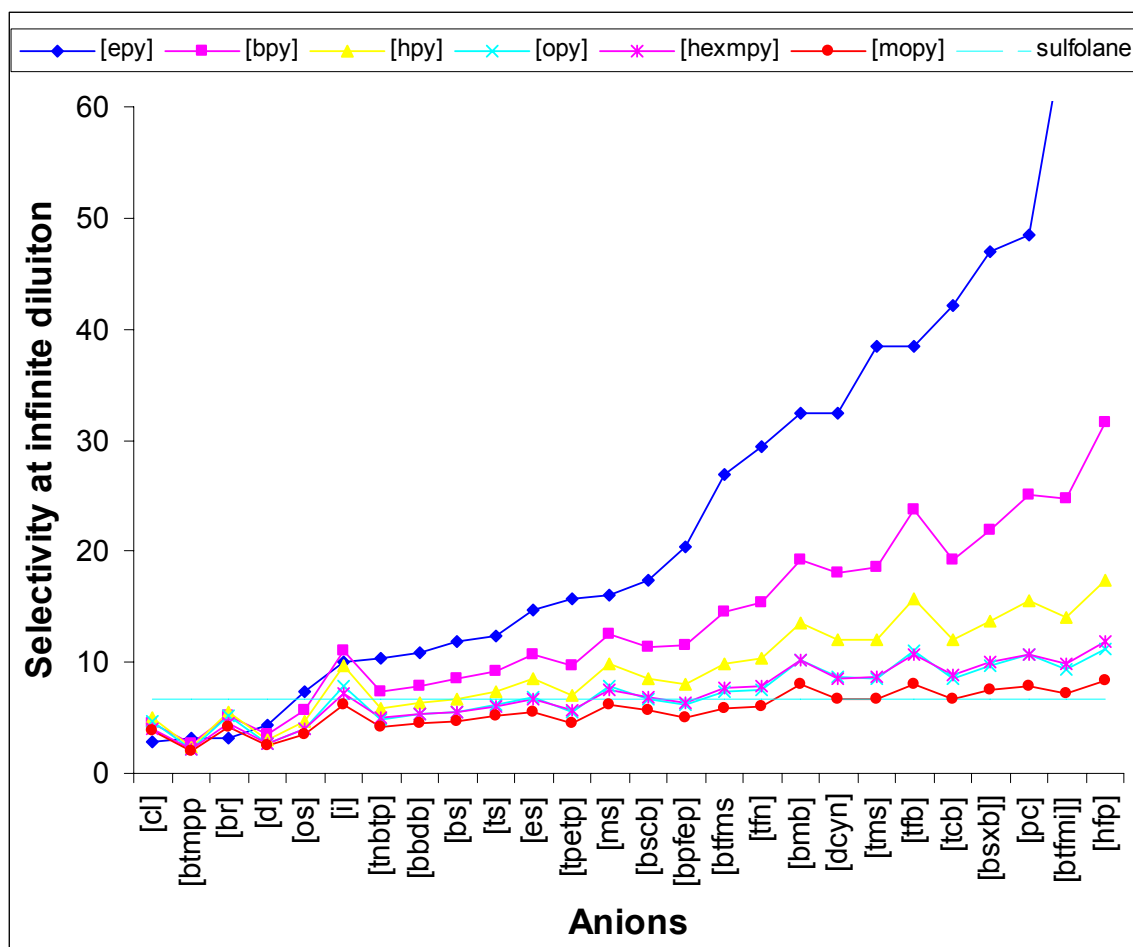


Figure 4.15: Selectivity at infinite dilution of pyridinium ILs consisting of cations with increasing alkyl chain length (ordered)

4.7.2.3 Pyrrolidinium Based ILs

Figure 4.16 shows capacity at infinite dilution for ILs based on pyrrolidinium cations versus the anions. It is observed that for a given anion, the capacity *increases* as the alkyl chain length increases. On the other hand, selectivities at infinite dilution of these ILs are shown in figure 4.17 as selectivity at infinite dilution versus anions. It is further observed that for a given anion, the selectivity *decreases* as the alkyl chain length increases. This is true for all the anions except little discrepancy in case of halide anions. The capacity and selectivity of sulfolane is also shown by broken horizontal line in figure 4.16 and 4.17 for comparison. It is observed that there are many pyridinium based ILs who have higher capacity or higher selectivity than the benchmark solvent sulfolane. Here any general pattern of the ranks of anions is not observed. The ranking of anions is *dependent* on the chain of associated alkyl chain length. Generally, the capacity of pyrrolidinium based IL is generally lower than pyridinium based IL but higher than imidazolium based IL for a fixed anion. For example, with tetrafluoroborate anion, 1-butyl-1-methyl-pyrrolidinium ([bmpy]), 4-methyl-N-butyl pyridinium ([bmpy]) and 1-butyl-3-methyl imidazolium ([bmi]) cations have capacities 0.31, 0.33 and 0.197 and selectivities 10, 15 and 19 respectively.

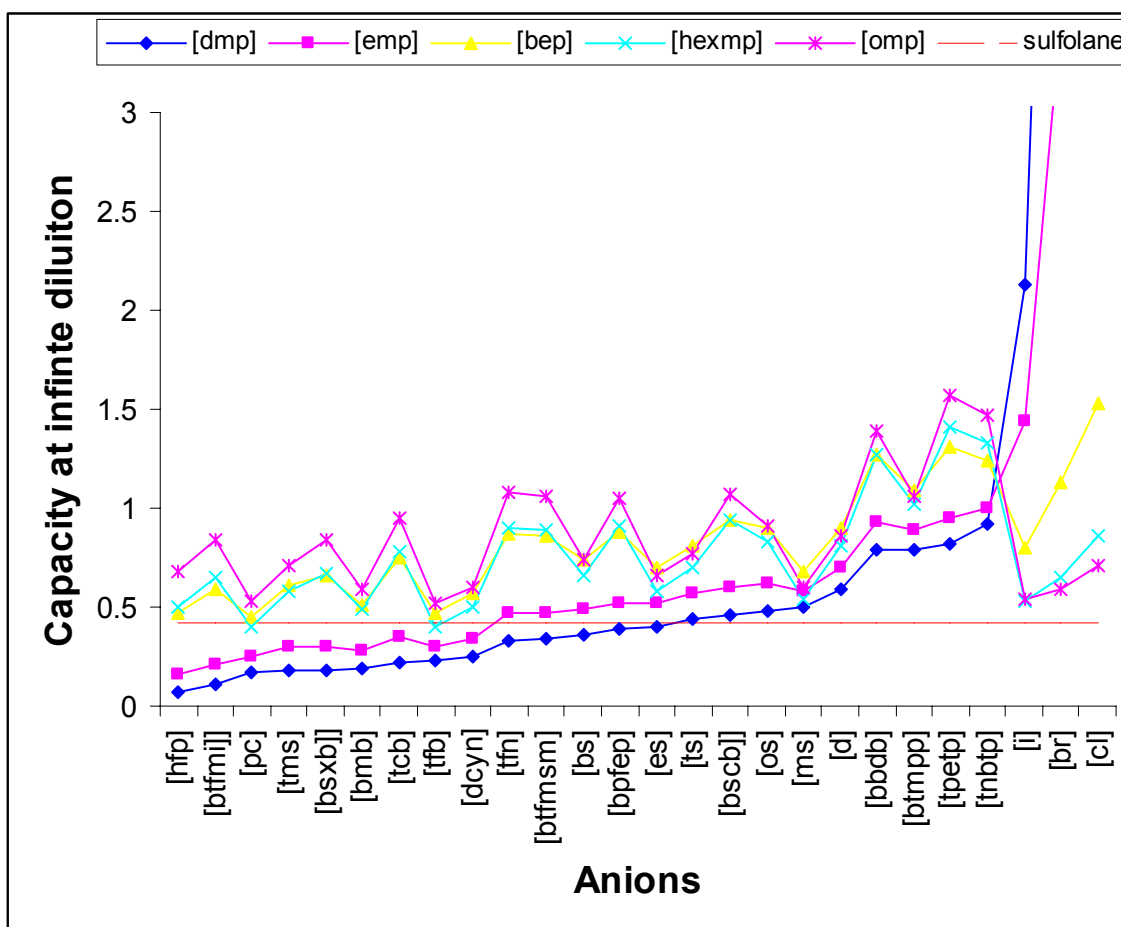


Figure 4.16: Capacity at infinite dilution of pyrrolidinium ILs consisting of cations with increasing alkyl chain length

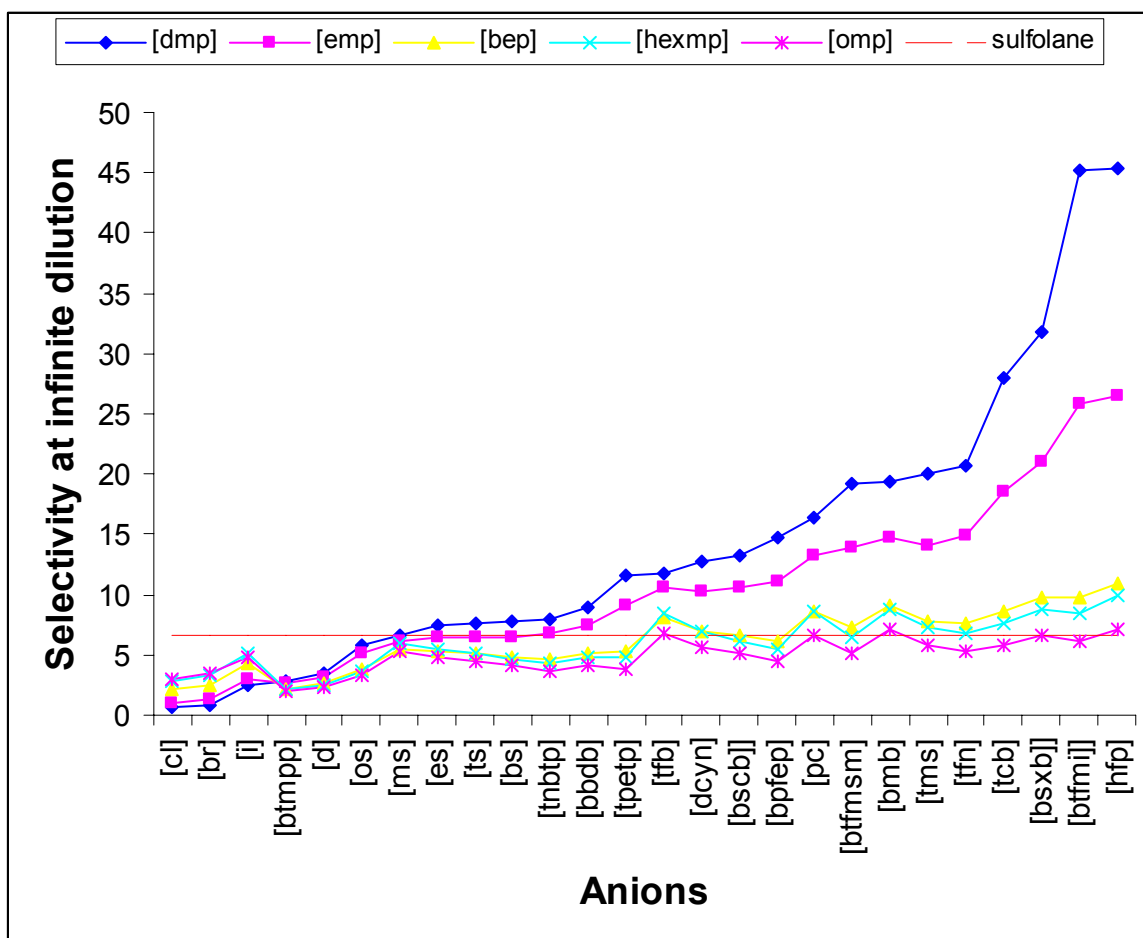


Figure 4.17: Selectivity at infinite dilution of pyrrolidinium ILs consisting of cations with increasing alkyl chain length

4.7.2.4 Other Cation Based ILs

Capacity and selectivity at infinite dilution of phosphonium based ILs is shown in figures 4.18 and 4.19. All the phosphonium based ILs has capacity higher than sulfolane but have selectivity lower than sulfolane. The ranking of anion is more or less representative of general phosphonium based IL even though the cation has many alkyl substitute or long chain with the phosphonium atom. The ranking of anions in ascending order with respect to capacity is [tfb]< [i]< [br]< [dcyn]< [bmb]< [pc]< [ms]< [tms]< [cl]< [es]< [hfp]< [ts]< [btfmi]< [bs]< [bsxb]< [tcb]< [bpfep]< [btfms]< [tfn]< [bscb]< [d]< [os]< [tnbtp]< [btmp]< [bbdb]< [tpetp]. The ranking of anions in ascending order with respect to selectivity is [btmpp]< [d]< [os]< [tnbtp]< [bbdb]< [tpetp]< [cl]< [br]< [bs]< [ts]< [bpfep]< [bscb]< [es]< [btfms]< [tfn]< [ms]< [i]< [tcb]< [tms]< [dcyn]< [btfmi]< [bsxb]< [bmb]< [pc]< [tfb]< [hfp]. Capacity and selectivity at infinite dilution of phosphonium based ILs are shown in figure 4.20 and 4.21. Ammonium based ILs also show high capacity but very low selectivity. Many of the ammonium based ILs have capacity higher than sulfolane but have selectivity lower than sulfolane. The ranking of anion is not a generalized one but specific to cations. Capacity of selectivity of other cation based ILs such as guanidium, uranium and quinilinium are shown in figures 4.22 and 4.23. Most of them have capacity higher than that of sulfolane but selectivity lower than that of sulfolane.

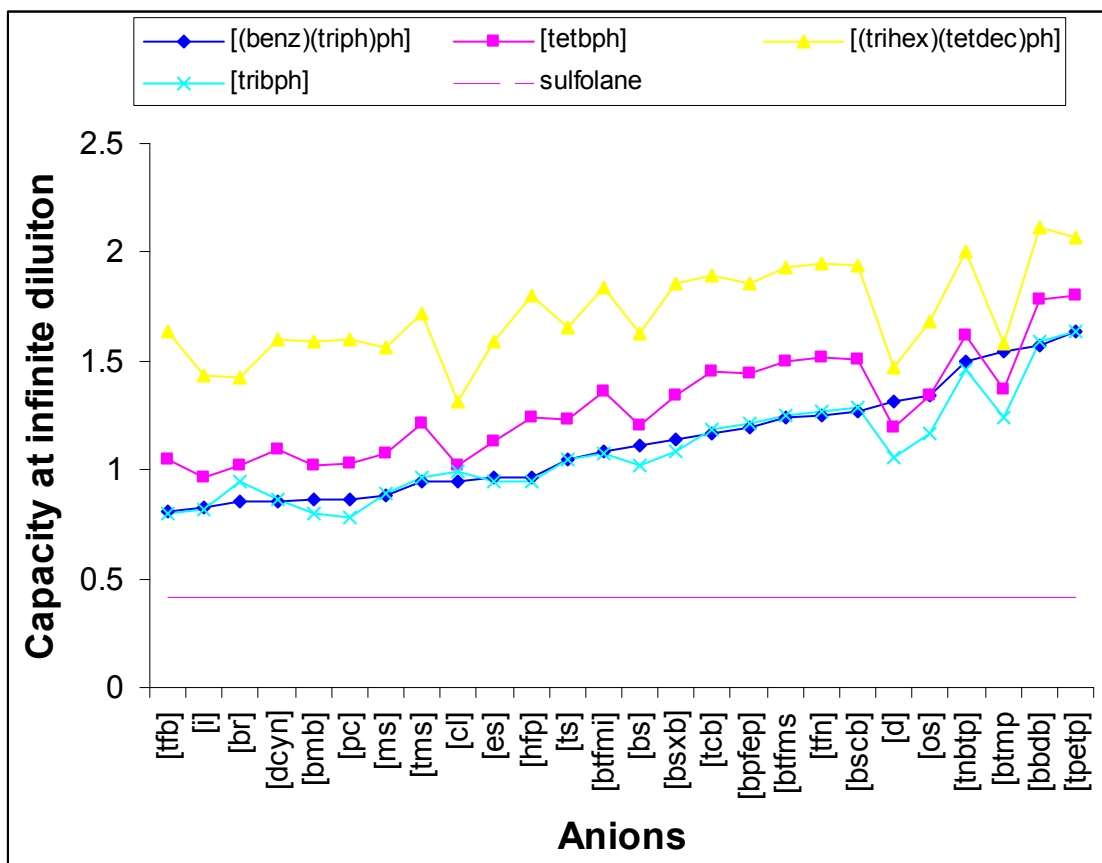


Figure 4.18: Capacity at infinite dilution of phosphonium ILs consisting of cations with increasing alkyl chain length

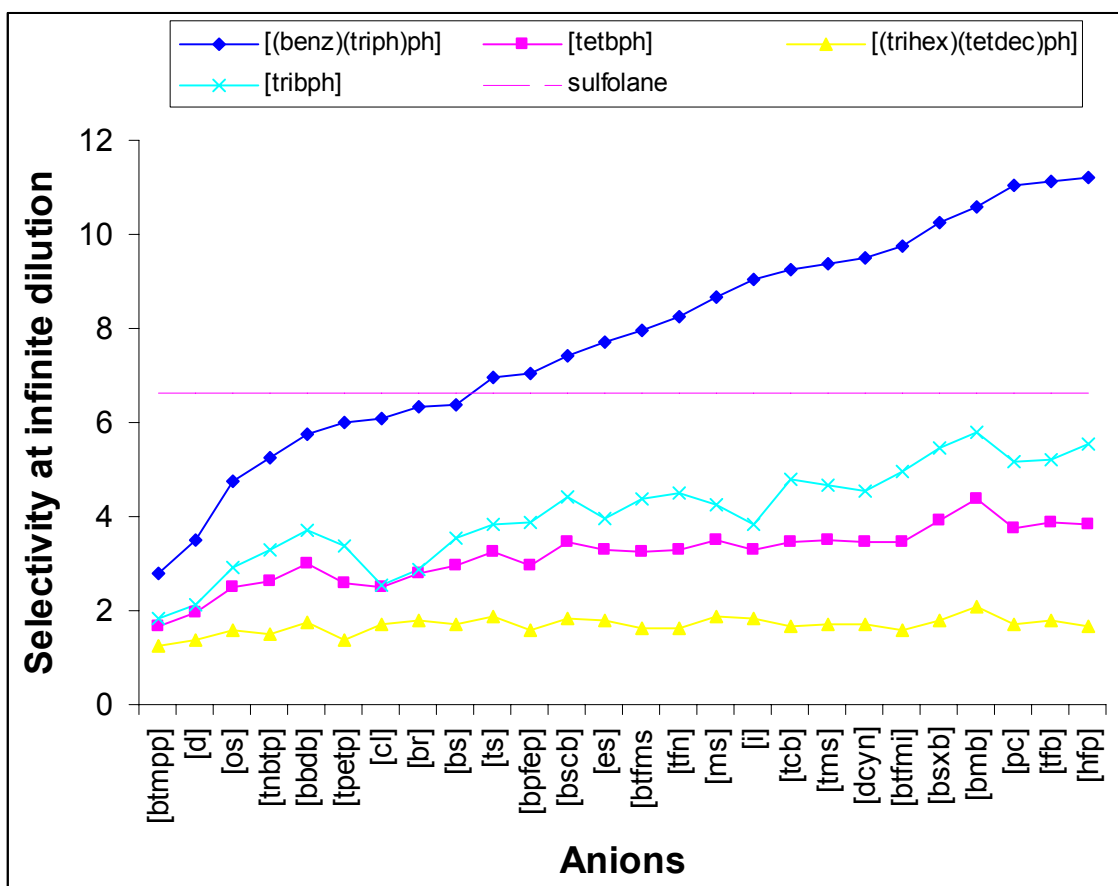


Figure 4.19: Selectivity at infinite dilution of phosphonium ILs consisting of cations with increasing alkyl chain length

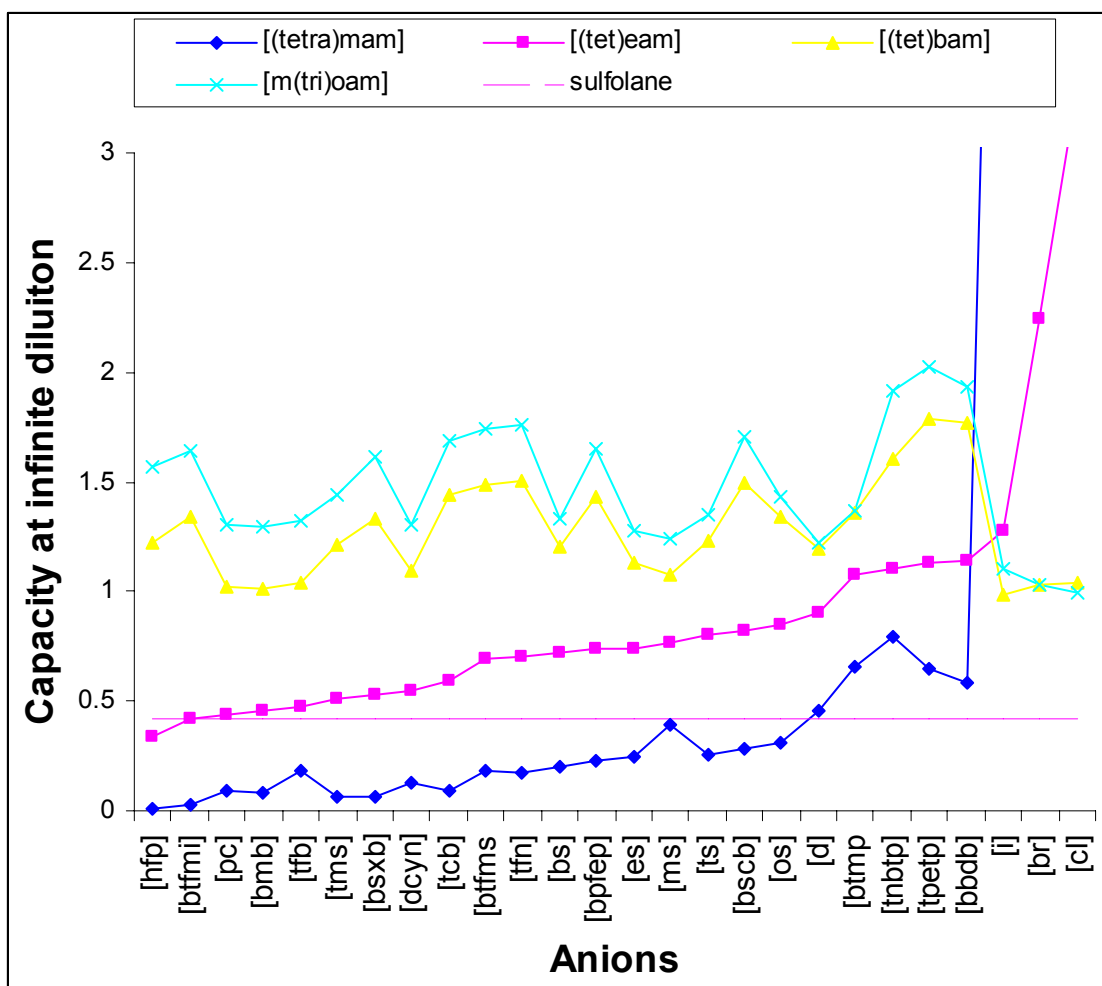


Figure 4.20: Capacity at infinite dilution of ammonium ILs consisting of cations with increasing alkyl chain length

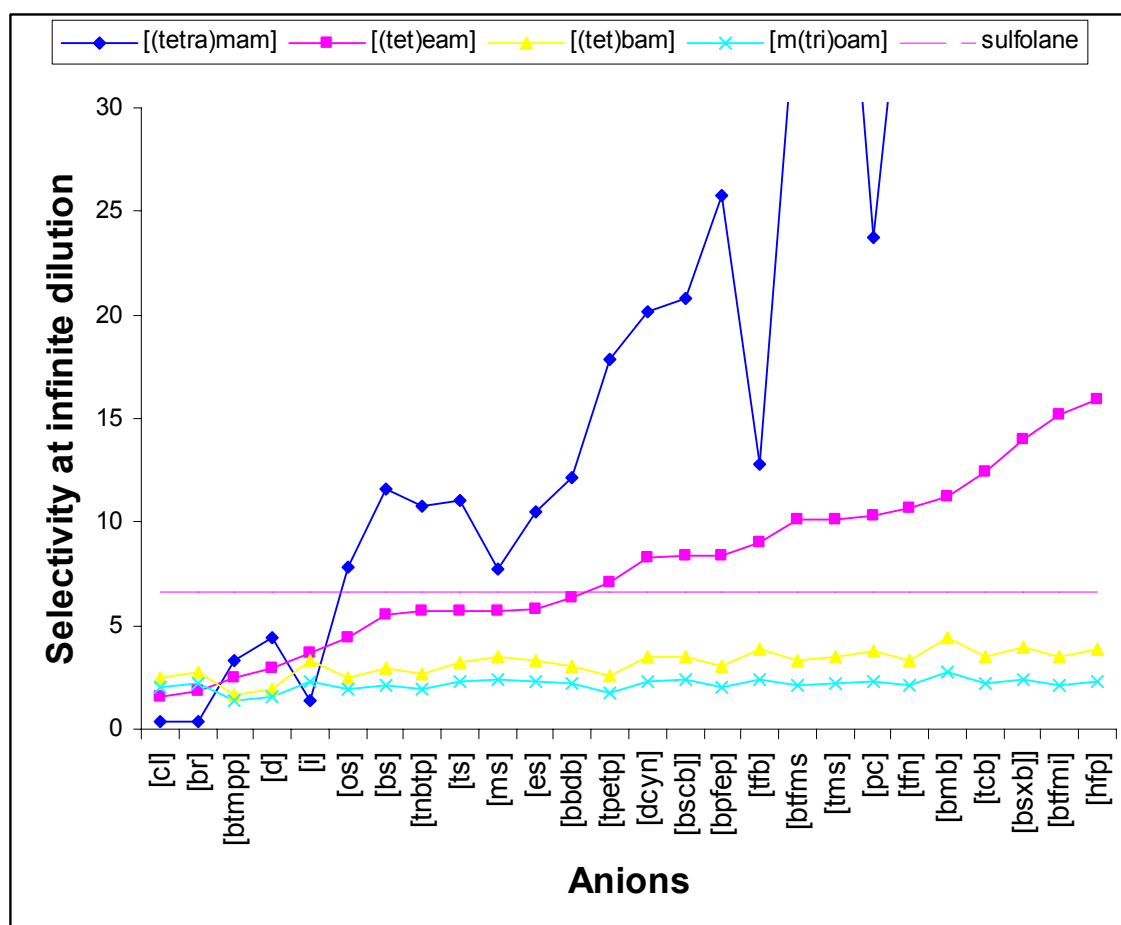


Figure 4.21: Selectivity at infinite dilution of ammonium ILs consisting of cations with increasing alkyl chain length

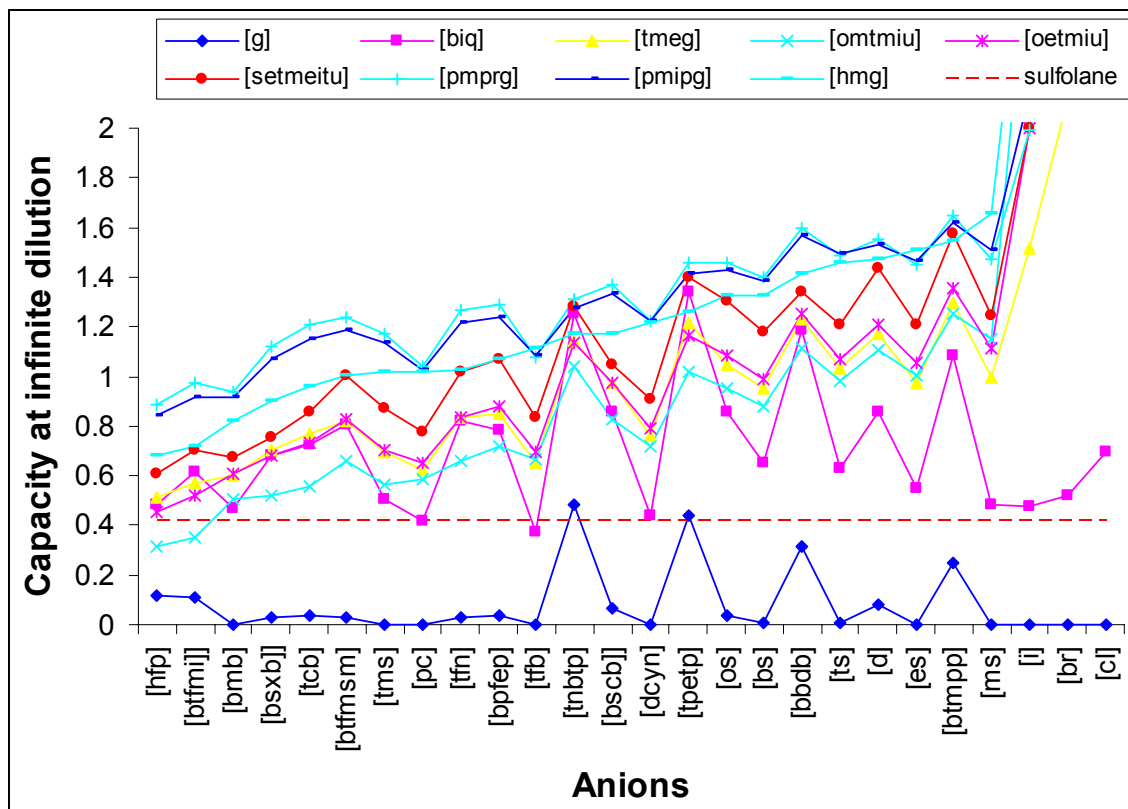


Figure 4.22: Capacity at infinite dilution of guanidinium, uranium and quinilinium based ILs

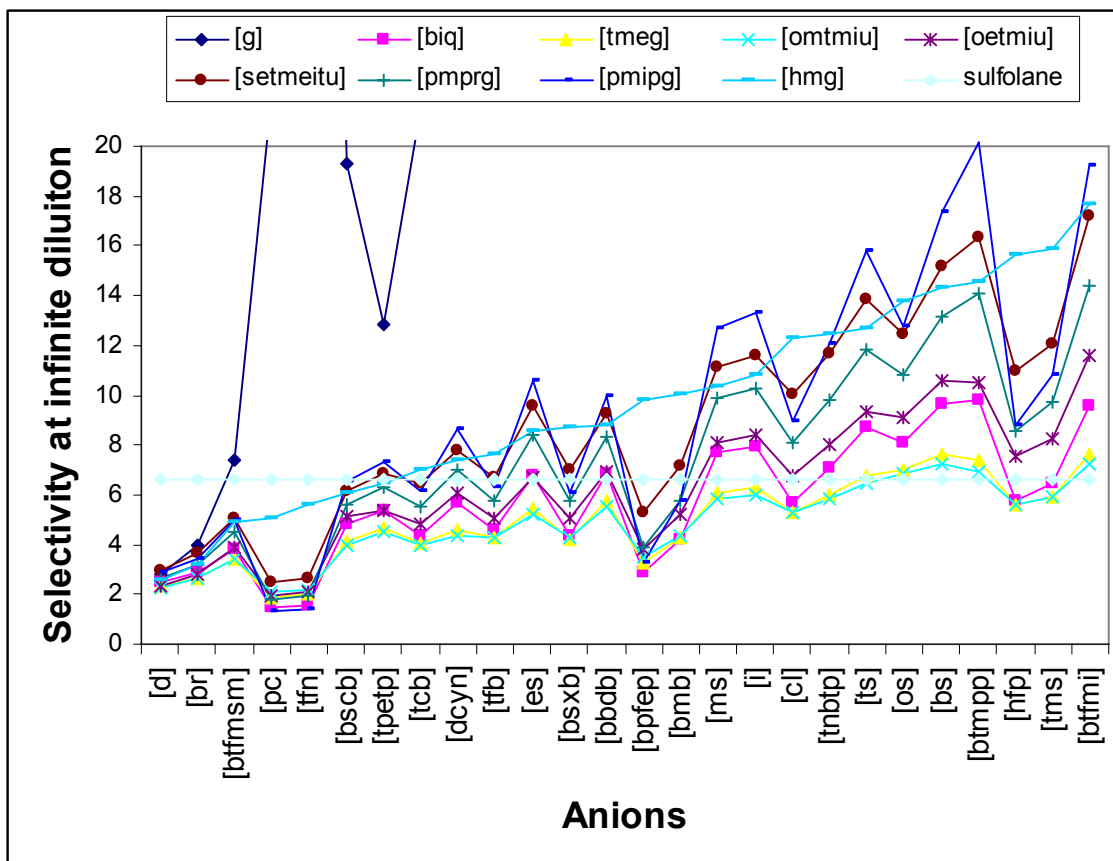


Figure 4.23: Selectivity at infinite dilution of guanidinium, uranium and quinilinium based

ILs

4.7.3 Computationally Recommended ILs

From previous results it is observed that the cations which give higher capacity usually give lower selectivity. Hence alkyl chain length has to be of moderate length. On the other hand, we found a ranking of anions which is more or less *independent* of the alkyl chain length unless the alkyl chain contains more than ten carbon. Therefore to screen anions a cation with moderate alkyl chain length is chosen as representative of that group of cations.

Figures 4.24 to 4.28 display the capacity and selectivity at infinite dilution for 1-butyl-1-methyl-pyrrolidinium, 1-butyl-1-methyl-imidazolium, 1-butyl-pyridinium, phosphonium and ammonium cation based ILs. The capacity has been scaled up in order for better viewing its trend with that of sulfolane. It is observed that anions those give high capacity also give low selectivity. But in the middle there are some which have capacity and selectivity both higher than sulfolane in cases of pyrrolidinium, imidazolium and pyridinium based IL. There are some anions in case of phosphonium based ILs but none in case of ammonium based ILs. Table 4-1 lists the anions for some representative cations discussed above.

Table 4.1: Computationally recommended anions for typical cations

Name of Cations	Computationally Recommended Anions That Satisfy the criteria: $C_{IL}^{\infty} = C_{sulfolane}^{\infty}$ and $S_{IL}^{\infty} = S_{sulfolane}^{\infty}$
1-butyl-1-methyl-pyrrolidinium	C^{∞} : [bsxb] > [tms] > [btfmi] > [dcyn] > [bmb] > [hfp] > [tfb] > [pc] S^{∞} : [hfp] > [btfmi] > [bsxb] > [bmb] > [pc] > [tfb] > [tms] > [dcyn]
1-butyl-1-methyl-imidazolium	C^{∞} : [bscb] > [tcb] > [btfmsm] > [bpfep] > [tfn] > [bscb] S^{∞} : [tcb] > [tfn] > [btfmsm] > [bpfep] > [bscb] > [ts]
1-butyl-pyridinium	C^{∞} : [tfn] > [bpfep] > [btfmsm] S^{∞} : [tfn] > [btfmsm] > [bpfep]
phosphonium	None
ammonium	C^{∞} : [tnbtp] > [tpetp] > [tnbtp] S^{∞} : [tpetp] > [bbdb] > [tnbtp]

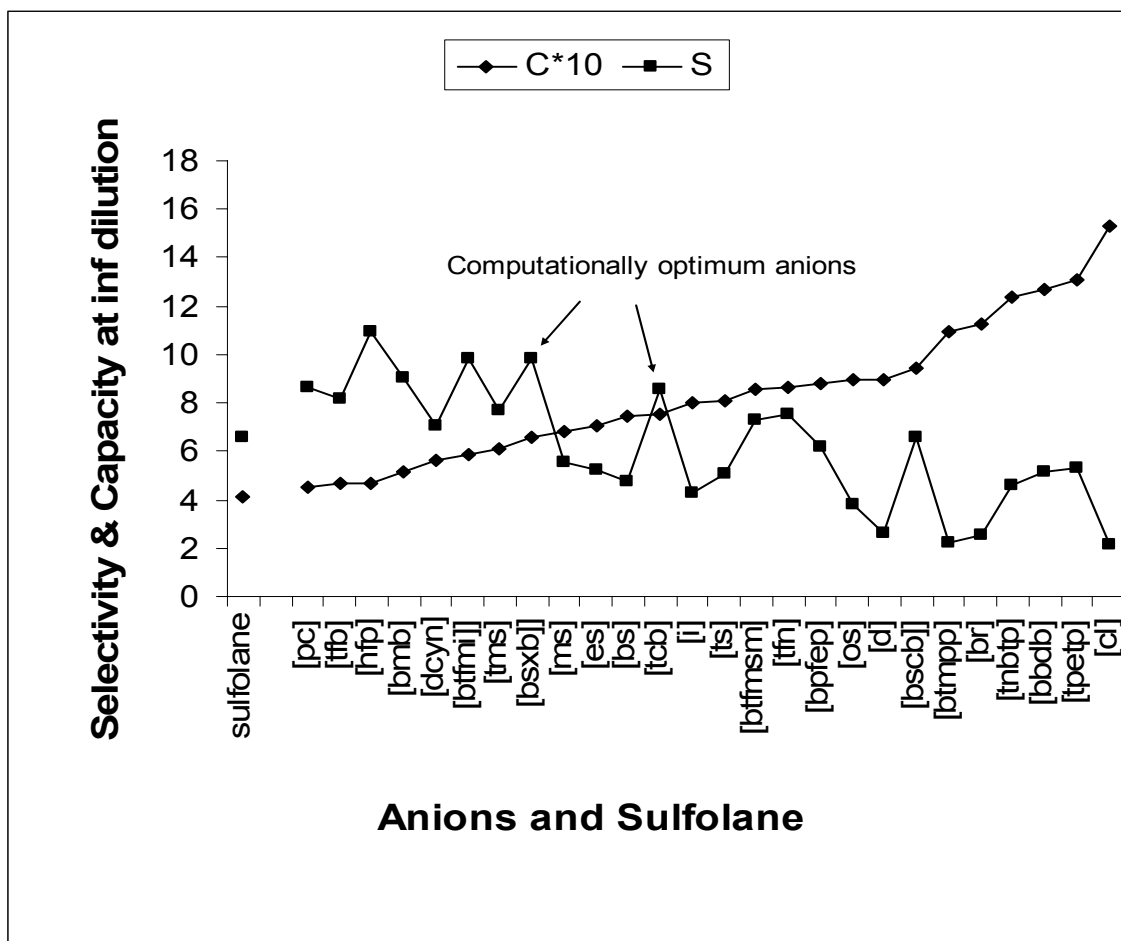


Figure 4.24: Trend of Capacity and Selectivity of a typical butyl-methyl-pyrrolidinium cation with different anions

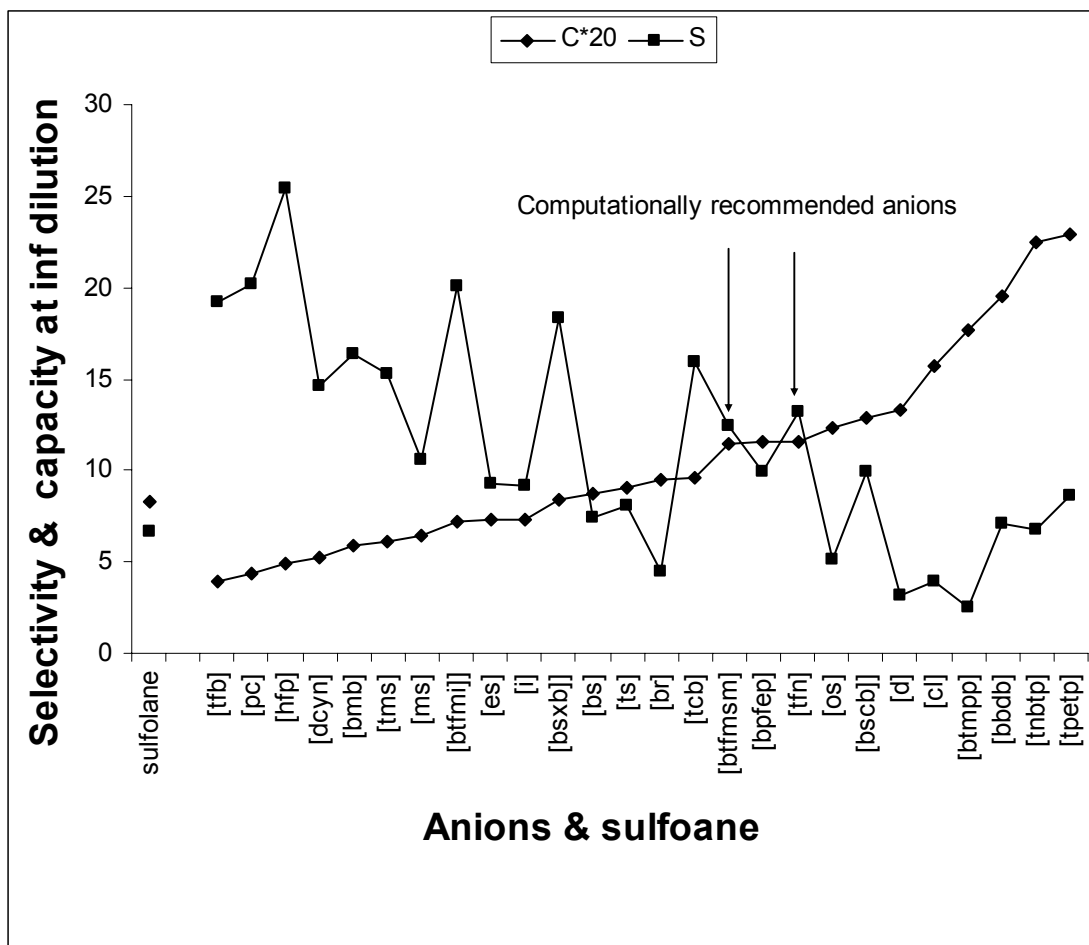


Figure 4.25: Trend of Capacity and Selectivity of a typical butyl-methyl-imidazolium cation with different anions

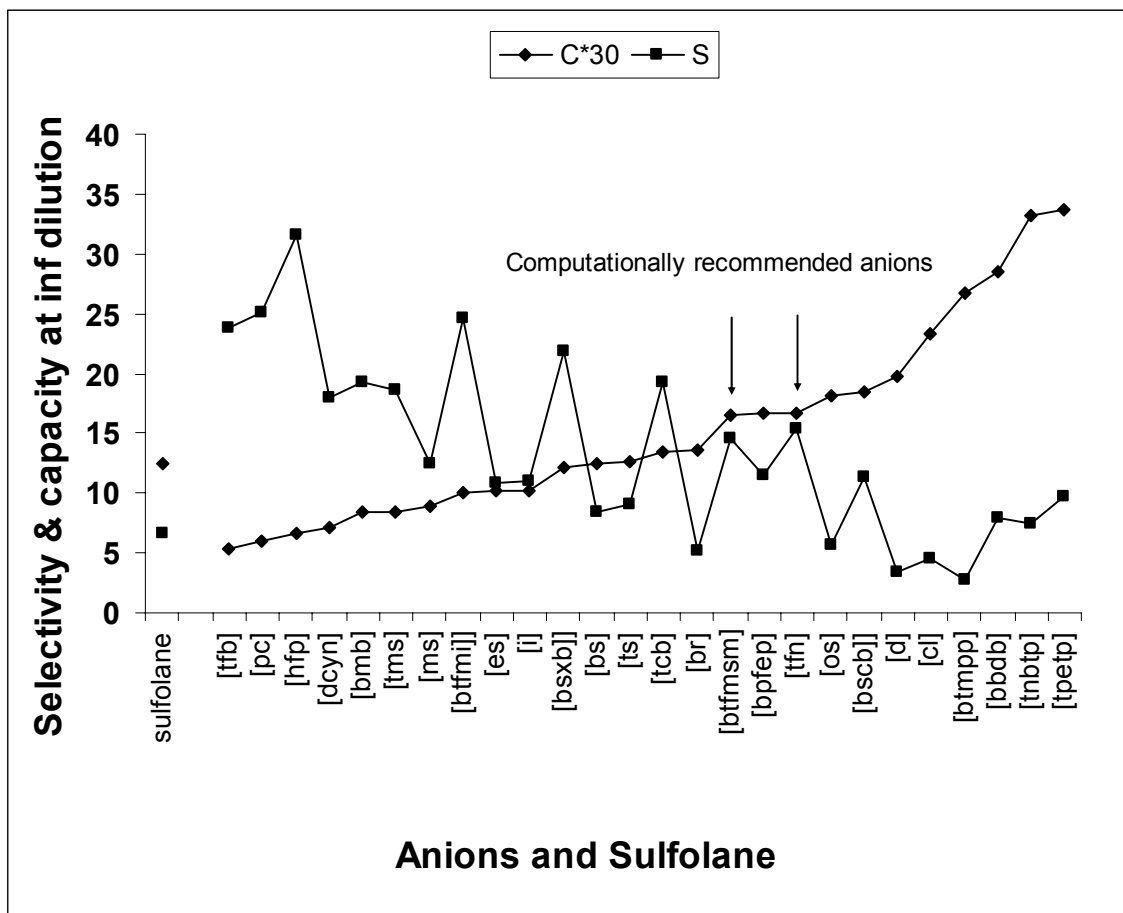


Figure 4.26: Trend of Capacity and Selectivity of a typical 1-butyl-pyridinium cation with different anions

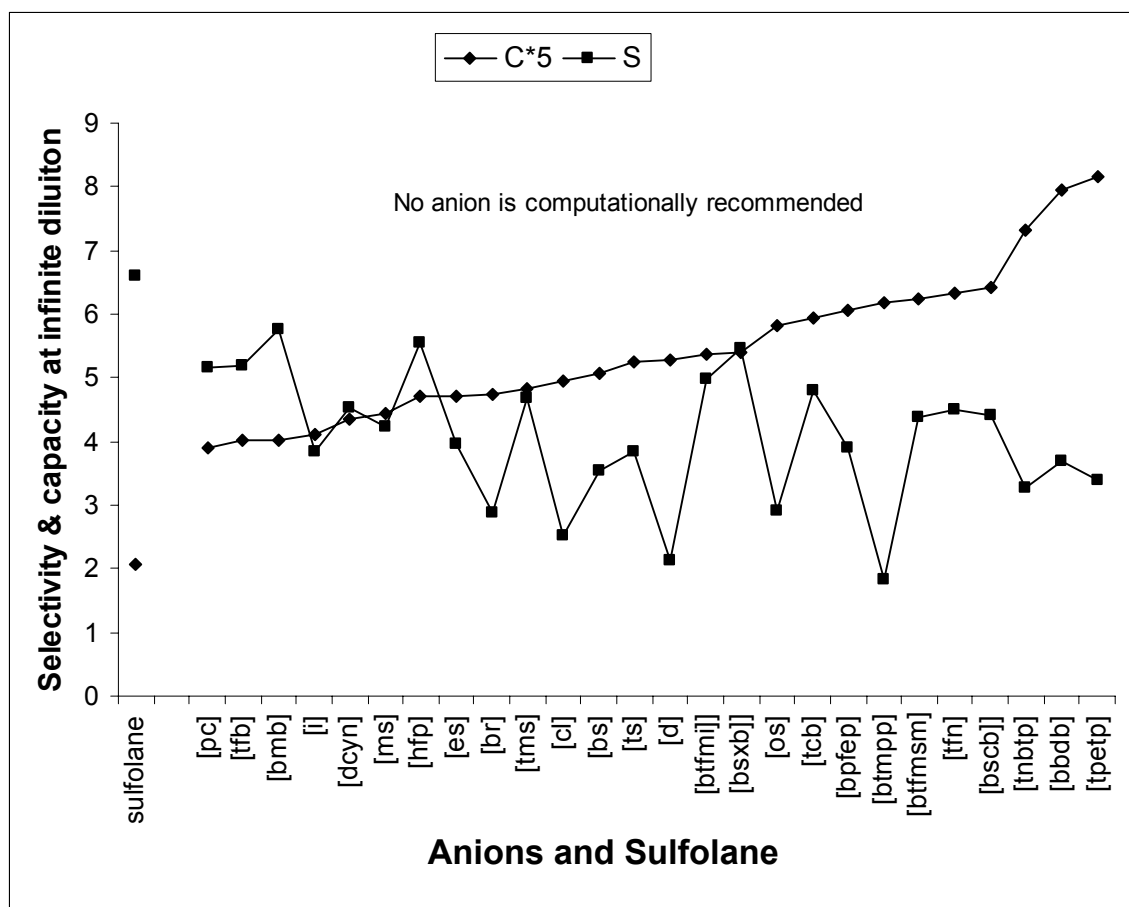


Figure 4.27: Trend of Capacity and Selectivity of a typical phosphonium cation with different anions

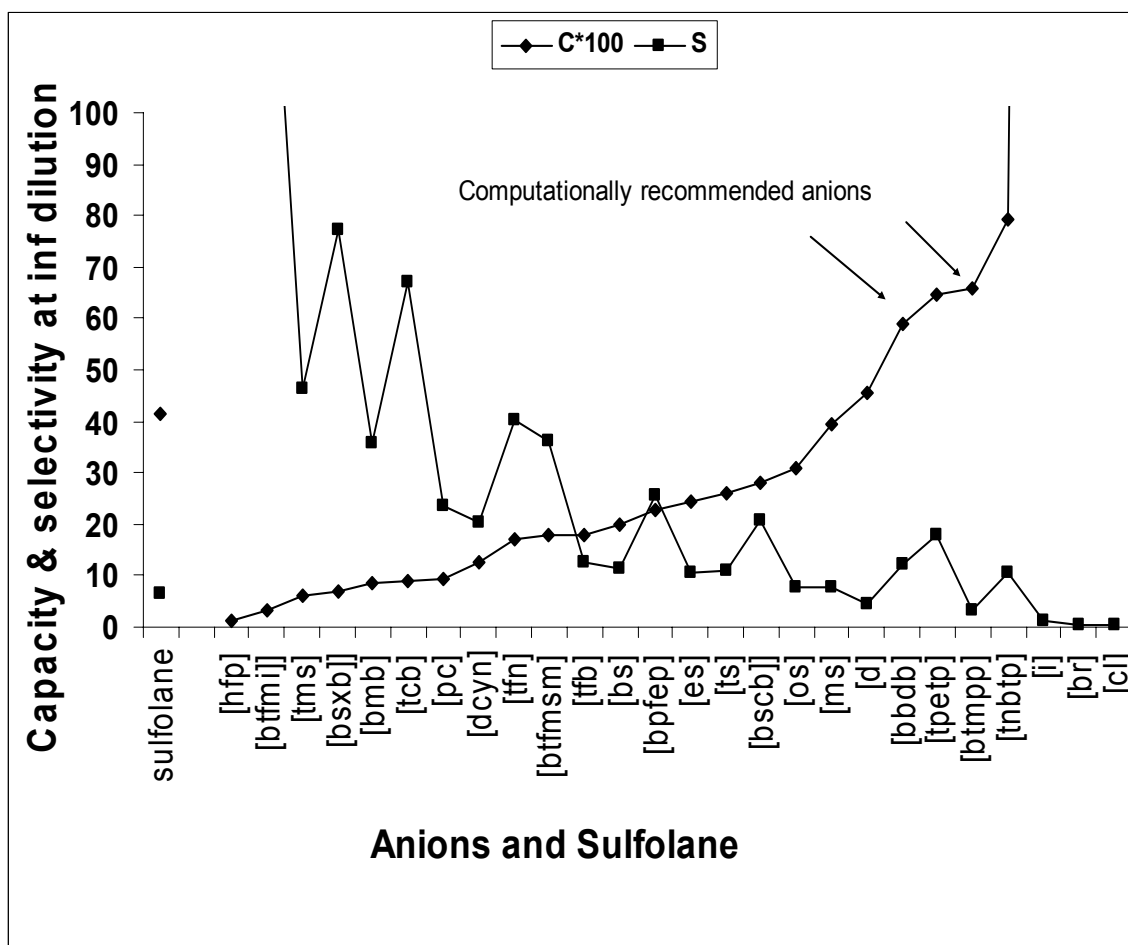


Figure 4.28: Trend of Capacity and Selectivity of a typical ammonium cation with different anions

4.7.4 Effect of Volume of Anions on Capacity and Selectivity

The size and structure of anions have considerable effect on the mutual interaction between cation and anion in an IL, and thereby affect its physical properties, capacity and selectivity when used as solvent. It is observed that capacity decreases with size of anions increases but after a threshold size of anion, capacity increases with the increase of size of anions. The effect of anions on selectivity is not that predictable. Superficially, it can be said that selectivity decreases with the increase of size of anions. Figure 4.29 and 4.30 displays the result of effect of size of anions on capacity of imidazolium based ILs. These ILs are all tailored using 1-butyl-3-methyl-imidazolium cation. Similar behavior pattern is observed for other cations as well. On the contrary, in case of phosphonium and ammonium based ILs, capacity was found to increase with increase in size of anions.

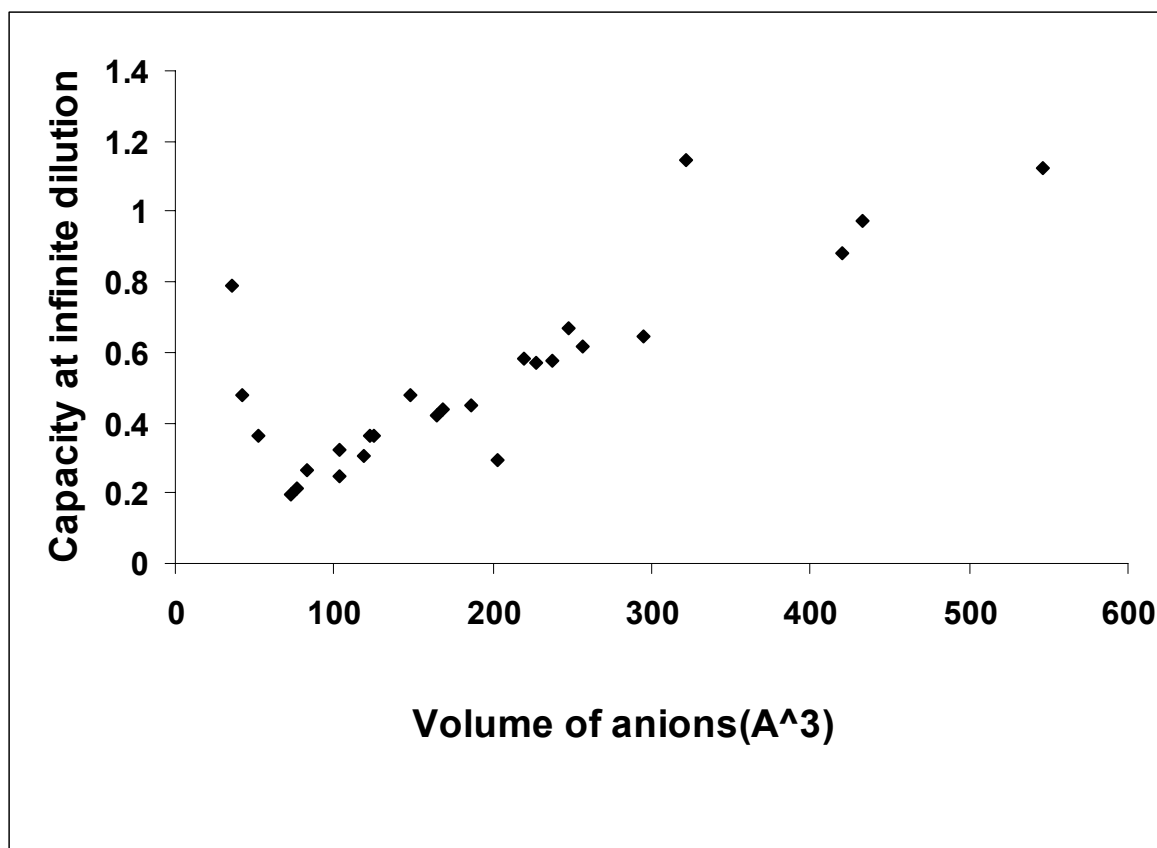


Figure 4.29: Capacity of 1-butyl-3-methyl- imidazolium with anions of increasing volume

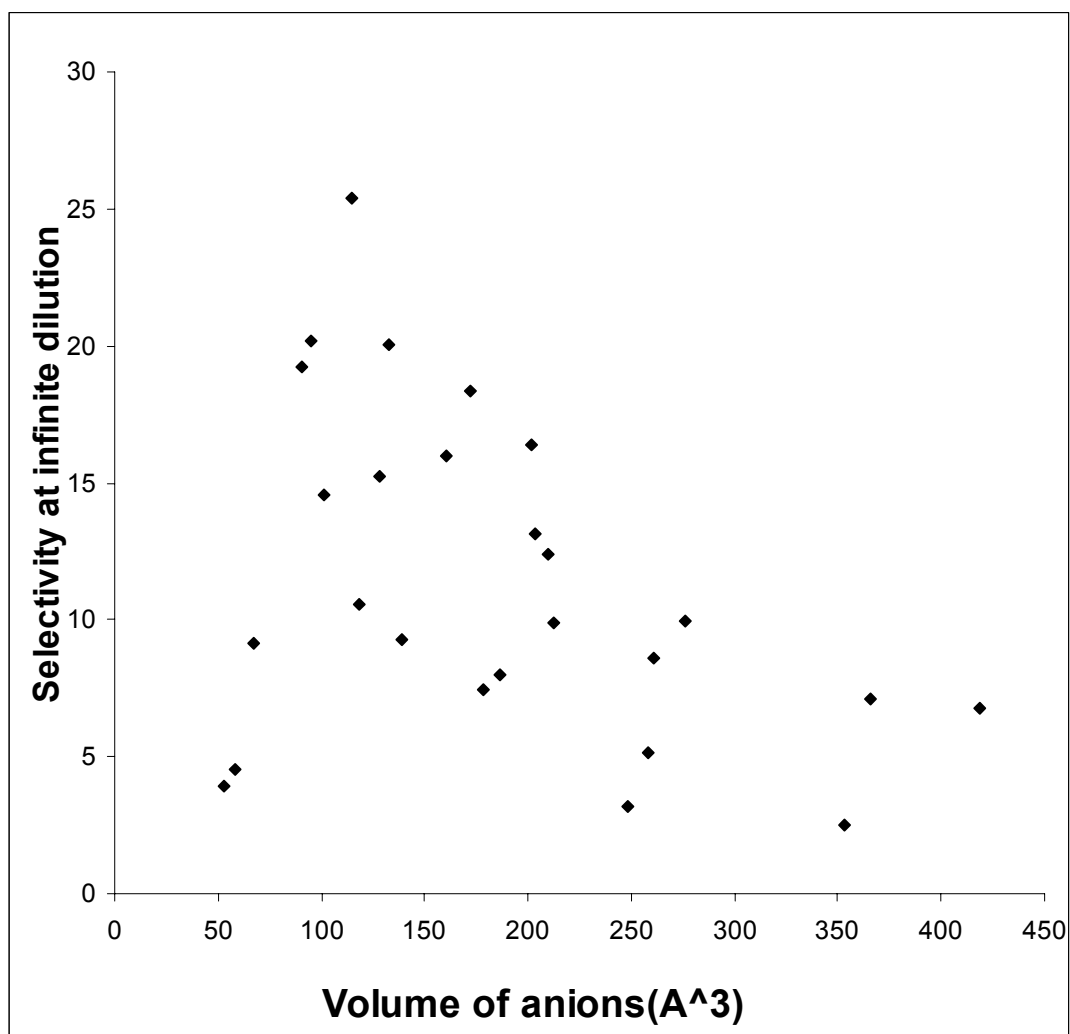


Figure 4.30: Selectivity of 1-butyl-3-methyl-imidazolium with anions of increasing volume

4.7.5 Effect of Volume of Cations on Capacity and Selectivity

The cations in ILs are considerably large and hence influence the physical properties of associated ILs. It is found that capacity of ILs increases with increase of volume of cations whereas selectivity decreases somewhat linearly. Figure 4-31 shows this trend for pyridinium based ILs all of which are consisted of tetrafluoroborate anions and pyridinium based cations of different volume.

4.7.6 Effect of Temperature on Capacity and Selectivity

Though it is observed that capacity increases with the increase in temperature, it is also accompanied by a decrease in selectivity. However the increase and decrease is insignificant. Figures 4-32 and 4-33 show the effect of temperature on 1-butyl-3-methylimidazolium tetrafluoroborate and 4-methyl-N-butyl pyridinium tetrafluoroborate ILs. This behavior is similar for other cations and anions as well.

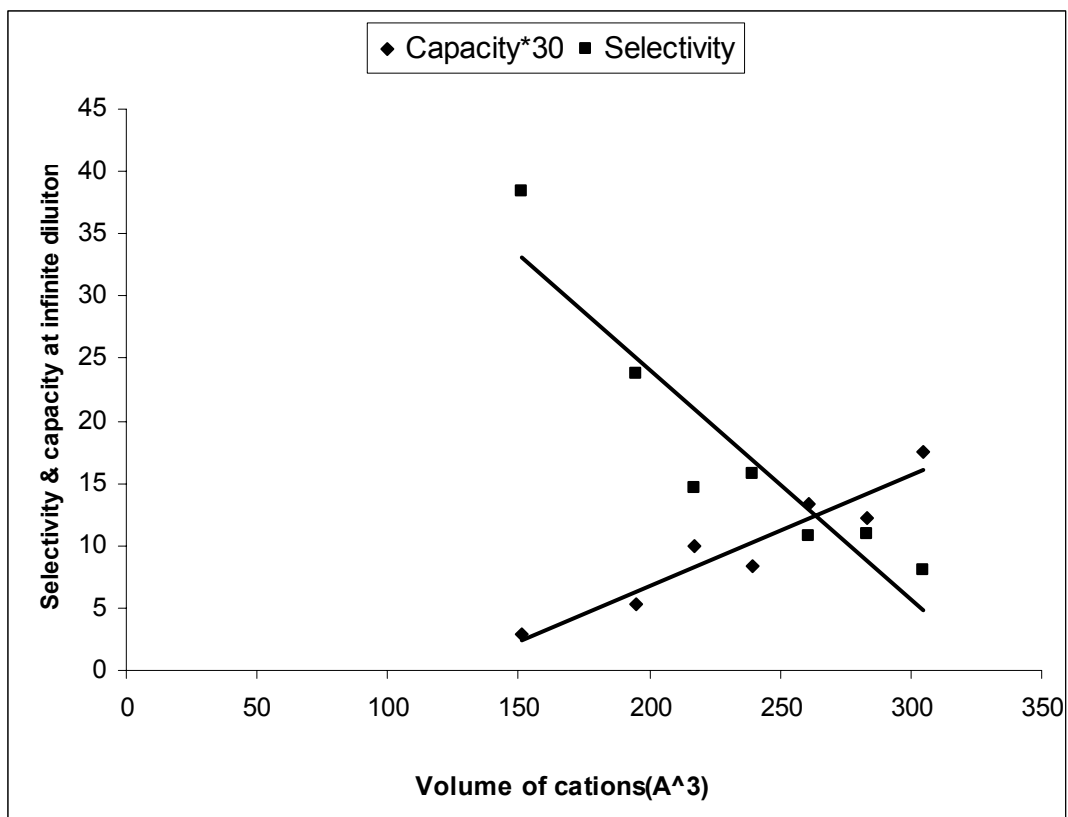


Figure 4.31: Trend of selectivity and capacity of ILs consisting tetrafluoroborate anion and pyridinium-based cations with increasing volume.

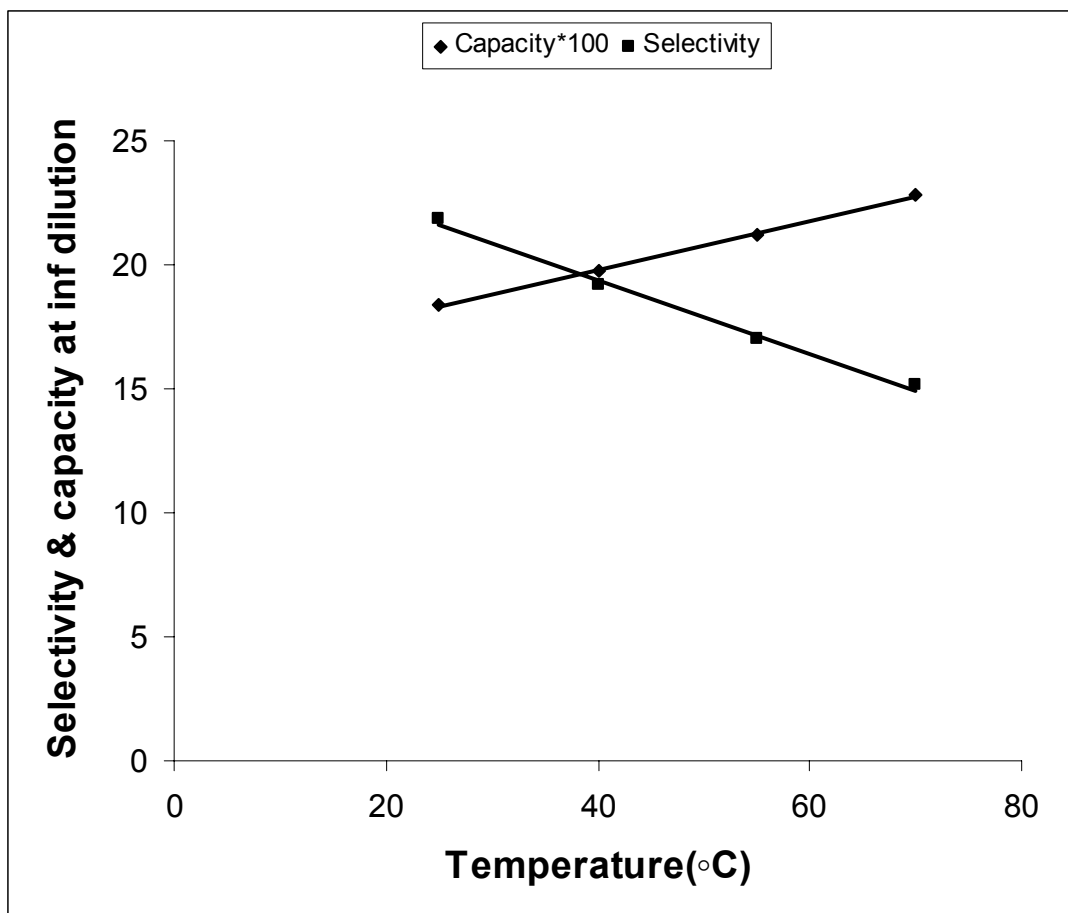


Figure 4.32: Effect of temperature on the infinite dilution selectivity and capacity of 1-butyl-3-methyl-imidazolium tetrafluoroborate

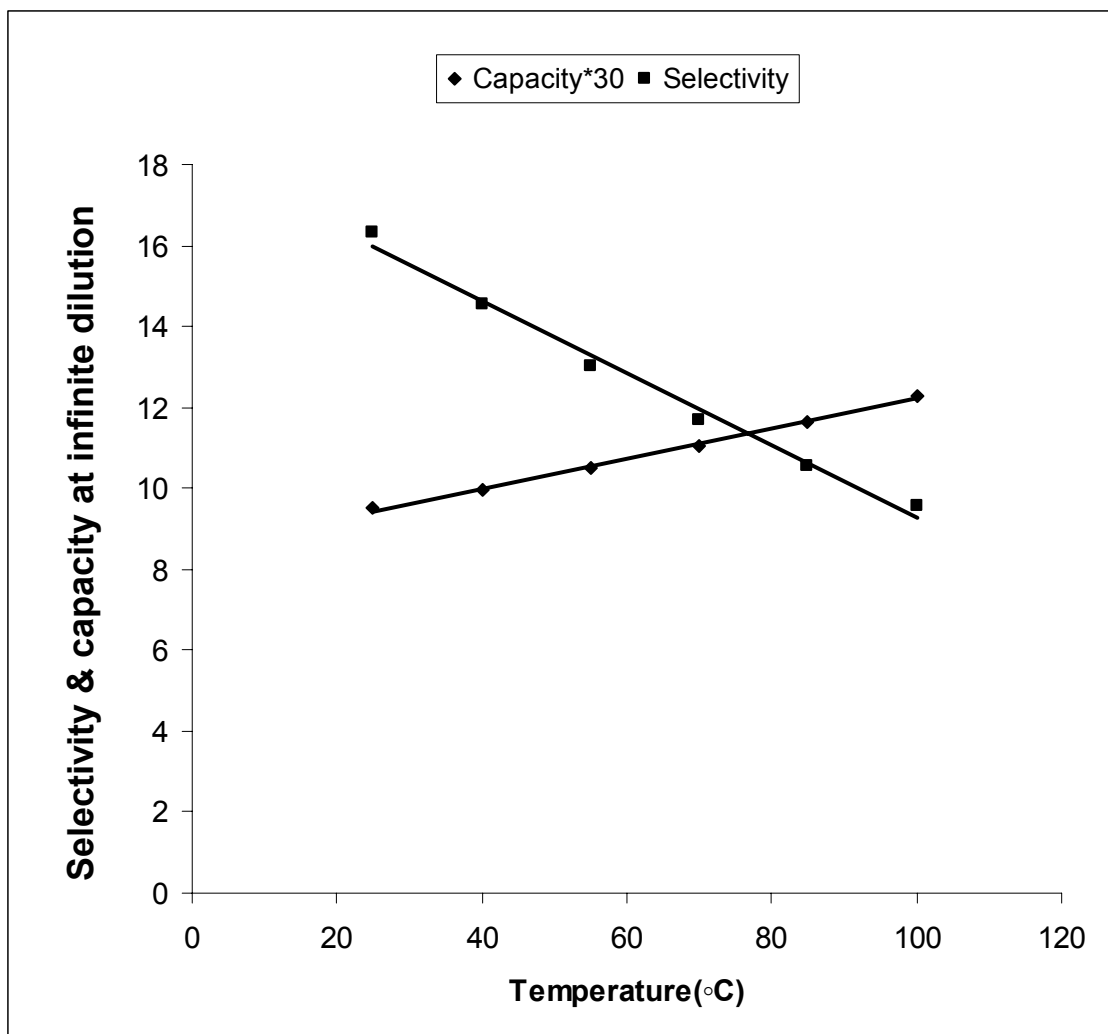


Figure 4.33: Effect of temperature on the infinite dilution selectivity and capacity of N-butyl-4-methyl-pyridinium tetrafluoroborate

CHAPTER 5

EXPERIMENT

5.1 INTRODUCTION

In the large pool of ionic liquids so far investigated, there is not a single one that possesses both high capacity and selectivity for aromatic extraction. But it is the combination of high capacity and selectivity that makes a solvent appropriate to use. Several attempts have been made to improve the properties of ILs, including the search for new and unusual ILs in addition to the mixing of 'green' co-solvents, such as water, ethanol and supercritical CO₂ existing ILs. However, the use of binary IL mixtures has rarely been investigated, although it has been shown that mixing two or more different ILs may confer on the mixture improved and unexpected properties (Fletcher et al., 2003).

Each ionic liquid based on imidazolium or pyridinium is unique in its polarity and aromaticity which results from its constituent cation and anion. High polarity facilitates the splitting of the IL-organic mixture into two phases. High aromaticity of ILs yields higher capacity but lower selectivity. Therefore, a good balance is needed between aromaticity and polarity which may be obtained from a synergized solvent tailored by mixing two suitable ionic liquids, for example, an IL having high capacity with one having high selectivity.

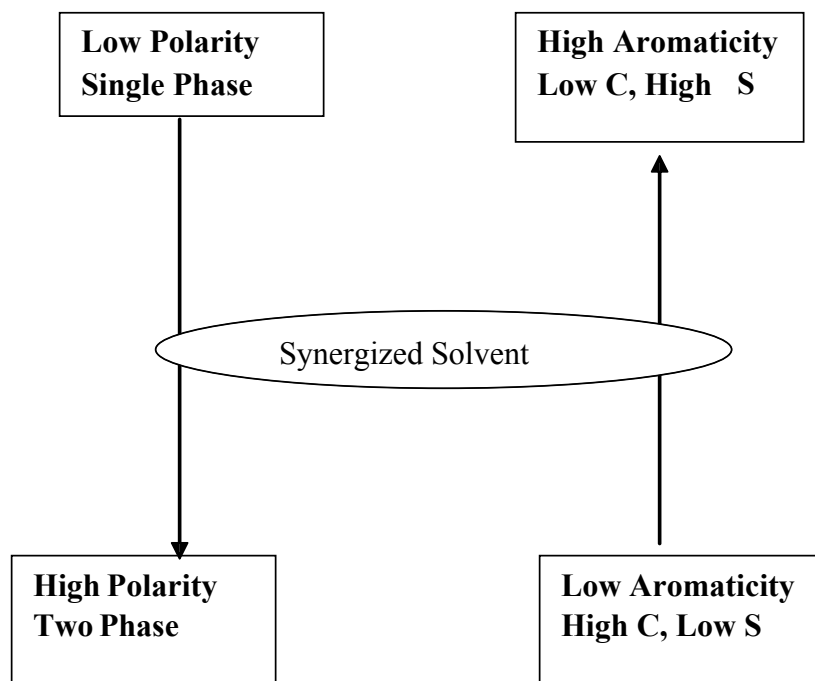


Figure 5.1: Physical Properties expected in synergized solvents

5.2 COMPUTATIONAL PREDICTION OF SYNERGISTIC BEHAVIOR OF BINARY IL MIXTURES

General behavior of binary mixtures is investigated by COSMO $therm$ in search of synergy. It is found that some mixtures behave ideally; some behave synergistically, whereas others display *negative* deviation from the ideal behavior.

The mixed solvent of [bmi][tcb] & [bmi][tnbtp] gives lower selectivity and capacity than those of their individual component ILs. Figure 5.2.1 shows the selectivity & capacity of the mixed solvent [bmi][tcb] & [bmi][tnbtp]. On the contrary, the mixed solvent of [bmi][os] & [bmi][cl] gives higher selectivity and capacity than those of their individual component ILs at all mixing ratio. Figure 5.2.2 shows the selectivity & capacity of the mixed solvent [bmi][os] & [bmi][cl]. It is postulated that the large difference between the sizes of anions might be the reason behind this synergistic behavior.

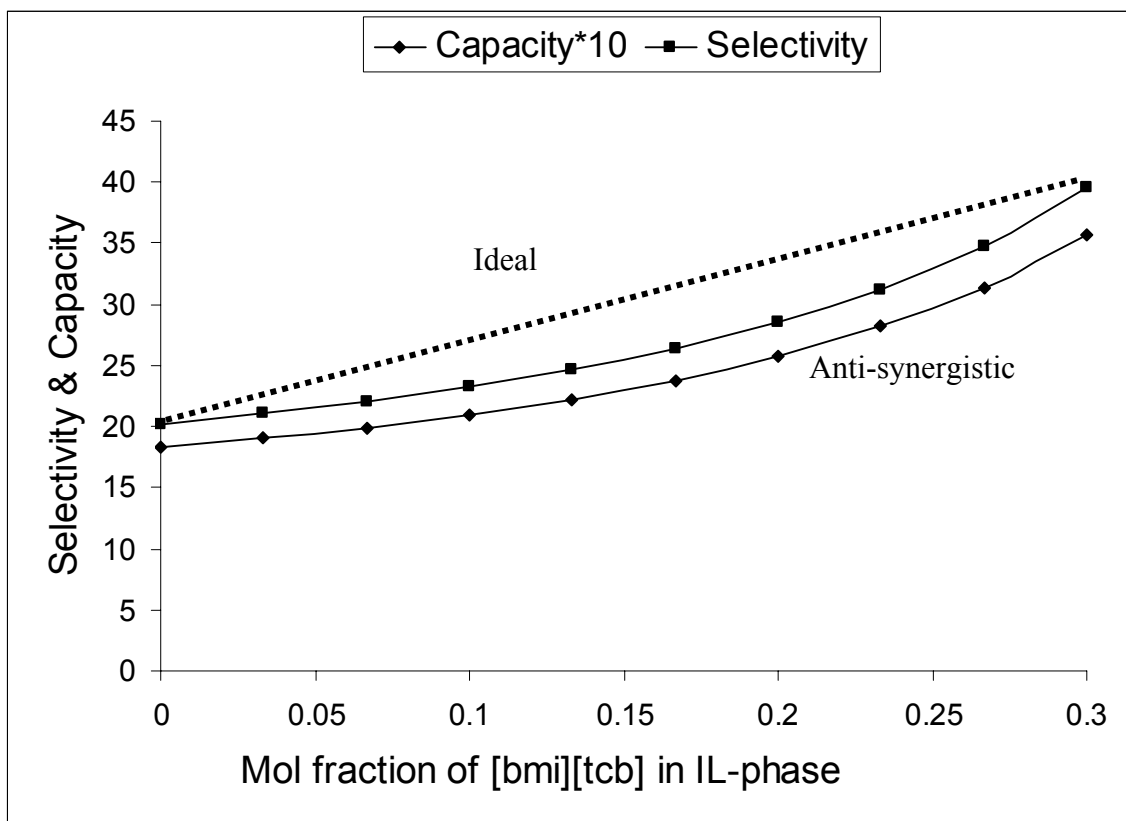


Figure 5.2: Selectivity & Capacity of the mixed solvent [bmi] [tcb] & [bmi] [tnbtp] for toluene and heptane mole fraction 0.01 and 0.09 in the IL-phase

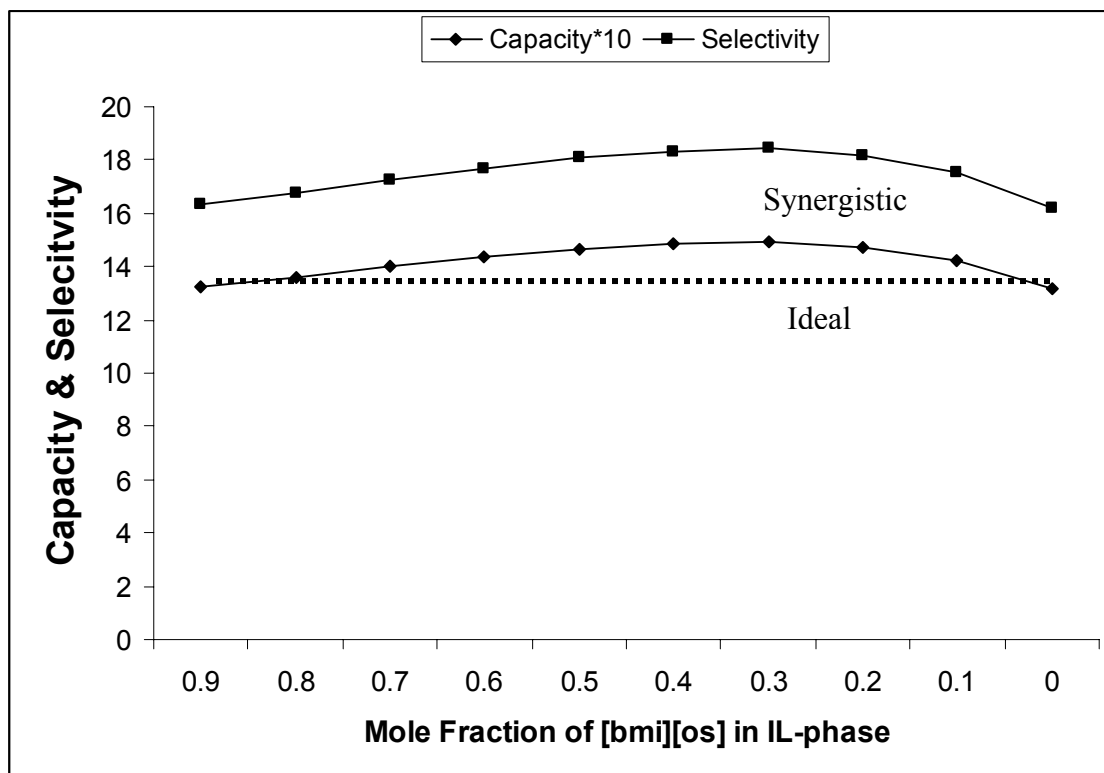
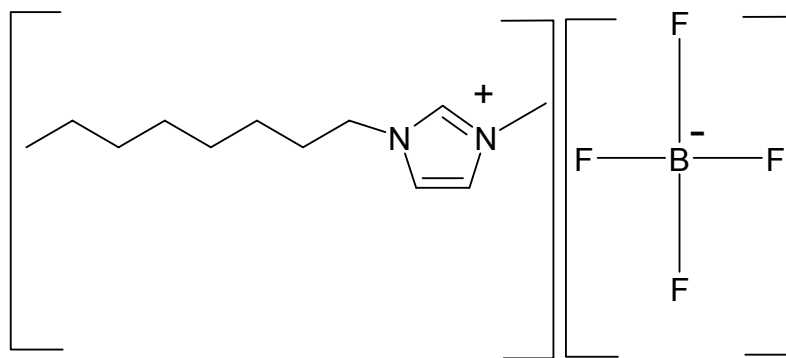


Figure 5.3: Selectivity & Capacity of the mixed solvent [bmi][os] & [bmi][cl] for toluene and heptane mole fractions 0.02 and 0.08 in the IL-phase

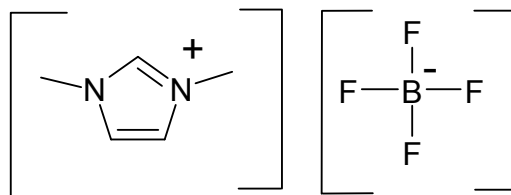
5.3 EXPERIMENTAL VERIFICATION OF SYNERGISTIC BEHAVIOR OF BINARY ILS MIXTURE

5.3.1 Materials

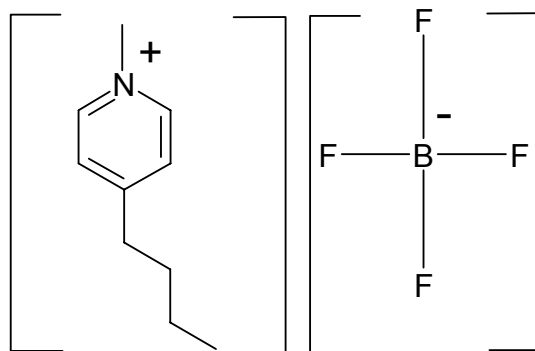
Meindersma et al. (2005) it was found that the ILs, dimethyl imidazolium methyl sulfate ([dmi][ms]) has high selectivity but low capacity and the IL octyl methyl imidazolium tetrafluroboarte ([omi][tfb]) has high capacity but low selectivity whereas the IL 4-methyl-N-butyl pyridinium tetrafluroborate ([bmpy][tfb]) shows a good compromise between selectivity and capacity. The chemical structures of the above mentioned ILs are shown in figure 5.4.



1-methyl-3-octyl imidazolium tetrafluroborate, [omi] [tfb]



1, 3-dimethyl imidazolium methyl sulfate, [dmi] [ms]



1-butyl-4-N-methyl pyridinium tetrafluoroborate, [bmpy] [tfb]

Figure 5.4: Chemical structure of components of synergized solvents

In this study, [dmi][ms] and [mbpy][tfb] are mixed with [omi][tfb] to seek for synergy in different ratios. Therefore, IL pairs [dmi][ms]+ [omi][tfb] & [bmpy][tfb]+ [omi][tfb] will be used to tailor new solvents.

Table 5.1: Solvents tailored from [omi][tfb] and [dmi][ms] for experiments

Mol Fraction of [omi][tfb]	Mol Fraction of [dmi][ms]
0.0	1.0
0.2	0.8
0.4	0.6
0.6	0.4
0.8	0.2
1.0	0.0

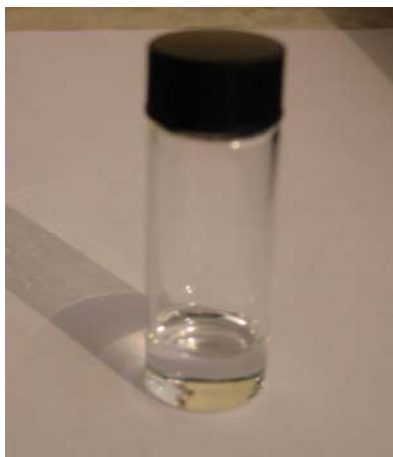
Table 5.2: Solvents tailored from [omi][tfb] & [mbpy][tfb] for experiment

Mol Fraction of [omi][tfb]	Mol Fraction of [mbpy][tfb]
0.0	1.0
0.2	0.8
0.4	0.6
0.6	0.4
0.8	0.2
1.0	0.0

1, 3 Dimethyl imidazolium methyl sulphate (97%), 1-methyl-3-octylimidazolium tetrafluoroborate (97%), 1-Butyl-4-methylpyridinium tetrafluoroborate (97%) were purchased from Fluka.

5.3.2 Phase Equilibrium Equipment

The liquid-liquid equilibrium measurement was made by using in 7 cm³ (1.5 cm inside diameter and 4 cm long) cylindrical vials. The top was closed using a PVC cap which was further wrapped by paraffin. The vials were put in constant temperature water bath with the sample inside.



(a)



(b)



(c)

Figure 5.5: Typical feed and solvent mixtures (a) Toluene+heptane
(b) [omi][tfb]+[dmi][ms]+toluene+heptane, (c) [omi][tfb]+[mbpy][tfb]+toluene+heptane.

5.3.3 Procedures

For each run, a measured mass (1 ± 0.001 g) of a pure ionic liquid or two pure ionic liquids (in specific ratios) was placed in the dried vile at room temperature. Fixed amount of toluene (0.1 ± 0.001 g) and heptane (0.9 ± 0.001 g) were then added. Therefore, solvent to feed ratio was 1 in all cases. When two ionic liquids were taken, mol fraction of one in the solvent was increased gradually in different samples. The viles were then kept at the constant temperature water bath for about 48 hours at 40° C to reach equilibrium.

Two samples of the each phases (5 ml each) were withdrawn by glass syringes and were taken in NMR tubes and mixed with 50 ml chloroform-d solvent to await chemical analysis.

5.3.4 Analysis

Both phases were analyzed by nuclear magnetic resonance (^1H NMR) instrument. Mole fraction of each component was calculated by analyzing the spectra. The precision of the composition measurements was considered to be ± 0.01 in mol fraction for the organic phase and ± 0.05 in mol fraction for the ionic liquid+toluene+heptane phase. The NMR instrument was operated at room temperature.

5.3.5 Experimental Results and Discussions

5.3.5.1 Binary Solvent, [dmi] [ms] + [omi] [tfb]

This two ILs are mixed to investigate the behavior of the mixed solvent. Capacity of the mixed solvent versus mol fraction of [dmi][ms] in the solvent is shown in figure 5.6 . It is observed that no synergy in capacity can be achieved from their mixture. At $X_{[dmi][ms]}=0$, the solvent is pure [omi][tfb], which has the highest capacity 0.8 . Now as $X_{[dmi][ms]}$ increases i.e. gradually [dmi][ms] is increased in the solvent, capacity starts falling. When $X_{[dmi][ms]}=1$, i.e., for pure [dmi][ms] capacity is the lowest of all, 0.4.

Selectivity of the mixed solvent is shown in figure 5.7 versus mol fraction of [dmi] [ms] in the solvent. It is observed that no synergy in capacity can be achieved from their mixture. At $X_{[dmi][ms]}=0$, the solvent is pure [omi][tfb], which has the lowest selectivity, 6 . Now as $X_{[dmi] [ms]}$ increases i.e. gradually [dmi][ms] is increased in the solvent selectivity starts increasing. When $x_{[dmi] [ms]}=1$, i.e., for pure [dmi] [ms] selectivity is the highest of all, 31. The effect of $x_{[dmi] [ms]}$ on capacity is not proportional but somewhat exponential. Selectivity increases slowly as $X_{[dmi] [ms]}$ increases and shoots up when it is close to 1.

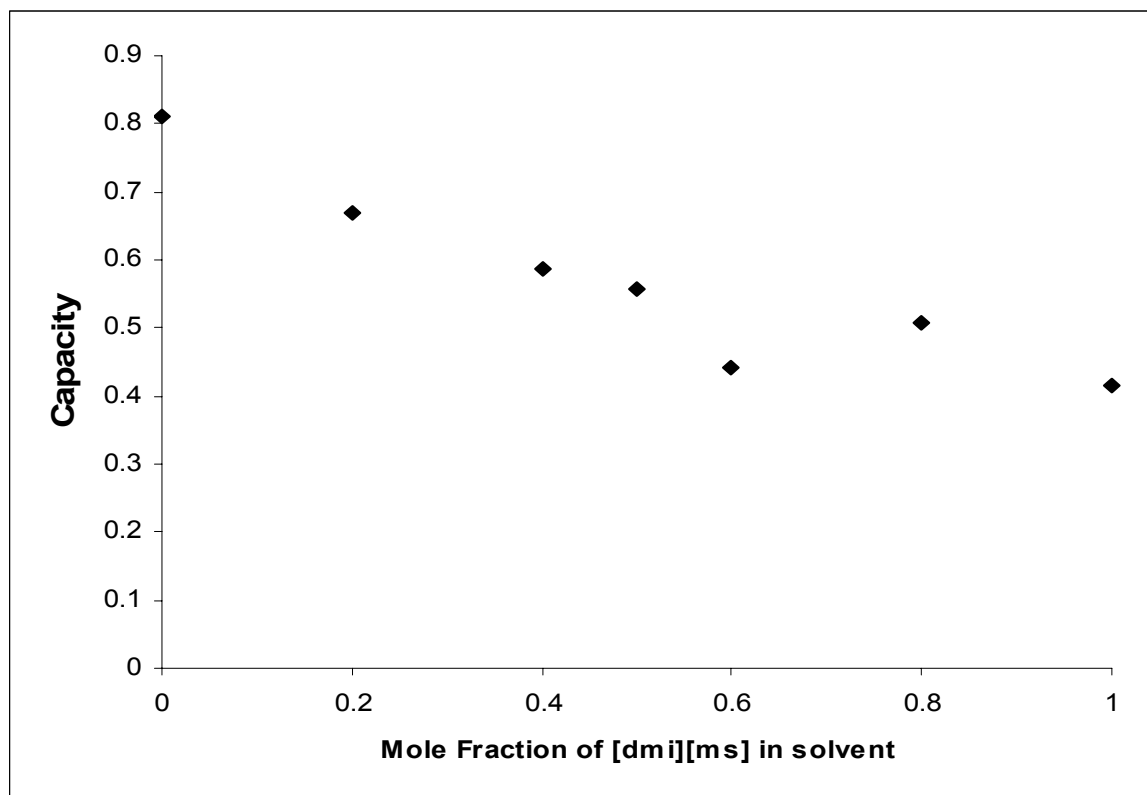


Figure 5.6: Experimental capacity for the system [dmi][ms]+[omi][tfb] at 40° C,0.1 Mpa, for the feed composition of toluele 0.1 gm, heptane 0.9 gm and total solvent ([dmi][ms]+[omi][tfb]) 1 gm.

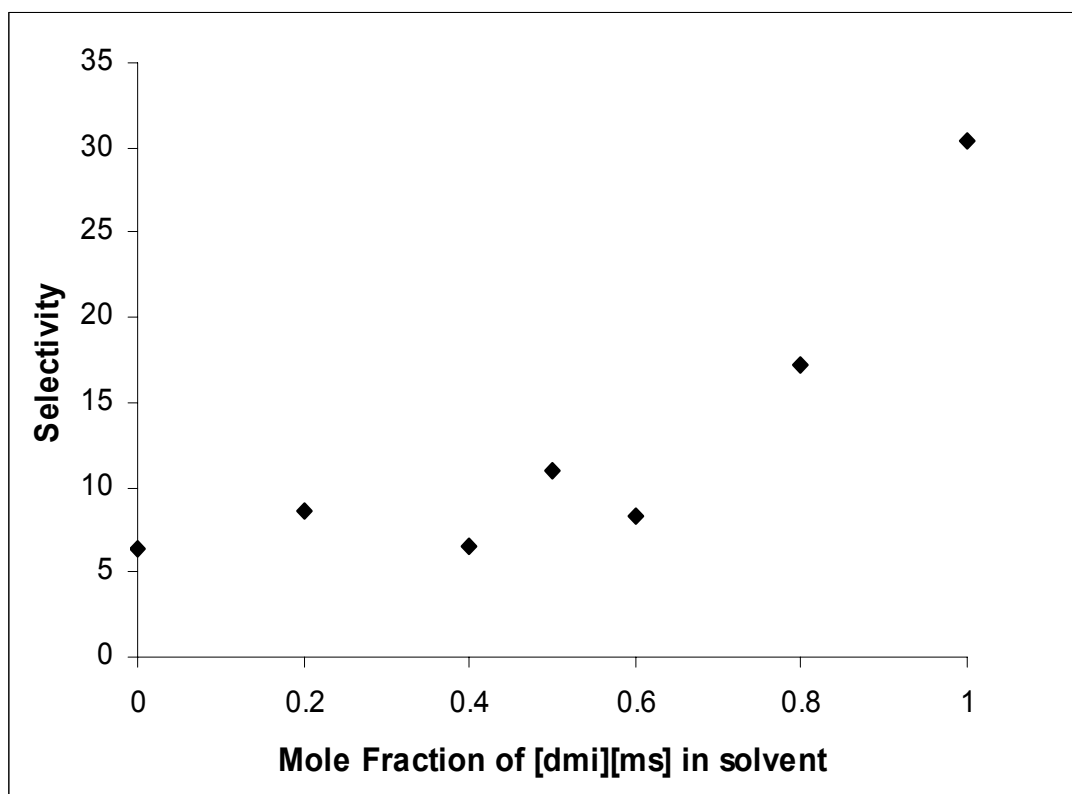


Figure 5.7: Experimental selectivity for the system [dmi][ms]+[omi][tfb] at 40° C, 0.1 Mpa, for the feed composition of toluene 0.1 gm, heptane 0.9 gm and total solvent ([dmi][ms]+[omi][tfb]) 1 gm.

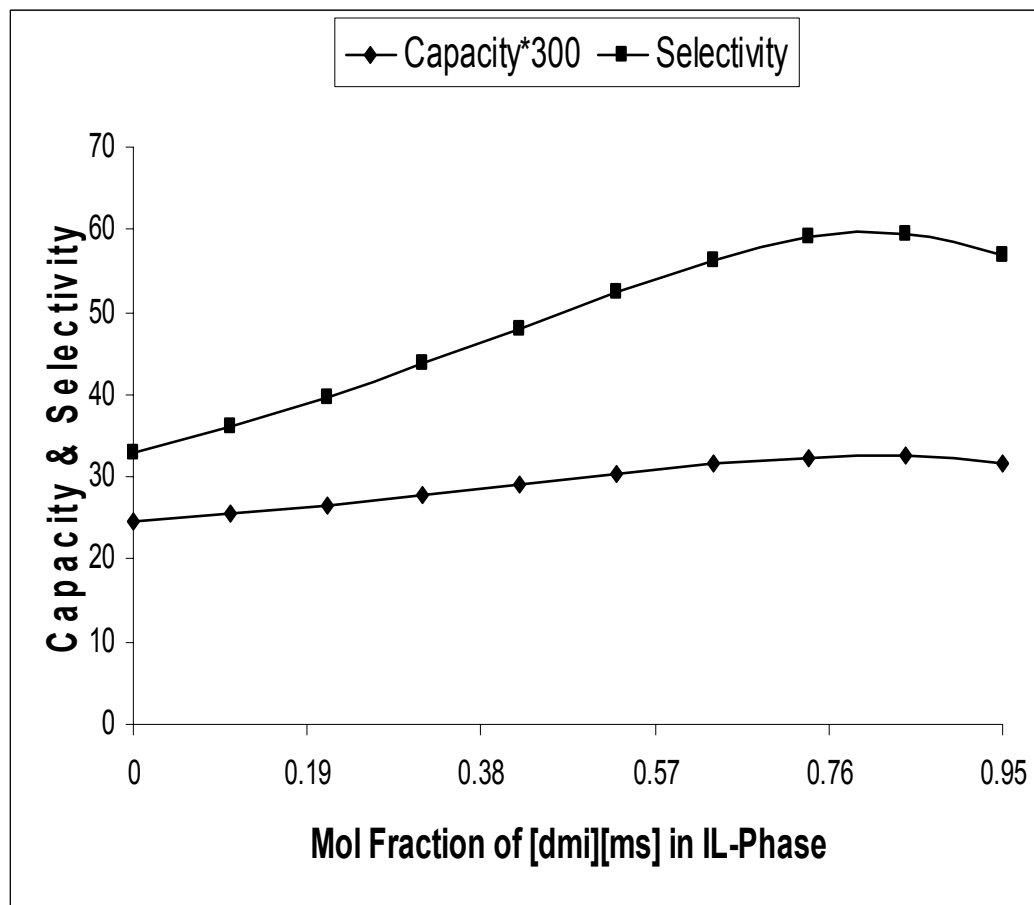


Figure 5.8: Calculated C & S for the system [dmi][ms]+[omi][tfb] at 40° C,0.1 Mpa,for the IL-Phase composition(MF): 0.95 IL,0.049 T,0.01 H

Figure 5.8 shows the capacity of this mixed solvent calculated by COSMO-RS versus mole fraction of [dmi][ms] in the IL-phase. It is notable here that the ratio of [dmi][ms] to [omi][tfb] is representative of their ratio in the solvent because all the solvent virtually goes to IL-phase and the presence of ILs in the organic phase is beyond the detectable limit. From experiment we have composition of both organic and IL-phase. Similar composition is fed to the COSMO-RS as IL-phase composition. COSMO-RS returns back the equilibrium organic phase when IL-phase composition is provided to it. It is seen from figure 5.8 that there might be a synergy in selectivity when $X_{[\text{dmi}][\text{ms}]}$ is near unity, though we did not get it from experiment.

5.3.5.2 Binary Solvent, [mbpy][tfb]+ [omi][tfb]

These two ILs are also mixed to investigate whether the capacity of [bmpy][tfb] can further be improved. Capacity of the mixed solvent is shown in figure 5.9 versus mol fraction of [omi][ms] in the solvent. It is observed that capacity increases somewhat linearly with $X_{[\text{omi}][\text{tfb}]}$. At $X_{[\text{omi}][\text{tfb}]}=0$, the solvent is pure [bmpy][tfb], which has the lowest capacity 0.41. Now as $X_{[\text{omi}][\text{tfb}]}$ increases i.e. gradually [omi][tfb] is increased in the solvent capacity falls and then starts increasing. When $X_{[\text{omi}][\text{tfb}]}=1$, i.e., pure [omi][tfb] capacity is 0.8. But At $X_{[\text{omi}][\text{tfb}]}$ close to 0.8, the capacity is higher (0.82) than that of pure [omi][tfb]. It is noted that [omi][tfb] has the highest capacity of all three ILs as pure. Therefore there seems synergy in capacity from the mixture of [bmpy][tfb] and [omi][tfb].

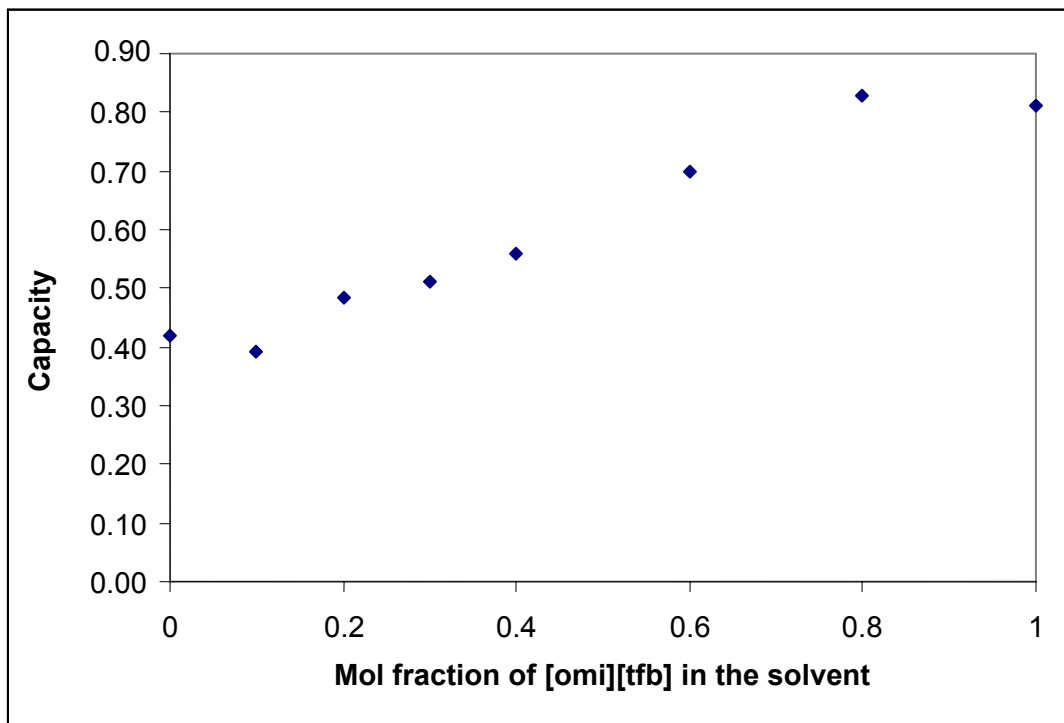


Figure 5.9: Experimental capacity for the solvent [omi][tfb]+[bmpy][tfb] at 40° C & 1 atm, for the feed composition of toluene 0.1 gm, heptane 0.9 gm and total solvent 1 gm.

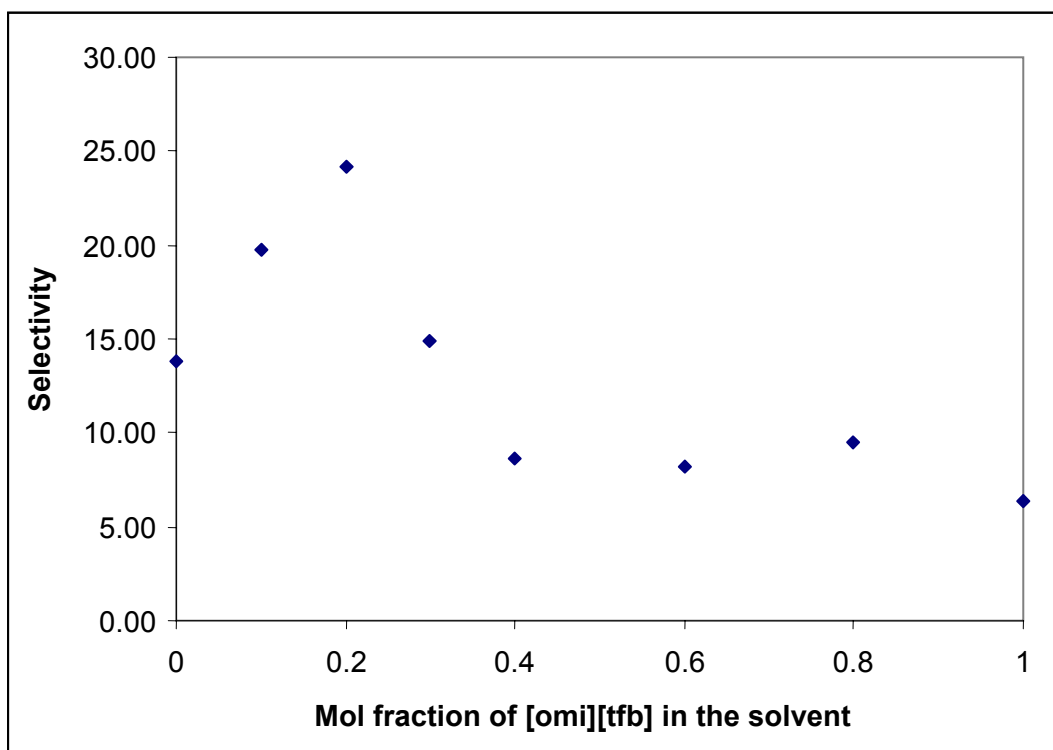


Figure 5.10: Experimental selectivity for the solvent [omi][tfb]+[bmpy][tfb] at 40°C & 1atm for the feed composition of toluene 0.1 gm, heptane 0.9 gm and total solvent 1 gm.

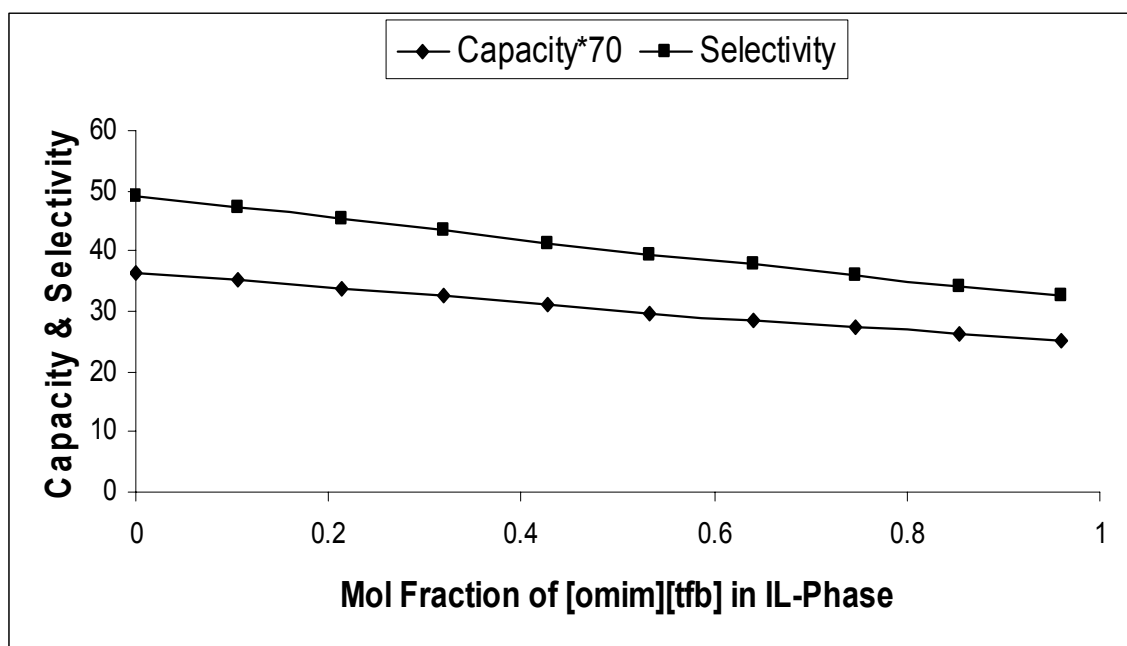


Figure 5.11: Calculated C & S for the system [bmpy][tfb]+[omi][tfb] at 40° C, 0.1 Mpa

Selectivity of the mixed solvent is shown in figure 5.10 versus mol fraction of [omi][tfb] in the solvent. It is observed that synergy in selectivity can be achieved from this mixture. At $X_{[\text{omi}][\text{tfb}]}=0$, the solvent is pure [bmpy][tfb], which has the selectivity 14. Now as $X_{[\text{omi}][\text{tfb}]}$ increases i.e. gradually [omi][tfb] is increased in the solvent, selectivity starts increasing. When $X_{[\text{omi}][\text{tfb}]}=0.2$, the selectivity is as high as 24. Then it starts decreasing with the increase of [omi][tfb]. When $X_{[\text{omi}][\text{tfb}]}=1$, that is, for pure [omi][tfb] selectivity is the lowest of all, 6. Initially the experiments were carried out at 0.2 mol fraction interval. Therefore, experiments were not done initially at the points where $X_{[\text{omi}][\text{tfb}]}=0.1$ & 0.3, but carried out later when a synergy was obtained at $X_{[\text{omi}][\text{tfb}]}=0.2$ to verify that there truly exists synergy around and at the point where $X_{[\text{omi}][\text{tfb}]}=0.2$.

Figure 5.11 shows the capacity of this mixed solvent predicted by *COSMOtherm* versus mole fraction of [bmpy][tfb] in the IL-phase. It is seen from figure 5.11 that there might be synergy in selectivity when $X_{[\text{omi}][\text{tfb}]}$ is near unity, though we did not get it from experiment. On the other hand, the synergy that was found in experiment is not predicted by *COSMOtherm* calculation.

CHAPTER 6

MODELING IONIC LIQUIDS SOLUTIONS

6.1 INTRODUCTION

It is important to characterize the fundamental thermodynamic properties and phase behavior of ILs for two reasons: to use them efficiently as solvents and to partition among different organic phases. A successful model will be very helpful in predicting the thermodynamic behavior of IL solutions in many important engineering applications. The development of proper thermodynamic models has made it possible to simulate industrial processes from minimum amount of experimental data. This facilitates process integration and optimization with a minimum of pilot plant tests.

6.2 NPT ENSEMBLE

An ensemble is an enormous collection of prototypes of a thermodynamic system. In an NPT ensemble, the containing walls of each system are heat conducting and flexible, so that each system of the ensemble can be described by the number of molecules (N), temperature (T) and pressure (P). The partition function would be on the total energy and total volume of the ensemble, and the partition function would turn out to be

$$\Delta(N, T, P) = \sum_E \sum_V \Omega(N, V, E) e^{-(E+PV)/kT} \quad (6-1)$$

whose characteristic thermodynamic function is the Gibbs free energy, expressed as,

$$G = -kT \ln \Delta \quad (6-2)$$

6.3 MODELING IL SOLUTIONS IN NPT ENSEMBLE

Although there are a few volume-explicit equations of state, almost all commonly used equations are volume-implicit (pressure is a function of volume and temperature). This is mainly because the energy levels needed to evaluate the partition function depend on volume. In classical mechanics, the intermolecular potential depends on the distances between the molecules, and the distance can easily be related to the volume. Another possible reason is that it is more convenient to work with a volume occupied by molecules than count the molecular collisions with the container wall. The volume-implicit equations have the advantage that more than one phase could be represented by one equation, as is the case for most cubic equations (representing the vapor and liquid phases). Representing multiple phases by volume-explicit equations require separate equations (roots) for each phase.

Volume-explicit equations have their advantages as well. In one-dimensional systems most exact results are given in the isothermal isobaric ensemble (volume explicit) (Lieb et al., 1966). In phase equilibrium calculations, the evaluation of density or the molar volume from a given pressure and temperature is one of the most frequently performed operations. Thus, the use of volume-implicit equations of state can slow down complex chemical engineering design programs and oil reservoir simulations to a rather unacceptable degree. In addition, root finding algorithms (such as the Cardanos formula for cubic roots) can lead to significant loss of numerical precision and unfortunately they do not exclude unphysical solutions thereby making it necessary to check whether the solutions are physically meaningful. These inconveniences make the use of volume-

explicit equations to be attractive especially in cases where a vapor phase can not be formed such as polymer systems, liquid-liquid equilibrium and at very high pressures.

6.4 ASSUMPTIONS

The following assumptions are made in this regard:

1. Only nearest neighbors interact.
2. Molecular interactions are pair wise additive.
3. The repulsive part can be modeled using hard-body mixtures
4. The square well potential may be used to represent short range attractive forces

6.5 APPROACH

Attempt will be taken first to model electrolyte solution in restrictive primitive model (RPM). RPM model will be described shortly. In this model, the overall compressibility factor is divided into three contributions such as the repulsive (Z^{hb}), attractive (Z^{att}) and ionic contribution (Z^{ionic}). The repulsive contribution, in the present model, will be presented by the compressibility factor for mixtures of hard spheres developed by Hamad (1997). For the ionic contribution, a mathematical expression can be developed that simulate behavior of long range ionic interaction. Parameters in this model will be found by satisfying some limiting conditions along with fitting with Monte Carlo simulation data. The model will be then extended to more realistic situation by adding a short range attractive term (Z^{att}) with it. This attractive term will be developed in the square well potential. The parameters in the square well potential, namely the width and depth of the well for pure and cross interactions, will be found by fitting the

model to experimental data for multicomponent solutions containing ILs and organic solutes.

6.6 THE RPM ELECTROLYTE MODEL IN NVT ENSEMBLE

The idealization of ionic solutions is called the primitive model. In this model, the solute molecules are considered as charged hard spheres of finite sizes. The solvent molecules, on the other hand, are not explicitly treated. Solvent molecules are removed and replaced by a dielectric continuum. As a consequence, the electrostatic forces of interaction, which are Columbic in nature, retain their values in water. The primitive model is an approximation for real electrolyte solutions. In the 1970s, Mean Spherical Approximation (MSA) was solved for the Restrictive Primitive Model (RPM) in the NVT ensemble (Anderson et al., 1971; Anderson et al., 1972). The anions and cations are charged hard spheres of equal size and the solvent is a dielectric continuum of dielectric constant ϵ_m .

The compressibility factor is found to be

$$Z = Z^{hs} + Z^{ionic} \quad (6-3)$$

$$Z^{ionic}(NVT) = \frac{3x + 3x\sqrt{1+2x} - 2\sqrt[3]{1+2x} + 2}{72\eta} \quad (6-4)$$

where, the hard sphere compressibility was developed by Carnahan and Starling (1969) and expressed as

$$z^{HS} = \frac{1 + \eta + \eta^2 - \eta^3}{(1 - \eta)^3} \quad (6-5)$$

and the quantity η is the packing fraction of the charged hard spheres and defined as

$$\eta = \frac{\pi \sum x_i \sigma_i^3}{6} \quad (6-6)$$

$$x = \sqrt{4\pi b^* \rho^*} \quad (6-7)$$

$$\rho^* = \rho \sum x_i \sigma_i^3 \quad (6-8)$$

b^* is the Bjerrum length divided by effective diameter of the system,

$$b^* = \frac{|z_+ z_-| e^2}{\epsilon_m kT \sum x_i \sigma_i} \quad (6-9)$$

6.7 PROPOSED MODEL

6.7.1 Proposed Model for RPM Electrolytes

The compressibility factor is divided into two parts- the repulsive contribution or the hard sphere contribution and ionic contribution and written as

$$Z = Z^{hs} + Z^{ionic} \quad (6-10)$$

6.7.1.1 Short Range Repulsive Forces in NPT

Hard body molecules are commonly used as reference systems for real fluids in perturbation theories due to the recognition that fluid structure is determined primarily by repulsive forces. The hard sphere is the simplest model of the hard body molecules. A recent review of twenty two different analytical expressions for the compressibility factor of the hard sphere system has been presented by Mulero et al. (2001). While the hard

sphere model serves as a reference in perturbation theories of simple fluids; it is also used to construct the hard core equations for chain molecules (Dickman et al., 1986; Wertheim et al., 1984; Wertheim et al., 1986; Boublik., 1986; Gonasgi et al., 1994).

The hard sphere potential is defined as:

$$U(r) = \begin{cases} \infty & 0 < r < \sigma \\ 0 & r > \sigma \end{cases} \quad (6-11)$$

Hamad [2], proposed the following hard sphere equation for mixtures of hard spheres:

$$Z^{HB} = 1 + \left(4 - \frac{3}{2}b_0\right)p^\circ + \frac{3}{4}b_1p^\circ \ln \left[\frac{3 + p^\circ}{3 + 25p^\circ} \right] + \frac{216b_0p^\circ}{(3 + p^\circ)(3 + 25p^\circ) \left\{ 16 + 3 \ln \left[\frac{3 + p^\circ}{3 + 25p^\circ} \right] \right\}} \quad (6-12)$$

There are two composition and size dependent parameters in this equation, namely: b_0 , b_1 which are defines as

$$b_0 = \frac{1152}{865} \frac{33\alpha^3 - 23\alpha\kappa - 13\alpha^2 + 3\kappa}{(3\alpha + 1)^3} \quad (6-13)$$

$$b_1 = \frac{8}{865} \frac{-729\alpha^3 + 3339\alpha\kappa + 5949\alpha^2 - 1639\kappa}{(3\alpha + 1)^3} \quad (6-14)$$

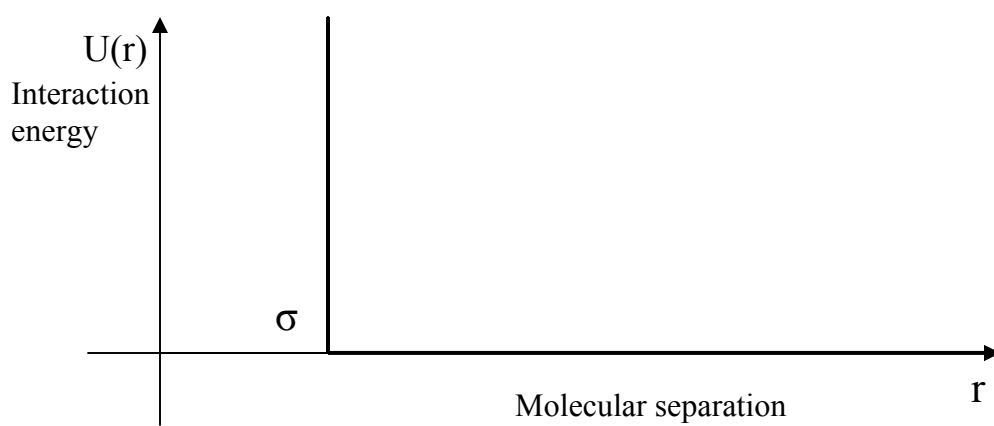


Figure 6.1: The hard-sphere potential

where,

$$\alpha = \frac{S_1 S_2}{S_3} \quad (6-15)$$

and

$$\kappa = \frac{S_2^3}{S_3^2} \quad (6-16)$$

$$S_i = \sum x_i \sigma_i^3 \quad (6-17)$$

The dimensionless pressure p° is defined as

$$p^\circ = ph \quad (6-18)$$

where,

$$h = \frac{(3S_1 S_2 + S_3)}{4} \quad (6-19)$$

$$p = \frac{\pi P}{6kT} \quad (6-20)$$

where P is the pressure, T is the temperature, σ_i and x_i are the diameter and mole fraction of the hard sphere species i . In the pure state both α and κ reduce to unity and the equation of state reduces to

$$Z(T, P) = 1 + 4p + \frac{3p}{4} \ln \frac{3+p}{3+25p} \quad (6-21)$$

At very high pressures, this equation predicts a close-packing reduced density,

$\eta_{\infty} = \pi\sigma^3\rho/6$, of 0.631, compared to the simulation values in the range 0.64-0.602 (Santiso et al., 2002). The Carnahan-Starling equation predicts a physically unattainable value of 1.

6.7.1.2 Ionic Interactions in NPT

The ionic contribution developed in the NVT ensemble [eq. (6-13)] was quite a great improvement over Debye-Huckel model and is successful in predicting restrictive primitive and primitive model electrolytes and some aqueous salt solutions. We propose the following general expression for the ionic contribution in NPT ensemble which has the ability to similarly to its NVT counterpart.

$$Z^{ionic}(NPT) = \sqrt{p^*} \left(\frac{m_1}{(p^* + a_0)^{n_1}} + \frac{m_2}{(p^* + a_0)^{n_2}} \right) \quad (6-21)$$

where, for pure component,

$$p^* = \frac{\pi P \sigma^3}{6kT} \quad (6-22)$$

Here, n_1 and n_2 are fixed to be $\frac{1}{2}$ and 3 respectively so that the expression has a limit at high pressure provides high pressure limit, $\frac{Z^{ionic}}{p^*}$ becomes integrable with respect to pressure and Z^{ionic} later gives good fitting to Monte Carlo data. Now, m_1, m_2, n_1 , and a_0 are yet to be found. The parameters m_1 and m_2 can be found from the two following limits

$$\lim\left[\frac{z^{ionic}(NVT)}{\eta^{1/2}}, \eta \rightarrow 0\right] = \lim\left[\frac{z^{ionic}(NPT)}{p^{*1/2}}, p^* \rightarrow 0\right] = f_1(T) \quad (6-23)$$

$$\lim[z^{ionic}(NVT), \eta \rightarrow 1] = \lim[z^{ionic}(NPT), p^* \rightarrow \infty] = f_2(T) \quad (6-24)$$

From the above equations, m_1 and m_2 are found as

$$m_2 = -\frac{a_0^{5/2}}{36} \left[1 - \sqrt{1 + 4\sqrt{6b^*}} - \sqrt{6b^*} (-3 + \sqrt{1 + 4\sqrt{6b^*}}) - \sqrt{\frac{2}{3}} a_0^3 b^{*3/2} \right] \quad (6-25)$$

$$m_1 = \frac{1}{36} \left[1 - \sqrt{1 + 4\sqrt{6b^*}} - \sqrt{6b^*} (-3 + \sqrt{1 + 4\sqrt{6b^*}}) \right] \quad (6-26)$$

The only unknown parameter left is a_0 which is found to be equal to -0.00796 by fitting the overall expression with Monte Carlo data.

6.7.2 Proposed Model for Multicomponent System Containing Ionic Liquids

The model is extended to real system by adding a short range attractive term in addition to repulsive and ionic contribution. The overall compressibility is expressed as:

$$Z = Z^{hb} + Z^{ionic} + Z^{att} \quad (6-27)$$

The repulsive part is similar to that used for hard spheres except that the hard sphere parameters will be replaced with hard body parameters as follows.

$$S_1 = 2 \sum x_i r_i \quad (6-28)$$

$$S_2 = \frac{\sum x_i a_i}{\pi} \quad (6-29)$$

$$S_3 = \frac{6(\sum x_i v_i)}{\pi} \quad (6-30)$$

where r , a , and v stands for average radius of curvature, surface area and volume of components respectively.

The ionic contribution is also the same as given in eq. (6-21) except that the dimensionless pressure for real multicomponent system is defined as

$$p^* = \frac{\pi P S_3}{6kT} \quad (6-31)$$

The only remaining contribution is short range attractive contribution whose expression is developed below. Short range attractive forces can be modeled using square well potential. This potential is defined as:

$$U(r) = \begin{cases} \infty & 0 < r < \sigma \\ -\varepsilon_{TW} & \sigma < r < \lambda\sigma \\ 0 & r > \sigma \end{cases} \quad (6-32)$$

In 1-dimension, that is, for hard rods with length, 1, the compressibility factor is expressed as

$$Z^{sw} = Z^{sw, hb} + Z^{sw, att} \quad (6-33)$$

where the square well attractive term is

$$Z^{sw, att} = \frac{(\lambda - 1)p^{sw}q}{q - e^{(\lambda - 1)p^{sw}}} \quad (6-34)$$

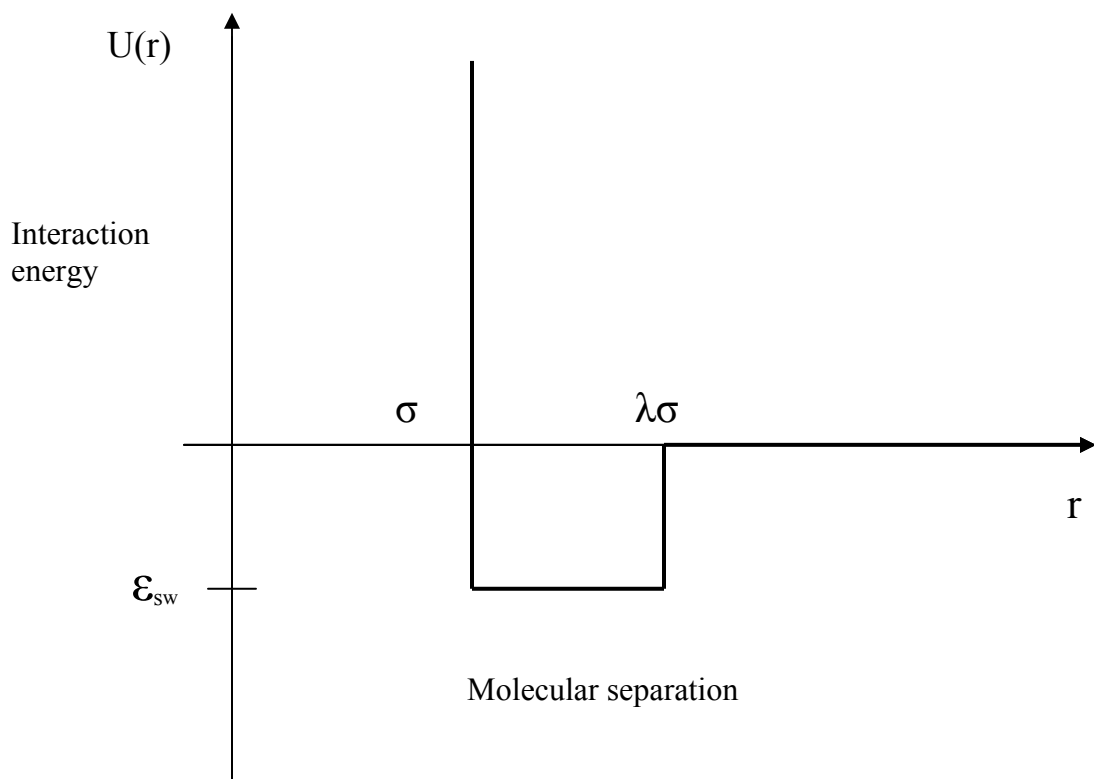


Figure 6.2: Square well potential

where,
$$q = 1 - e^{1/T_{sw}^*} \quad (6-35)$$

The dimensionless pressure is defined as,

$$P^{sw} = \frac{Pl}{kT} \quad (6-36)$$

and the dimensionless temperature T_{sw}^* is

$$T_{sw}^* = \frac{kT}{\varepsilon_{sw}} \quad (6-37)$$

where P , l and T , ε_{sw} are the system pressure, length of hard rods, temperature and depth of square well.

The above attractive term is used in our model for 3-dimension molecules by changing the volume in the definition of dimensionless pressure as below for pure component:

$$Z^{sw,att,3d} = \frac{(\lambda-1)p^{sw,3d}q}{q - e^{(\lambda-1)p^{sw,3d}}} \quad (6-38)$$

where the dimensionless pressure is defined in 3-d as

$$p^{sw,3d} = \frac{\pi P \sigma^3}{6kT} \quad (6-39)$$

for multicomponent mixture,

$$Z^{att} = \sum_i \sum_j x_i x_j \frac{(\lambda_{ij} - 1)p^{sw,3d} q_{ij}}{q_{ij} - \exp[(\lambda_{ij} - 1)p^{sw,3d}]} \quad (6-40)$$

where the dimensionless pressure,

$$p^{sw,3d} = \frac{\pi Ph}{6kT} \quad (6-41)$$

6.7.3 Excess Molar Gibbs Energy

The excess molar Gibbs energy is defined as

$$\begin{aligned} \frac{G^{ex}}{RT} &= \frac{G^{mixture}}{RT} - \frac{G^{ideal\ solution}}{RT} \\ &= \frac{G^{R,mixture}}{RT} - \sum_i x_i \frac{G^{R,pure,i}}{RT} \\ &= \frac{G^{R,mixture}}{RT} - \sum_i x_i \left(\text{Limit}_{x_i \rightarrow 1} \frac{G^{R,mixture}}{RT} \right) \end{aligned} \quad (6-42)$$

where, $G^{mixture}$ = absolute molar Gibbs free energy of the mixture

$G^{ideal\ solution}$ = absolute molar Gibbs free energy of the mixture if it behaved as an ideal solution at the same temperature, pressure and composition of the mixture.

$G^{R,mixture}$ = Residual molar Gibbs free energy of mixture

$G^{R,pure,i}$ = Residual molar Gibbs free energy of component i

x_i = Mole fraction of component i

Now, residual Gibbs energy can be divided into three parts as

$$\begin{aligned} \frac{G^{R,mixture}}{RT} &= \int_0^P \frac{Z^{mixture} - 1}{P} dP \\ &= \int_0^P \frac{Z^{hb} - 1}{P} dP + \int_0^P \frac{Z^{att}}{P} dP + \int_0^P \frac{Z^{ionic}}{P} dP \end{aligned}$$

$$= \frac{G^{R,hb}}{RT} + \frac{G^{R,att}}{RT} + \frac{G^{R,ionic}}{RT} \quad (6-42)$$

On performing the integration, for multicomponent systems each expression becomes -

$$\frac{G^{R,hb}}{RT} = (4 - \frac{3b_0}{2})p^o + b_1[\frac{3(3+p^o)}{4} \ln(\frac{3+p^o}{3+25p^o}) + \frac{54}{25} \ln(1 + \frac{25p^o}{3})] - b_0 \ln[1 + \frac{3}{16} \ln(\frac{3+p^o}{3+25p^o})] \quad (6-43)$$

$$\frac{G^{R,att}}{RT} = \sum_i \sum_j x_i x_j \ln[\frac{(q_{ij}-1) \exp\{(\lambda_{ij}-1)p^o\}}{(q_{ij}-1)}] \quad (6-44)$$

$$\frac{G^{R,ionic}}{RT} = \frac{3m_2(a_0 + p^*)^2 \arctan[\frac{\sqrt{p^*}}{\sqrt{a_0}}] + \sqrt{a_0} \{m_2 \sqrt{p^*} (5a_0 + 3p^*) + 8a_0^2 m_1 (a_0 + p^*)^2 \ln[\sqrt{p^*} + \sqrt{a_0 + p^*}]\}}{4a_0^{5/2} (a_0 + p^*)^2} - 2m_1 \ln[\sqrt{a_0}] \quad (6-45)$$

The molar Gibbs energy of mixing can be calculated from the molar residual energy by using the following relationship:

$$\frac{\Delta G}{RT} = \frac{G^{ex}}{RT} + \sum_i x_i \ln x_i \quad (6-46)$$

6.8 RESULTS AND DISCUSSIONS

6.8.1 Application to RPM electrolyte

The model is applied to the mean spherical approximation in the RPM model of electrolytes. Table 6.1 displays the compressibility factor calculated using the present

model along with its counterpart model in the NVT Ensemble. The corresponding simulation data (Larsen et al., 1976) is also enumerated.

Table 6.1: Comparison of compressibility factor for MSA in RPM

η	b^*	MC	Compressibility factor	
			Eq. of state(NVT)	Eq. of state(NPT)
0.1498	1.8823	1.62	1.66	1.63
	4.7055	1.43	1.34	1.35
	9.4111	0.79	0.89	0.77
0.2507	1.5873	3.02	2.86	2.89
	3.9684	2.70	2.59	2.55
	7.9368	1.99	2.21	1.87
	15.8737	1.34	1.55	1.00
0.3503	1.4191	5.04	5.09	4.91
	3.5476	4.69	4.93	4.52
	7.0952	4.48	4.65	4.14
	14.1905	3.57	4.13	3.10
	35.476	1.49	2.74	0.42
0.3945	1.3634	6.71	6.64	6.50
	3.4086	6.44	6.54	6.16
	6.8172	6.15	6.31	5.73
	13.6344	4.47	5.86	4.11
	34.0859	2.61	4.58	1.59

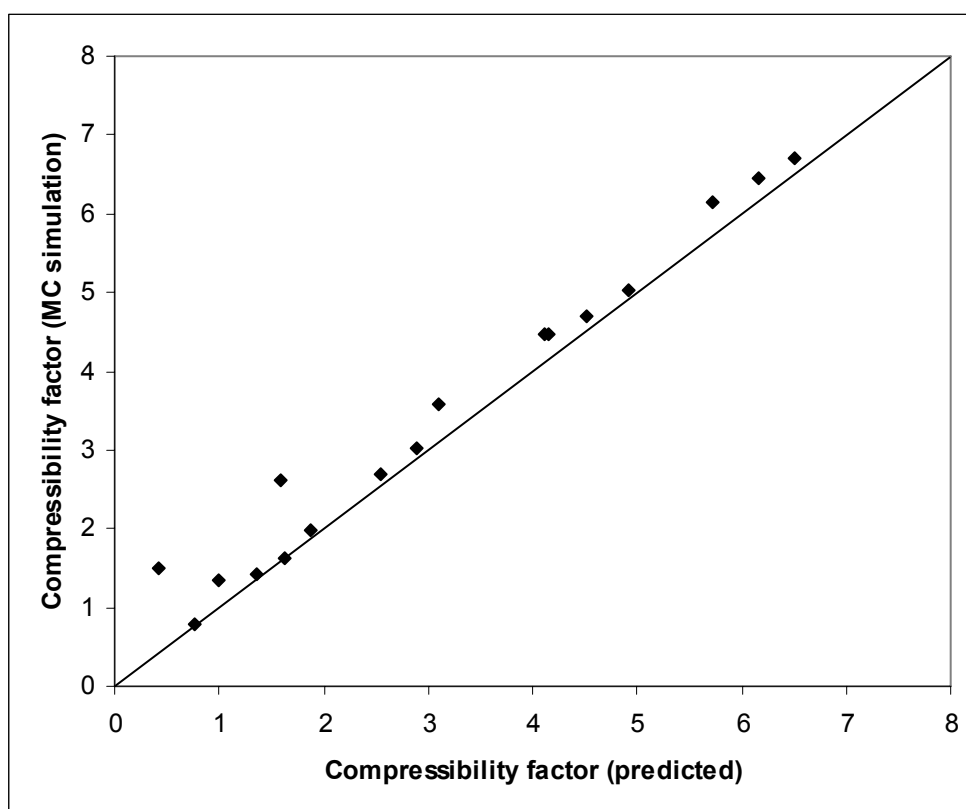


Figure 6.3: Comparison of compressibility factor of restricted primitive model electrolyte between MC simulation results and the ones calculated with the model proposed.

The compressibility factors predicted by the present model are compared with those of MC simulation data graphically in figure 6.3. The diagonal line represents the points where simulation and predicted data are exactly equal. When simulation results are higher than the predicted values, the points fall above the line. Most of the data are close to the diagonal line which means the prediction is quite close to that of simulation data.

6.8.2 Application to Real Solution: [bmpy] [tfb] +Toluene+Heptane System

The model is employed to predict phase diagram of the real solution consisting of N-butyl-methyl-pyridinium, toluene and heptane at 1 atm and 40°C under some simplified assumptions which are listed below:

- (i) In the calculation of the radius of curvature, geometric shape of the four components is assumed to be similar to that of a prolate spherocylinder.
- (ii) Molecular area and volume of the cation, toluene, and heptane is calculated by UNIFAC group contribution method. The volume of anion is found from COSMOtherm and is scaled up to reflect UNIFAC volume.
- (iii) Dielectric constant of the ionic liquid solvent is close to that of water.
- (iv) The depth of square-well for toluene and heptane are found by comparing the model for pure component to the Tait equation.
- (v) The depth of square-well for cation is found from following assumption as molecular weight of the cation is closely equal to that of heptadecane.

$$t_{cation} = t_{toluene} \frac{T_{c,C_{17}H_{36}}}{T_{c,toluene}} \quad (6-47)$$

T_c is critical temperature

- (vi) The depth of square-well for anion will be fitted to experimental data.
- (vii) The depth of square-well in case of cross interaction is found from following rule and will be fitted to experimental data.

$$t_{ij} = c_{ij} \sqrt{t_{ii} t_{jj}} \quad (6-48)$$

- (viii) The mol fraction of ionic liquid in the organic phase is in the order of 10^{-4} and mol fraction of heptane in the ionic liquid phase is in the order of 10^{-3} .

After fitting the parameters with experimental data, the model is employed for the system consisting of N-methyl butyl pyridinium, toluene and heptane. For best fit, the depth of depth of square-well for anion is kept close to that of toluene and all c_{ij} values are found to be equal to 1 except the cross parameters between toluene and heptane which is related to the mol number of toluene in the feed as follows,

$$c_{12} = 46.602 \exp[2.1263n_{\text{toluene}}] \quad (6-49)$$

The phase diagram predicted by the model is shown in figure in 6.4 while figure 6.5 compares it with the one found from experiment. The prediction seems well unto 50 mol% of toluene in the feed. When the toluene content is higher than that the prediction is not well.

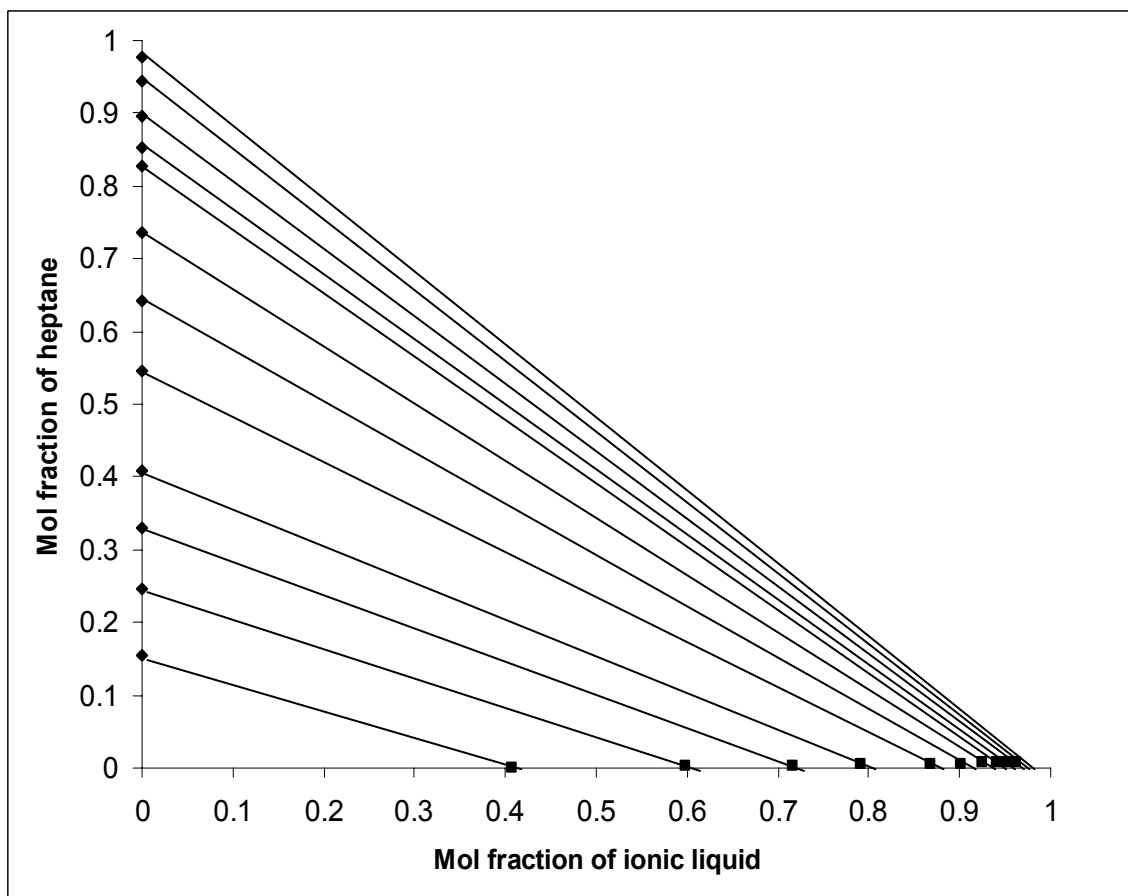


Figure 6.4: Predicted phase diagram of [bmpy] [tfb] + toluene+ heptane system at 1 atm and 40°C by the model developed.

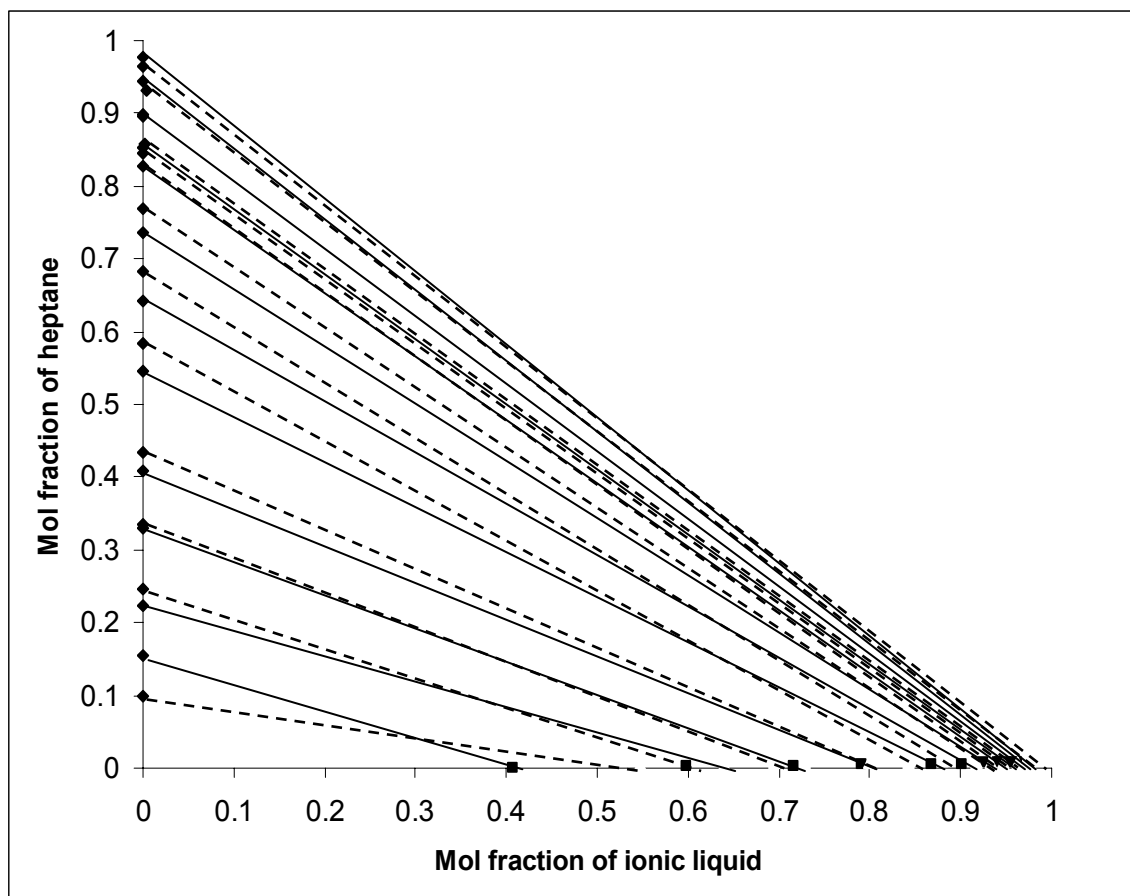


Figure 6.5: Comparison of phase diagram of ionic liquid ([bmpy] [tfb]) +toluene+heptane system at 1 atm and 40°C (—, prediction; ---, experimental)

CHAPTER 7

CONCLUSIONS & RECOMMENDATIONS

This work comprises of mainly three parts. Chapter 4 deals with the screening of ionic liquids possessing high selectivity and capacity and in parallel explores effect of some thermodynamic and molecular parameters on selectivity and capacity. Chapter 5 validates synergistic behavior of binary ionic liquids. Chapter 6 describes an excess Gibbs energy models. Specific conclusions that are obtained during these works are summarized below.

7.1 CONCLUSIONS

The following conclusions are deduced from the results and discussions

- ❖ Like organic solvents, ILs are also characterized by the dilemma of having high selectivity at the cost of low capacity and vice versa.
- ❖ There are many ILs which show
$$C_{IL}^{\infty} \geq C_{sulfolane}^{\infty} \text{ and } S_{IL}^{\infty} \geq S_{sulfolane}^{\infty}$$
- ❖ Cations from the same precursor behave predictively with the same anion.
- ❖ The ranking of anions changes to some extent from cation to cation.
- ❖ Ammonium and Phosphonium ILs show very high capacity but very low selectivity.

- ❖ Cations based on imidazolium and pyridinium are more suitable than other cations in terms of tunability as response of these cations to capacity and selectivity is well predictable.
- ❖ Moderate alkyl chain length of cations provides good compromise between selectivity and capacity.
- ❖ Effect of temperature and pressure on capacity and selectivity is insignificant.
- ❖ Irregular behavior might provide efficient solvents.
- ❖ The feed composition and price of IL will influence the optimum solvent choice.

- ❖ Mixing ionic liquids may be a viable approach in the design and modification of IL based solvents toward specific ends.
- ❖ Some binary IL mixtures behave ideally, others deviate positively or negatively from the ideal behavior.
- ❖ Synergy in capacity & selectivity was found in case of the binary IL mixture containing 1-butyl-4-methyl pyridinium tetrafluoroborate and 1-methyl-3-octyl imidazolium tetrafluoroborate.
- ❖ The proposed model predicts compressibility factor for electrolyte solutions of primitive model and molten salts.

7.2 SUGGESTIONS FOR FUTURE WORK

Below is a list of points that are suggested for consideration for further work

- ❖ We recommend use of binary ILs with synergy

- ❖ Conduct experiments with the other screened ILs
- ❖ Improve capacity and selectivity by mixing ILs with other additives

*APPENDIX A: Identification Number and Full Name of
Cations & Anions*

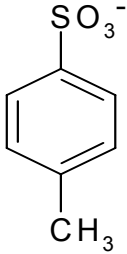
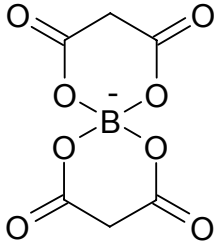
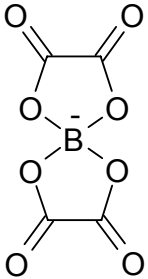
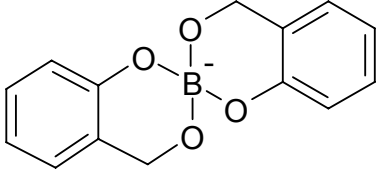
CATION ID #	Full Name in COSMO-RS
1	1,1-dimethyl-pyrrolidinium.cosmo
2	1,1-dipropyl-pyrrolidinium.cosmo
3	1-ethyl-1-methyl-pyrrolidinium0.cosmo
4	1-butyl-1-methyl-pyrrolidinium0.cosmo
5	1-butyl-1-ethyl-pyrrolidinium.cosmo
6	1-hexyl-1-methyl-pyrrolidinium0.cosmo
7	1-octyl-1-methyl-pyrrolidinium0.cosmo
8	3-methyl-imidazolium.cosmo
9	1-butyl-imidazolium0.cosmo
10	1,3-methyl-imidazolium.cosmo
11	1-ethyl-3-methyl-imidazolium0.cosmo
12	1-butyl-3-methyl-imidazolium0.cosmo
13	1-pentyl-3-methyl-imidazolium0.cosmo
14	1-hexyl-3-methyl-imidazolium0.cosmo
15	1-octyl-3-methyl-imidazolium0.cosmo
16	1-decyl-3-methyl-imidazolium0.cosmo
17	1-dodecyl-3-methyl-imidazolium0.cosmo
18	1-tetradecyl-3-methyl-imidazolium0.cosmo
19	1-hexadecyl-3-methyl-imidazolium0.cosmo
20	1-octadecyl-3-methyl-imidazolium0.cosmo
21	1-benzyl-3-methyl-imidazolium0.cosmo
22	1-ethyl-2-3-methyl-imidazolium0.cosmo
23	1-propyl-2-3-methyl-imidazolium0.cosmo
24	1-butyl-2-3-methyl-imidazolium0.cosmo
25	1-hexyl-2-3-methyl-imidazolium0.cosmo
26	1-hexadecyl-2-3-methyl-imidazolium0.cosmo
27	1-methyl-3-(3-phenyl-propyl)-imidazolium0.cosmo
28	4-methyl-n-butylpyridinium.cosmo
29	1-ethyl-pyridinium0.cosmo
30	1-butyl-pyridinium0.cosmo
31	1-hexyl-pyridinium0.cosmo
32	1-octyl-pyridinium0.cosmo
33	1-butyl-3-ethyl-pyridinium0.cosmo
34	1-butyl-3-methyl-pyridinium0.cosmo
35	1-butyl-4-methyl-pyridinium.cosmo
36	1-hexyl-3-methyl-pyridinium0.cosmo
37	1-hexyl-4-methyl-pyridinium0.cosmo
38	3-methyl-1-octyl-pyridinium0.cosmo
39	4-methyl-1-octyl-pyridinium0.cosmo
40	1-butyl-3,4-dimethyl-pyridinium0.cosmo
41	1-butyl-3,5-dimethyl-pyridinium0.cosmo
42	methyl-trioctyl-ammonium.cosmo
43	tetra-methylammonium.cosmo
44	tetra-ethylammonium.cosmo

45	tetra-n-butylammonium.cosmo
46	benzyl-triphenyl-phosphonium.cosmo
47	tetrabutyl-phosphonium.cosmo
48	trihexyl-tetradecyl-phosphonium.cosmo
49	triisobutyl-methyl-phosphonium.cosmo
50	guanidinium.cosmo
51	hexamethylguanidinium.cosmo
52	N,N,N,N,N-pentamethyl-N-isopropyl-guanidinium.cosmo
53	N,N,N,N,N-pentamethyl-N-propyl-guanidinium.cosmo
54	N,N,N,N-tetramethyl-N-ethylguanidinium.cosmo
55	S-ethyl-N,N,N,N-tetramethylisothiuronium.cosmo
56	O-ethyl-N,N,N,N-tetramethylisouronium.cosmo
57	O-methyl-N,N,N,N-tetramethylisouronium.cosmo
58	N-butyl-isoquinolinium0.cosmo

ID # of Anions	Full Name in COSMOtherm	Symbol Used
1	bf4.cosmo	[tfb]
2	pf6.cosmo	[hfp]
3	methylsulfate.cosmo	[ms]
4	ethylsulfate0.cosmo	[es]
5	butylsulfate0.cosmo	[bs]
6	octylsulfate0.cosmo	[os]
7	clo4.cosmo	[pc]
8	cl.cosmo	[cl]
9	br.cosmo	[br]
10	i.cosmo	[i]
11	toluene-4-sulfonate.cosmo	[ts]
12	trifluoromethane-sulfonate.cosmo	[tms]
13	tris(nonafluorobutyl)trifluorophosphate.cosmo	[tnbtp]
14	tris(pentafluoroethyl)trifluorophosphate.cosmo	[tpetp]
15	bisbiphenyldiolatoborate.cosmo	[bbdb]
16	bismalonatoborate.cosmo	[bmb]
17	bisoxalatoborate.cosmo	[bsxb]
18	bissalicylatoborate.cosmo	[bscb]
19	tetracyanoborate.cosmo	[tcb]
20	bis(2,4,4-trimethylpentyl)phosphinate.cosmo	[btmpp]
21	bis-pentafluoroethyl-phosphinate.cosmo	[bpfep]
22	bis(trifluoromethyl)imide.cosmo	[btfmi]
23	bis(trifluoromethylsulfonyl)methane0.cosmo	[btfmsm]
24	tf2n0.cosmo	[tfn]
25	decanoate.cosmo	[d]
26	dicyanamide.cosmo	[dcyn]

APPENDIX B: Chemical Formula/Structure of Some

Anions

F_4B^- ID#1: [tfb]	F_6P^- ID#2: [hfp]	ClO_4^- ID#7: [pc]	$F_3C-SO_3^-$ ID#12: [tms]
 ID#11: [ts]	 ID#16: [bmb]	 ID#17: [bsxb]	 ID#18: [bscb]
$(CN)_4B^-$ ID#19: [tcb]	$(OC_8H_{17})_2P^-$ ID#20: [btmpp]	$(OC_2F_5)_2P^-$ ID#21: [bpfep]	$(CF_3)_2N^-$ ID#22: [btfmi]
$F_{18}C_6P^-$ ID#14: [tpetp]	$(SO_2CF_3)_2HC^-$ ID#23: [btfmsm]	$(SO_2CF_3)_2HN^-$ ID#24: [tfn]	$(CN)_2N^-$ ID#26: [dcyn]

*APPENDIX C: Calculated Infinite Dilution Capacity and
Selectivity of the ILs*

Cation #	Anion #	C [∞]	S [∞]
1	1	0.231424	11.82103
1	2	0.074467	45.40989
1	3	0.4984	6.588528
1	4	0.40495	7.484319
1	5	0.363341	7.750288
1	6	0.484047	5.872674
1	7	0.174078	16.30954
1	8	13.31828	0.742918
1	9	7.22406	0.889585
1	10	2.126138	2.412926
1	11	0.444203	7.642846
1	12	0.183836	20.01476
1	13	0.916097	7.937672
1	14	0.822207	11.56485
1	15	0.7882	8.916915
1	16	0.191767	19.37144
1	17	0.184005	31.81348
1	18	0.460219	13.30886
1	19	0.224369	28.04611
1	20	0.792009	2.833436
1	21	0.392494	14.68902
1	22	0.111337	45.1396
1	23	0.338865	19.2573
1	24	0.332834	20.70489
1	25	0.594995	3.524153
1	26	0.245055	12.72769
3	1	0.299826	10.61332
3	2	0.156938	26.48583
3	3	0.577959	6.137024
3	4	0.517895	6.515279
3	5	0.489215	6.479543
3	6	0.615222	5.078571
3	7	0.251339	13.19912
3	8	5.874772	1.070408
3	9	3.470044	1.282344
3	10	1.436554	3.013674
3	11	0.573841	6.533874
3	12	0.298411	14.06768
3	13	0.998239	6.726938
3	14	0.949706	9.095138
3	15	0.928669	7.525671
3	16	0.283024	14.72122
3	17	0.300372	20.98819
3	18	0.598276	10.56895
3	19	0.354487	18.52609
3	20	0.892113	2.619098
3	21	0.523828	11.06548
3	22	0.211802	25.75838
3	23	0.472729	13.97486

Cation #	Anion #	C [∞]	S [∞]
2	1	0.521569	7.841499
2	2	0.506707	10.58111
2	3	0.743257	5.382699
2	4	0.764753	5.148318
2	5	0.799897	4.69468
2	6	0.945565	3.77247
2	7	0.501138	8.299788
2	8	1.683756	2.101329
2	9	1.253171	2.437761
2	10	0.894006	4.156652
2	11	0.86343	4.980698
2	12	0.651308	7.556212
2	13	1.234637	4.569665
2	14	1.316158	5.246651
2	15	1.296149	5.144818
2	16	0.548278	8.848076
2	17	0.697096	9.614285
2	18	0.979246	6.547675
2	19	0.789076	8.430533
2	20	1.135743	2.213777
2	21	0.910435	6.157679
2	22	0.622755	9.578586
2	23	0.887699	7.219675
2	24	0.897867	7.484169
2	25	0.947249	2.606061
2	26	0.617965	6.823073
4	1	0.318506	10.23691
4	2	0.321881	14.76471
4	3	0.508346	6.340769
4	4	0.531393	6.017729
4	5	0.576862	5.394716
4	6	0.734847	4.168599
4	7	0.306063	10.9895
4	8	1.467936	2.078216
4	9	0.998538	2.504753
4	10	0.636925	4.631821
4	11	0.635786	5.683402
4	12	0.443223	9.540444
4	13	1.17827	5.129663
4	14	1.210771	6.137331
4	15	1.125252	5.791319
4	16	0.384977	10.92933
4	17	0.496822	12.32242
4	18	0.788264	7.604194
4	19	0.584217	10.68745
4	20	0.960979	2.288508
4	21	0.7347	7.248684
4	22	0.436982	12.85059
4	23	0.70408	8.762051

3	24	0.470423	14.81929
3	25	0.699134	3.173801
3	26	0.344889	10.26726
5	1	0.4693	8.171643
5	2	0.469976	10.96403
5	3	0.678037	5.529846
5	4	0.703018	5.26431
5	5	0.744947	4.766155
5	6	0.896047	3.796008
5	7	0.452819	8.614872
5	8	1.530795	2.144036
5	9	1.125534	2.508638
5	10	0.802196	4.280972
5	11	0.807314	5.057488
5	12	0.606972	7.727845
5	13	1.238272	4.587017
5	14	1.310616	5.277223
5	15	1.266209	5.17842
5	16	0.512747	9.051677
5	17	0.658538	9.800173
5	18	0.944421	6.602511
5	19	0.752772	8.567277
5	20	1.091789	2.203881
5	21	0.882089	6.190959
5	22	0.590549	9.806447
5	23	0.858574	7.296538
5	24	0.86781	7.565663
5	25	0.898415	2.603535
5	26	0.565326	7.024612
7	1	0.515982	6.824233
7	2	0.677468	7.171107
7	3	0.601125	5.249538
7	4	0.655588	4.791292
7	5	0.740379	4.137038
7	6	0.909134	3.267581
7	7	0.525302	6.694458
7	8	0.706817	3.000053
7	9	0.586482	3.456823
7	10	0.541603	4.842204
7	11	0.774271	4.500237
7	12	0.713265	5.740349
7	13	1.467906	3.638931
7	14	1.572548	3.873312
7	15	1.391423	4.176986
7	16	0.594251	7.069219
7	17	0.838004	6.649289
7	18	1.069143	5.090927
7	19	0.952274	5.804015
7	20	1.064311	1.952284
7	21	1.052436	4.483079
7	22	0.839094	6.198888
7	23	1.059818	5.155994

4	24	0.707999	9.143379
4	25	0.75656	2.738855
4	26	0.403793	8.576792
6	1	0.402583	8.508877
6	2	0.49724	9.868718
6	3	0.535962	5.923219
6	4	0.582589	5.43397
6	5	0.6565	4.71279
6	6	0.825891	3.657427
6	7	0.404699	8.584086
6	8	0.861455	2.756495
6	9	0.654874	3.250536
6	10	0.528431	5.098213
6	11	0.700254	5.073901
6	12	0.579017	7.247525
6	13	1.333967	4.243719
6	14	1.41224	4.734187
6	15	1.270191	4.841768
6	16	0.486396	8.697712
6	17	0.673012	8.720617
6	18	0.937768	6.10196
6	19	0.778993	7.568539
6	20	1.016665	2.099649
6	21	0.906175	5.533995
6	22	0.646002	8.460261
6	23	0.894677	6.500181
6	24	0.904753	6.715914
6	25	0.807653	2.4967
6	26	0.49585	6.997409
8	1	0.003411	272.9777
8	2	0.007644	578.2174
8	3	0.032862	41.86667
8	4	0.046491	32.42922
8	5	0.084879	19.97577
8	6	0.210565	9.34209
8	7	0.003903	366.6068
8	8	1.301031	3.314942
8	9	0.423267	4.39053
8	10	0.071389	22.0506
8	11	0.092918	21.71254
8	12	0.018978	126.4516
8	13	0.693695	14.91698
8	14	0.604833	24.96213
8	15	0.500042	13.4484
8	16	0.034649	80.02347
8	17	0.060642	107.6387
8	18	0.211339	25.51024
8	19	0.079087	89.77621
8	20	0.559852	3.36282
8	21	0.150916	32.27329
8	22	0.047211	167.2367
8	23	0.12913	46.6424

7	24	1.075222	5.290432
7	25	0.856413	2.302464
7	26	0.603691	5.688918
9	1	0.054272	37.14875
9	2	0.119777	42.5483
9	3	0.104404	16.42115
9	4	0.13816	12.9939
9	5	0.206899	9.149507
9	6	0.363647	5.541305
9	7	0.067208	36.19098
9	8	0.169146	6.32519
9	9	0.088889	7.900057
9	10	0.078211	16.91516
9	11	0.215675	10.05168
9	12	0.131955	21.27622
9	13	0.990275	8.545971
9	14	0.998808	11.17702
9	15	0.757537	7.663586
9	16	0.140985	22.80044
9	17	0.240594	23.86254
9	18	0.429436	11.28822
9	19	0.289499	20.11629
9	20	0.64379	2.441274
9	21	0.361804	11.24384
9	22	0.237088	26.51233
9	23	0.350518	14.92071
9	24	0.350799	16.12515
9	25	0.411563	3.213498
9	26	0.099458	22.37401
11	1	0.125061	28.20192
11	2	0.093134	61.47865
11	3	0.285523	12.74756
11	4	0.296899	11.93458
11	5	0.342394	9.937843
11	6	0.507193	6.53858
11	7	0.122246	34.64003
11	8	2.297536	2.525603
11	9	1.258559	2.870166
11	10	0.550294	8.000148
11	11	0.364816	10.36578
11	12	0.166501	28.26177
11	13	0.926675	9.141825
11	14	0.865903	13.39726
11	15	0.789486	9.535198
11	16	0.188171	25.84275
11	17	0.230394	36.27831
11	18	0.466675	14.76767
11	19	0.262934	31.99245
11	20	0.828322	2.944179
11	21	0.385004	16.484
11	22	0.154668	48.51097
11	23	0.358401	21.73426

8	24	0.122964	53.54005
8	25	0.320497	4.979453
8	26	0.011497	145.47
10	1	0.09137	35.71176
10	2	0.034648	140.8718
10	3	0.260549	14.80744
10	4	0.244077	14.89521
10	5	0.266897	12.78778
10	6	0.418649	7.950939
10	7	0.076148	52.19047
10	8	7.407753	1.65308
10	9	3.852827	1.818806
10	10	0.992049	6.423673
10	11	0.291699	13.11308
10	12	0.091919	49.21803
10	13	0.82481	11.31241
10	14	0.717614	18.35001
10	15	0.666088	11.86402
10	16	0.123796	37.96292
10	17	0.133014	63.91985
10	18	0.355275	20.05262
10	19	0.155172	56.77068
10	20	0.784583	3.34364
10	21	0.277967	24.60845
10	22	0.070646	105.8751
10	23	0.244331	33.57998
10	24	0.239838	37.15209
10	25	0.568865	4.559532
10	26	0.107329	35.3734
12	1	0.197193	19.22516
12	2	0.247468	25.41704
12	3	0.322484	10.55321
12	4	0.36321	9.267559
12	5	0.439067	7.453472
12	6	0.617564	5.142195
12	7	0.216048	20.15394
12	8	0.787027	3.932636
12	9	0.476383	4.518726
12	10	0.3649	9.141002
12	11	0.452081	8.019932
12	12	0.306299	15.26633
12	13	1.124948	6.755385
12	14	1.146045	8.592932
12	15	0.975492	7.10167
12	16	0.295743	16.40703
12	17	0.422028	18.35148
12	18	0.644544	9.957838
12	19	0.479298	15.98163
12	20	0.884332	2.517459
12	21	0.578051	9.883434
12	22	0.361808	20.02637
12	23	0.572889	12.42648

11	24	0.357402	23.5706
11	25	0.613544	3.86113
11	26	0.164591	23.5772
13	1	0.245885	15.96167
13	2	0.33671	18.93951
13	3	0.354413	9.582514
13	4	0.401643	8.36202
13	5	0.485351	6.719609
13	6	0.666435	4.722744
13	7	0.273279	16.1723
13	8	0.635583	4.277377
13	9	0.407158	4.878218
13	10	0.361283	8.86774
13	11	0.495101	7.27963
13	12	0.377395	12.36772
13	13	1.216706	6.024292
13	14	1.268579	7.315168
13	15	1.053415	6.386779
13	16	0.350343	13.88501
13	17	0.516029	14.56003
13	18	0.724088	8.65364
13	19	0.583044	12.67397
13	20	0.913426	2.390159
13	21	0.667756	8.292571
13	22	0.46969	15.08393
13	23	0.67349	10.24347
13	24	0.685702	10.76306
13	25	0.696148	2.998284
13	26	0.318516	12.10054
15	1	0.420402	9.667502
15	2	0.61678	9.998349
15	3	0.473434	7.054178
15	4	0.52717	6.233824
15	5	0.619624	5.12387
15	6	0.795509	3.813548
15	7	0.465929	9.396244
15	8	0.525223	4.224834
15	9	0.385585	4.691207
15	10	0.431179	6.974147
15	11	0.622126	5.60254
15	12	0.585223	7.618961
15	13	1.455861	4.581837
15	14	1.567461	5.071162
15	15	1.25043	4.924142
15	16	0.518268	9.177272
15	17	0.779383	8.682938
15	18	0.931208	6.20081
15	19	0.862006	7.616523
15	20	0.984755	2.096501
15	21	0.900772	5.572813
15	22	0.774643	8.285276
15	23	0.939476	6.633881

12	24	0.58067	13.15866
12	25	0.667435	3.193923
12	26	0.263658	14.56877
14	1	0.30009	13.35713
14	2	0.428724	14.84703
14	3	0.391025	8.656063
14	4	0.442032	7.55863
14	5	0.530581	6.100679
14	6	0.711284	4.37414
14	7	0.334833	13.26064
14	8	0.568086	4.389784
14	9	0.382333	4.959376
14	10	0.376536	8.301365
14	11	0.537163	6.645833
14	12	0.447279	10.32595
14	13	1.301539	5.454658
14	14	1.377785	6.385693
14	15	1.122948	5.815112
14	16	0.405687	11.95082
14	17	0.606705	11.98313
14	18	0.795971	7.664506
14	19	0.68034	10.45395
14	20	0.93895	2.282885
14	21	0.749812	7.148339
14	22	0.574335	11.98241
14	23	0.76659	8.706675
14	24	0.783117	9.093319
14	25	0.722771	2.833691
14	26	0.375062	10.22596
16	1	0.55578	7.289027
16	2	0.804147	7.295225
16	3	0.571482	5.790566
16	4	0.624838	5.198135
16	5	0.716281	4.36955
16	6	0.88328	3.370463
16	7	0.607482	7.025525
16	8	0.547259	3.835002
16	9	0.430769	4.193602
16	10	0.51308	5.756732
16	11	0.715844	4.777465
16	12	0.72424	5.919488
16	13	1.588845	3.931575
16	14	1.72102	4.178156
16	15	1.36786	4.251365
16	16	0.637932	7.279557
16	17	0.94393	6.671936
16	18	1.060624	5.158986
16	19	1.029556	5.889847
16	20	1.033527	1.943655
16	21	1.038759	4.533526
16	22	0.959913	6.190588
16	23	1.098337	5.296944

15	24	0.963327	6.865576
15	25	0.772076	2.551828
15	26	0.491196	7.613173
17	1	0.684441	5.797229
17	2	0.970783	5.707437
17	3	0.664658	4.882903
17	4	0.715608	4.445267
17	5	0.803223	3.810879
17	6	0.959203	3.030507
17	7	0.739011	5.569025
17	8	0.584778	3.4514
17	9	0.483452	3.728664
17	10	0.595804	4.848745
17	11	0.800913	4.159105
17	12	0.847323	4.832868
17	13	1.703419	3.461112
17	14	1.843853	3.572587
17	15	1.466307	3.750953
17	16	0.749385	6.004385
17	17	1.086017	5.403679
17	18	1.171093	4.426504
17	19	1.170425	4.801172
17	20	1.07448	1.819024
17	21	1.154419	3.835002
17	22	1.117146	4.933408
17	23	1.232121	4.417438
17	24	1.266221	4.51981
17	25	0.875594	2.147426
17	26	0.725748	4.820415
19	1	0.921168	4.062181
19	2	1.248368	3.945478
19	3	0.843814	3.682014
19	4	0.887202	3.429313
19	5	0.963635	3.036635
19	6	1.09646	2.53347
19	7	0.974245	3.89935
19	8	0.683805	2.820319
19	9	0.604809	2.994838
19	10	0.762355	3.633295
19	11	0.958829	3.296166
19	12	1.059988	3.530361
19	13	1.883849	2.805467
19	14	2.018768	2.786733
19	15	1.628236	3.047282
19	16	0.9546	4.406056
19	17	1.321447	3.898571
19	18	1.357612	3.450917
19	19	1.395841	3.505769
19	20	1.148673	1.625491
19	21	1.341404	2.94969
19	22	1.365809	3.505349
19	23	1.447875	3.323904

16	24	1.128058	5.445666
16	25	0.827412	2.327698
16	26	0.614103	5.915583
18	1	0.806515	4.786072
18	2	1.117939	4.670705
18	3	0.755842	4.20494
18	4	0.803311	3.875327
18	5	0.885766	3.380454
18	6	1.030349	2.758481
18	7	0.861188	4.593673
18	8	0.632046	3.111142
18	9	0.54273	3.329127
18	10	0.679592	4.162476
18	11	0.882186	3.679806
18	12	0.959222	4.081522
18	13	1.800829	3.096709
18	14	1.941105	3.127769
18	15	1.552936	3.36161
18	16	0.85489	5.089451
18	17	1.210965	4.532846
18	18	1.270026	3.878661
18	19	1.291555	4.052565
18	20	1.113599	1.71635
18	21	1.255341	3.332324
18	22	1.25108	4.098742
18	23	1.348007	3.792138
18	24	1.385093	3.866153
18	25	0.921905	1.999846
18	26	0.829375	4.062222
20	1	1.02398	3.540613
20	2	1.359174	3.429519
20	3	0.925276	3.285142
20	4	0.964599	3.085797
20	5	1.035161	2.767654
20	6	1.157297	2.352198
20	7	1.074685	3.401376
20	8	0.73598	2.584986
20	9	0.665183	2.726313
20	10	0.840152	3.233354
20	11	1.029658	2.995736
20	12	1.149397	3.125643
20	13	1.95517	2.574512
20	14	2.08106	2.525376
20	15	1.694109	2.796923
20	16	1.045701	3.892494
20	17	1.41654	3.434221
20	18	1.435463	3.119959
20	19	1.484528	3.103809
20	20	1.182886	1.551341
20	21	1.416837	2.660729
20	22	1.461652	3.0784
20	23	1.53389	2.972817

19	24	1.487114	3.378899
19	25	0.96541	1.873484
19	26	0.924425	3.506015
21	1	0.125482	36.04831
21	2	0.17065	47.21303
21	3	0.227582	17.19691
21	4	0.272406	14.46468
21	5	0.360984	10.89049
21	6	0.559242	6.886135
21	7	0.137146	38.66249
21	8	0.569212	6.180134
21	9	0.372372	7.219892
21	10	0.232905	15.6611
21	11	0.359809	11.67967
21	12	0.217233	26.15054
21	13	1.065748	8.804386
21	14	1.027046	12.24099
21	15	0.874351	9.382348
21	16	0.221097	25.75349
21	17	0.315814	30.12424
21	18	0.536809	14.05221
21	19	0.3605	26.35953
21	20	0.89585	3.171422
21	21	0.486644	14.86545
21	22	0.27143	35.06032
21	23	0.466563	18.89184
21	24	0.464802	20.26084
21	25	0.646073	4.240156
21	26	0.176643	26.14322
23	1	0.328804	14.81722
23	2	0.290732	23.1004
23	3	0.548777	8.627718
23	4	0.566639	8.081359
23	5	0.612129	7.023559
23	6	0.780038	5.143018
23	7	0.331058	16.52294
23	8	1.995605	2.717032
23	9	1.281405	3.000743
23	10	0.807806	6.474815
23	11	0.64024	7.434416
23	12	0.407831	14.35502
23	13	1.094697	6.602115
23	14	1.111341	8.534101
23	15	1.067348	7.213686
23	16	0.384523	15.09434
23	17	0.483897	18.16215
23	18	0.741594	10.05269
23	19	0.538917	16.07701
23	20	1.048895	2.66971
23	21	0.658209	10.31738
23	22	0.383072	20.19369
23	23	0.634757	12.59601

20	24	1.574389	3.015151
20	25	1.007032	1.770921
20	26	1.009633	3.099064
22	1	0.299407	16.57756
22	2	0.195741	33.4958
22	3	0.558985	9.104602
22	4	0.543181	8.916023
22	5	0.558382	8.017687
22	6	0.7146	5.806396
22	7	0.28249	20.03859
22	8	3.666499	2.109857
22	9	2.285231	2.291508
22	10	1.104604	5.760533
22	11	0.594882	8.324975
22	12	0.319693	18.78953
22	13	0.998888	7.720198
22	14	0.969609	10.72664
22	15	0.960652	8.386389
22	16	0.320872	18.4645
22	17	0.36919	25.02061
22	18	0.63524	12.24442
22	19	0.408631	22.41947
22	20	1.01698	2.899157
22	21	0.542828	13.32018
22	22	0.259372	30.51963
22	23	0.508397	16.62188
22	24	0.511441	17.72879
22	25	0.820778	3.652091
22	26	0.349091	15.12365
24	1	0.359309	13.57229
24	2	0.378718	18.00123
24	3	0.544699	8.376666
24	4	0.581547	7.641776
24	5	0.648105	6.482913
24	6	0.824999	4.755158
24	7	0.376592	14.38074
24	8	1.348762	3.293497
24	9	0.894203	3.642936
24	10	0.674507	7.022856
24	11	0.667148	6.959516
24	12	0.478589	12.04223
24	13	1.182685	5.893618
24	14	1.233884	7.250134
24	15	1.147089	6.487712
24	16	0.4358	13.19133
24	17	0.582164	14.60027
24	18	0.822059	8.797785
24	19	0.648273	12.85831
24	20	1.072591	2.53271
24	21	0.752674	8.660998
24	22	0.494651	15.37204
24	23	0.740461	10.41305

23	24	0.642292	13.29596
23	25	0.847832	3.319586
23	26	0.400592	12.65396
25	1	0.474254	10.22934
25	2	0.58192	11.42176
25	3	0.604071	7.186685
25	4	0.657216	6.4591
25	5	0.742812	5.427942
25	6	0.923317	4.077443
25	7	0.509741	10.26284
25	8	0.921085	3.775225
25	9	0.661707	4.151543
25	10	0.627631	6.702295
25	11	0.752501	5.916648
25	12	0.640444	8.59551
25	13	1.350868	4.789423
25	14	1.453591	5.458696
25	15	1.303088	5.337621
25	16	0.558717	9.992152
25	17	0.785132	9.949875
25	18	0.987674	6.871483
25	19	0.8684	8.754694
25	20	1.125669	2.291737
25	21	0.941884	6.39336
25	22	0.726859	9.747589
25	23	0.950133	7.479306
25	24	0.970346	7.748506
25	25	0.91817	2.791056
25	26	0.564806	8.422107
27	1	0.228129	20.97497
27	2	0.30067	25.22057
27	3	0.331863	12.28649
27	4	0.382639	10.64329
27	5	0.475023	8.464492
27	6	0.670177	5.812554
27	7	0.244788	21.6436
27	8	0.55139	5.792882
27	9	0.390201	6.632223
27	10	0.322571	11.63514
27	11	0.476989	9.04489
27	12	0.348446	16.16648
27	13	1.20194	7.206043
27	14	1.180251	9.271823
27	15	1.000407	7.712173
27	16	0.323462	17.372
27	17	0.449301	18.99147
27	18	0.674264	10.66898
27	19	0.513625	16.65649
27	20	0.967546	2.921946
27	21	0.6382	10.60452
27	22	0.417199	20.24768
27	23	0.622568	13.0874

24	24	0.752524	10.91208
24	25	0.867419	3.131243
24	26	0.442129	11.22721
26	1	1.10758	3.717458
26	2	1.386035	3.55356
26	3	1.047857	3.482742
26	4	1.093406	3.266046
26	5	1.168659	2.919697
26	6	1.297432	2.465612
26	7	1.153727	3.572087
26	8	0.891818	2.770949
26	9	0.809278	2.915613
26	10	0.970511	3.436385
26	11	1.165438	3.192103
26	12	1.264134	3.321346
26	13	1.884886	2.570036
26	14	2.026433	2.528585
26	15	1.791507	2.910951
26	16	1.118733	4.109577
26	17	1.488855	3.599518
26	18	1.544742	3.288758
26	19	1.56696	3.247969
26	20	1.323311	1.660519
26	21	1.530871	2.821842
26	22	1.501744	3.220092
26	23	1.612244	3.088576
26	24	1.649376	3.127175
26	25	1.145392	1.906616
26	26	1.124802	3.334424
28	1	0.332604	14.55522
28	2	0.389367	18.41637
28	3	0.473813	8.952206
28	4	0.519882	7.987997
28	5	0.600608	6.590439
28	6	0.783901	4.740582
28	7	0.362072	15.14893
28	8	0.882909	3.840183
28	9	0.591518	4.248135
28	10	0.523911	7.997348
28	11	0.603317	7.1097
28	12	0.451074	12.25851
28	13	1.189338	6.064912
28	14	1.252933	7.441631
28	15	1.117716	6.468343
28	16	0.420432	13.51459
28	17	0.588968	14.68255
28	18	0.794754	8.782754
28	19	0.641104	12.94721
28	20	1.000647	2.437566
28	21	0.716209	8.588035
28	22	0.508112	15.36773
28	23	0.726975	10.47698

27	24	0.625438	13.79478
27	25	0.728555	3.763389
27	26	0.292815	16.01186
29	1	0.098988	38.47659
29	2	0.071048	88.79319
29	3	0.246776	16.01555
29	4	0.260789	14.68681
29	5	0.3109	11.80603
29	6	0.481479	7.373924
29	7	0.099698	48.52747
29	8	2.521659	2.91066
29	9	1.316961	3.249789
29	10	0.507838	10.00945
29	11	0.322784	12.40538
29	12	0.135587	38.37208
29	13	0.901015	10.28462
29	14	0.828215	15.74669
29	15	0.749917	10.81766
29	16	0.164688	32.4435
29	17	0.204703	46.98508
29	18	0.428827	17.46432
29	19	0.226889	42.05802
29	20	0.827743	3.204384
29	21	0.35193	20.44503
29	22	0.126451	67.68266
29	23	0.324343	26.95449
29	24	0.323349	29.42987
29	25	0.600986	4.302903
29	26	0.130467	32.47238
31	1	0.279461	15.68681
31	2	0.404165	17.37096
31	3	0.369065	9.88205
31	4	0.420495	8.523014
31	5	0.51203	6.754912
31	6	0.699015	4.72728
31	7	0.322532	15.5939
31	8	0.54953	4.973183
31	9	0.355467	5.576827
31	10	0.358634	9.644039
31	11	0.509873	7.390608
31	12	0.424776	11.97535
31	13	1.291103	5.903704
31	14	1.366205	7.054248
31	15	1.105367	6.329745
31	16	0.391546	13.5495
31	17	0.597254	13.6813
31	18	0.775558	8.498673
31	19	0.659434	12.00988
31	20	0.942497	2.420805
31	21	0.736974	8.096728
31	22	0.551418	13.97346
31	23	0.750562	9.8249

28	24	0.741906	11.00357
28	25	0.791296	3.038275
28	26	0.399931	11.62165
30	1	0.176	23.77132
30	2	0.22166	31.60104
30	3	0.297613	12.4698
30	4	0.338916	10.77825
30	5	0.417892	8.463646
30	6	0.603244	5.64387
30	7	0.200189	25.06444
30	8	0.779204	4.551059
30	9	0.45149	5.173606
30	10	0.342517	11.01029
30	11	0.421906	9.139814
30	12	0.279763	18.60983
30	13	1.106207	7.421269
30	14	1.120592	9.72082
30	15	0.950381	7.857433
30	16	0.278423	19.25864
30	17	0.404686	21.8502
30	18	0.617669	11.30913
30	19	0.449813	19.20691
30	20	0.889209	2.699023
30	21	0.556152	11.57491
30	22	0.332807	24.67893
30	23	0.548103	14.50437
30	24	0.556436	15.40866
30	25	0.65987	3.468215
30	26	0.235948	18.00969
32	1	0.406211	10.95001
32	2	0.600884	11.27773
32	3	0.45912	7.852328
32	4	0.513655	6.874714
32	5	0.609063	5.577162
32	6	0.790798	4.082134
32	7	0.463322	10.65288
32	8	0.51401	4.680898
32	9	0.364706	5.160998
32	10	0.422484	7.862857
32	11	0.602919	6.116561
32	12	0.572437	8.56822
32	13	1.45333	4.903994
32	14	1.568527	5.511683
32	15	1.242378	5.302243
32	16	0.511753	10.15981
32	17	0.782593	9.656584
32	18	0.921067	6.764241
32	19	0.854454	8.512196
32	20	0.993022	2.210061
32	21	0.900277	6.181
32	22	0.763858	9.350969
32	23	0.93595	7.325416

31	24	0.768332	10.28041
31	25	0.713843	3.030325
31	26	0.350175	11.99356
33	1	0.403938	11.79776
33	2	0.503751	13.83027
33	3	0.520054	7.834053
33	4	0.571196	6.999929
33	5	0.657814	5.813891
33	6	0.839799	4.281956
33	7	0.439269	11.98505
33	8	0.767541	3.827378
33	9	0.540942	4.230372
33	10	0.533763	7.257678
33	11	0.657584	6.300947
33	12	0.537878	9.829322
33	13	1.266031	5.356335
33	14	1.362454	6.281633
33	15	1.203913	5.727104
33	16	0.488394	11.25193
33	17	0.696099	11.63421
33	18	0.88253	7.533653
33	19	0.756364	10.23978
33	20	1.023581	2.278142
33	21	0.806991	7.134485
33	22	0.633103	11.63689
33	23	0.833357	8.57928
33	24	0.852389	8.95328
33	25	0.816937	2.800618
33	26	0.470856	9.458464
35	1	0.331336	14.44661
35	2	0.387007	18.34982
35	3	0.472644	8.879897
35	4	0.518164	7.934894
35	5	0.597487	6.564393
35	6	0.78003	4.725248
35	7	0.359766	15.05003
35	8	0.888534	3.783388
35	9	0.594822	4.194231
35	10	0.523906	7.898398
35	11	0.601305	7.074311
35	12	0.449148	12.19188
35	13	1.188447	6.054731
35	14	1.25078	7.428099
35	15	1.115059	6.457421
35	16	0.41872	13.45015
35	17	0.585059	14.64238
35	18	0.791977	8.758021
35	19	0.637875	12.90726
35	20	0.996244	2.427568
35	21	0.714	8.558886
35	22	0.50529	15.3263
35	23	0.723994	10.44883

32	24	0.961863	7.589457
32	25	0.768601	2.709218
32	26	0.474614	8.631083
34	1	0.32916	14.65102
34	2	0.384338	18.60425
34	3	0.472115	8.978475
34	4	0.517533	8.014962
34	5	0.597105	6.624733
34	6	0.779975	4.759012
34	7	0.358139	15.26282
34	8	0.906474	3.824547
34	9	0.600602	4.233038
34	10	0.527291	7.992871
34	11	0.600788	7.142551
34	12	0.447471	12.34758
34	13	1.187888	6.08648
34	14	1.249655	7.480652
34	15	1.112697	6.499986
34	16	0.416732	13.5981
34	17	0.582473	14.80774
34	18	0.790395	8.825277
34	19	0.635526	13.05055
34	20	1.002621	2.449956
34	21	0.713479	8.639805
34	22	0.502901	15.51023
34	23	0.721991	10.54793
34	24	0.736775	11.0791
34	25	0.793467	3.054512
34	26	0.397519	11.69709
36	1	0.452231	10.71645
36	2	0.590041	11.77772
36	3	0.548761	7.495853
36	4	0.60421	6.661402
36	5	0.695605	5.515598
36	6	0.877654	4.089407
36	7	0.498684	10.65629
36	8	0.713636	4.093621
36	9	0.512414	4.48541
36	10	0.543159	7.203666
36	11	0.691686	6.015623
36	12	0.605838	8.761087
36	13	1.357001	4.957294
36	14	1.470816	5.654604
36	15	1.262113	5.368776
36	16	0.540315	10.23333
36	17	0.784003	10.12067
36	18	0.949345	6.916916
36	19	0.850286	8.916826
36	20	1.055081	2.227211
36	21	0.892541	6.407826
36	22	0.732272	9.896686
36	23	0.92561	7.613249

35	24	0.738715	10.97357
35	25	0.787854	3.024543
35	26	0.398737	11.53666
37	1	0.447194	10.71613
37	2	0.585814	11.78762
37	3	0.542096	7.483047
37	4	0.597356	6.649023
37	5	0.689015	5.501826
37	6	0.8706	4.079686
37	7	0.492691	10.65426
37	8	0.69667	4.075527
37	9	0.503263	4.476359
37	10	0.532798	7.189632
37	11	0.685229	5.997724
37	12	0.600146	8.742096
37	13	1.356241	4.963197
37	14	1.469199	5.660714
37	15	1.257238	5.360836
37	16	0.536332	10.21646
37	17	0.778954	10.10954
37	18	0.94393	6.903786
37	19	0.84476	8.90631
37	20	1.045941	2.215438
37	21	0.886262	6.389717
37	22	0.727965	9.893025
37	23	0.920385	7.605335
37	24	0.943883	7.896977
37	25	0.838624	2.712552
37	26	0.517119	8.582798
39	1	0.583108	8.084996
39	2	0.786201	8.329638
39	3	0.632723	6.224792
39	4	0.689794	5.58263
39	5	0.783713	4.682677
39	6	0.957219	3.584934
39	7	0.638954	7.878835
39	8	0.661932	3.912631
39	9	0.510925	4.245714
39	10	0.595262	6.134815
39	11	0.775031	5.129048
39	12	0.748142	6.658805
39	13	1.502435	4.202628
39	14	1.646163	4.558073
39	15	1.382823	4.576296
39	16	0.659401	8.03406
39	17	0.95927	7.546999
39	18	1.081833	5.664225
39	19	1.03073	6.674605
39	20	1.090523	2.03998
39	21	1.038001	5.069438
39	22	0.933389	7.106075
39	23	1.095288	5.915346

36	24	0.94945	7.903613
36	25	0.847688	2.727376
36	26	0.522865	8.606606
38	1	0.585925	8.1187
38	2	0.786862	8.36294
38	3	0.637894	6.252554
38	4	0.695292	5.606575
38	5	0.789123	4.704173
38	6	0.963288	3.598906
38	7	0.642375	7.915398
38	8	0.676791	3.928431
38	9	0.519555	4.257533
38	10	0.603468	6.158911
38	11	0.780982	5.153829
38	12	0.752689	6.697873
38	13	1.501804	4.204814
38	14	1.645521	4.564003
38	15	1.387061	4.593857
38	16	0.662011	8.071425
38	17	0.961883	7.583312
38	18	1.086647	5.688235
38	19	1.034096	6.708196
38	20	1.100338	2.054413
38	21	1.044582	5.099895
38	22	0.934753	7.141194
38	23	1.09915	5.940243
38	24	1.129796	6.118702
38	25	0.898056	2.479111
38	26	0.647541	6.656807
40	1	0.508544	10.7305
40	2	0.56639	13.02148
40	3	0.665223	7.286767
40	4	0.713514	6.619236
40	5	0.789589	5.627864
40	6	0.96377	4.230711
40	7	0.540904	11.05574
40	8	1.088126	3.532373
40	9	0.783517	3.805053
40	10	0.73412	6.600464
40	11	0.789455	6.086846
40	12	0.630746	9.423344
40	13	1.254977	5.262678
40	14	1.360194	6.172414
40	15	1.264551	5.664508
40	16	0.565835	10.70959
40	17	0.77189	11.25745
40	18	0.960335	7.409404
40	19	0.826114	9.972288
40	20	1.134052	2.315441
40	21	0.868522	7.067805
40	22	0.682036	11.24721
40	23	0.893479	8.414194

39	24	1.125905	6.093911
39	25	0.888818	2.459874
39	26	0.642864	6.612753
41	1	0.546346	9.89441
41	2	0.601137	11.96517
41	3	0.705942	6.848091
41	4	0.752674	6.260374
41	5	0.824529	5.370709
41	6	0.993787	4.084789
41	7	0.574771	10.17669
41	8	1.146034	3.371845
41	9	0.840496	3.630281
41	10	0.780803	6.171735
41	11	0.828273	5.804712
41	12	0.667255	8.779154
41	13	1.265513	5.05112
41	14	1.37751	5.856897
41	15	1.292188	5.446755
41	16	0.591921	10.07251
41	17	0.801899	10.52275
41	18	0.991751	7.060953
41	19	0.859751	9.313268
41	20	1.153865	2.271567
41	21	0.897114	6.690041
41	22	0.714521	10.40244
41	23	0.923326	7.931721
41	24	0.945328	8.251954
41	25	0.973806	2.773528
41	26	0.615825	8.273106
43	1	0.180206	12.76504
43	2	0.012179	180.1014
43	3	0.393119	7.757654
43	4	0.245602	10.46357
43	5	0.199939	11.56357
43	6	0.310273	7.85272
43	7	0.093647	23.73095
43	8	103.1534	0.335562
43	9	54.13155	0.387589
43	10	7.012941	1.378602
43	11	0.259476	11.0384
43	12	0.060744	46.49803
43	13	0.791296	10.75564
43	14	0.64648	17.87852
43	15	0.587533	12.15827
43	16	0.084236	35.62259
43	17	0.067875	77.41805
43	18	0.279196	20.8145
43	19	0.089827	67.01725
43	20	0.658288	3.32211
43	21	0.225877	25.77513
43	22	0.031043	153.9934
43	23	0.17939	36.12987

40	24	0.914779	8.769326
40	25	0.946975	2.841721
40	26	0.577907	8.901947
42	1	1.321764	2.428612
42	2	1.56627	2.296555
42	3	1.23607	2.414784
42	4	1.275001	2.312502
42	5	1.332794	2.133108
42	6	1.430633	1.890857
42	7	1.307997	2.329142
42	8	0.994154	2.038797
42	9	1.033475	2.17005
42	10	1.106683	2.345058
42	11	1.34883	2.326768
42	12	1.440913	2.251237
42	13	1.915957	1.899613
42	14	2.02287	1.790455
42	15	1.931056	2.173155
42	16	1.292033	2.801122
42	17	1.617363	2.418458
42	18	1.70381	2.365383
42	19	1.687448	2.195544
42	20	1.368817	1.380492
42	21	1.652001	2.002307
42	22	1.641642	2.127973
42	23	1.737778	2.13926
42	24	1.764059	2.153792
42	25	1.219239	1.545102
42	26	1.300303	2.258498
44	1	0.47461	9.026458
44	2	0.341744	15.92739
44	3	0.769771	5.736045
44	4	0.73904	5.757999
44	5	0.722836	5.500946
44	6	0.84857	4.41448
44	7	0.433158	10.33494
44	8	3.307019	1.579977
44	9	2.239107	1.816879
44	10	1.274287	3.686399
44	11	0.801722	5.684653
44	12	0.514617	10.16337
44	13	1.106871	5.681697
44	14	1.128283	7.10643
44	15	1.136493	6.31413
44	16	0.45413	11.24496
44	17	0.525596	13.98926
44	18	0.820048	8.393604
44	19	0.590702	12.42487
44	20	1.080039	2.46135
44	21	0.734384	8.413436
44	22	0.41714	15.21695
44	23	0.694813	10.15514

43	24	0.170745	40.16797
43	25	0.457274	4.423981
43	26	0.124237	20.18803
45	1	1.043622	3.87006
45	2	1.225498	3.852761
45	3	1.078237	3.476757
45	4	1.133893	3.269869
45	5	1.205274	2.941766
45	6	1.335929	2.487753
45	7	1.022946	3.754669
45	8	1.042401	2.480326
45	9	1.032845	2.734723
45	10	0.980833	3.285701
45	11	1.233662	3.226732
45	12	1.211183	3.507698
45	13	1.601751	2.646267
45	14	1.784195	2.603144
45	15	1.765082	3.029962
45	16	1.012039	4.394615
45	17	1.334527	3.943505
45	18	1.499223	3.489261
45	19	1.438883	3.49943
45	20	1.361269	1.686339
45	21	1.433727	3.002274
45	22	1.341592	3.494115
45	23	1.483504	3.2906
45	24	1.507416	3.342236
45	25	1.197813	1.938123
45	26	1.094171	3.479227
47	1	1.049157	3.862096
47	2	1.240516	3.81309
47	3	1.074308	3.489715
47	4	1.130248	3.28012
47	5	1.206179	2.943649
47	6	1.340024	2.484496
47	7	1.027868	3.73882
47	8	1.017234	2.517761
47	9	1.023775	2.781888
47	10	0.968204	3.310933
47	11	1.23201	3.231253
47	12	1.217765	3.489575
47	13	1.616636	2.618234
47	14	1.800091	2.571682
47	15	1.779348	3.007472
47	16	1.018995	4.37226
47	17	1.346148	3.903291
47	18	1.50986	3.464159
47	19	1.451021	3.464714
47	20	1.365659	1.685648
47	21	1.446226	2.976774
47	22	1.358332	3.45399
47	23	1.497291	3.257076

44	24	0.700828	10.63829
44	25	0.901142	2.929964
44	26	0.547396	8.282957
46	1	0.808857	11.10749
46	2	0.968833	11.21924
46	3	0.886874	8.683112
46	4	0.96862	7.726763
46	5	1.107591	6.369175
46	6	1.341498	4.730259
46	7	0.866136	11.04779
46	8	0.949791	6.098239
46	9	0.857604	6.350287
46	10	0.82853	9.036392
46	11	1.043664	6.974077
46	12	0.948605	9.367441
46	13	1.496348	5.239363
46	14	1.635105	6.012256
46	15	1.570207	5.739603
46	16	0.863041	10.56282
46	17	1.144167	10.23906
46	18	1.2683	7.398594
46	19	1.17046	9.24331
46	20	1.543754	2.778191
46	21	1.194906	7.042125
46	22	1.087484	9.770328
46	23	1.240603	7.961361
46	24	1.253535	8.249479
46	25	1.31236	3.486157
46	26	0.858445	9.499603
48	1	1.636807	1.785253
48	2	1.805572	1.67118
48	3	1.560829	1.860937
48	4	1.588432	1.81006
48	5	1.624495	1.706373
48	6	1.68475	1.563786
48	7	1.59499	1.713109
48	8	1.317383	1.720612
48	9	1.422445	1.794865
48	10	1.434257	1.816207
48	11	1.653174	1.86049
48	12	1.715642	1.707585
48	13	2.00034	1.508099
48	14	2.066006	1.394659
48	15	2.112257	1.731763
48	16	1.592042	2.084419
48	17	1.852465	1.791315
48	18	1.937614	1.840652
48	19	1.891135	1.649249
48	20	1.578409	1.244881
48	21	1.85265	1.568171
48	22	1.839451	1.580135
48	23	1.926158	1.631435

47	24	1.520314	3.307359
47	25	1.197693	1.941071
47	26	1.097173	3.474394
49	1	0.801642	5.204741
49	2	0.94343	5.557565
49	3	0.890624	4.242743
49	4	0.943798	3.966008
49	5	1.016238	3.538596
49	6	1.1651	2.913369
49	7	0.78253	5.14945
49	8	0.990701	2.526184
49	9	0.946378	2.879337
49	10	0.822413	3.851182
49	11	1.050249	3.837841
49	12	0.96568	4.669117
49	13	1.462266	3.272355
49	14	1.631773	3.379372
49	15	1.587796	3.702914
49	16	0.803729	5.773566
49	17	1.080385	5.466235
49	18	1.28487	4.414701
49	19	1.186998	4.8091
49	20	1.237134	1.838923
49	21	1.212406	3.888137
49	22	1.072505	4.97572
49	23	1.24913	4.38759
49	24	1.268312	4.491649
49	25	1.058335	2.137271
49	26	0.868122	4.529266
51	1	1.11341	5.768027
51	2	0.68291	9.546743
51	3	1.658589	4.23524
51	4	1.509317	4.370468
51	5	1.324013	4.39567
51	6	1.322729	3.824279
51	7	1.018741	6.477276
51	8	6.879371	1.454075
51	9	4.691898	1.539504
51	10	2.988935	2.858251
51	11	1.460395	4.593949
51	12	1.017641	7.049876
51	13	1.173918	4.839977
51	14	1.259692	5.714861
51	15	1.414671	5.404381
51	16	0.823944	8.062712
51	17	0.897706	9.637869
51	18	1.174881	6.815027
51	19	0.958139	8.745769
51	20	1.544186	2.473168
51	21	1.069485	6.747823
51	22	0.715894	9.829912
51	23	1.004608	7.709166

48	24	1.946995	1.63529
48	25	1.471036	1.37505
48	26	1.601206	1.724626
50	1	0.000105	1695.58
50	2	0.118572	72.99274
50	3	0.000277	166.1581
50	4	0.001263	63.15992
50	5	0.007015	21.47415
50	6	0.03932	7.363313
50	7	0.000714	321.4558
50	8	0.001657	21.88344
50	9	4.02E-05	82.85897
50	10	2.69E-06	939.9437
50	11	0.009275	25.92273
50	12	0.001203	162.2584
50	13	0.485924	19.28659
50	14	0.437905	29.12771
50	15	0.312534	12.87375
50	16	0.00356	121.2446
50	17	0.026364	67.80799
50	18	0.067737	22.0645
50	19	0.036833	64.29681
50	20	0.249222	2.763837
50	21	0.036644	33.94393
50	22	0.109138	66.81783
50	23	0.029074	43.97758
50	24	0.026554	52.36822
50	25	0.082101	3.986246
50	26	0.000602	296.8123
52	1	1.083208	5.566575
52	2	0.842971	7.595151
52	3	1.508412	4.254469
52	4	1.466762	4.202586
52	5	1.382837	4.030901
52	6	1.42649	3.444435
52	7	1.028907	5.926714
52	8	3.98237	1.884307
52	9	2.907365	2.004651
52	10	2.13577	3.287476
52	11	1.491149	4.296196
52	12	1.138802	5.972944
52	13	1.276851	4.132903
52	14	1.416639	4.594041
52	15	1.565863	4.652757
52	16	0.91339	7.006582
52	17	1.07168	7.589912
52	18	1.332007	5.733522
52	19	1.152908	6.802499
52	20	1.618172	2.296968
52	21	1.238334	5.44229
52	22	0.918932	7.365596
52	23	1.189291	6.100129

51	24	1.025425	7.972993
51	25	1.472287	2.852113
51	26	1.213838	5.687894
53	1	1.077935	5.60607
53	2	0.885341	7.264867
53	3	1.475589	4.341717
53	4	1.453315	4.242616
53	5	1.397839	4.002583
53	6	1.454798	3.388204
53	7	1.042693	5.882489
53	8	3.515414	2.078715
53	9	2.552612	2.191815
53	10	1.995026	3.493835
53	11	1.490508	4.303119
53	12	1.170215	5.820872
53	13	1.308704	3.986685
53	14	1.459417	4.373572
53	15	1.599302	4.516557
53	16	0.938246	6.85652
53	17	1.122285	7.220542
53	18	1.37031	5.546239
53	19	1.205962	6.458519
53	20	1.646459	2.276251
53	21	1.286515	5.20823
53	22	0.973651	6.937698
53	23	1.240243	5.80477
53	24	1.266867	5.960355
53	25	1.55365	2.638762
53	26	1.22442	5.2591
55	1	0.834658	10.99642
55	2	0.610985	17.21119
55	3	1.244828	7.12258
55	4	1.209222	6.977705
55	5	1.181822	6.459617
55	6	1.306533	5.066499
55	7	0.774806	12.0754
55	8	4.544679	2.508588
55	9	3.221404	2.67559
55	10	2.002502	5.315037
55	11	1.205166	6.727207
55	12	0.871541	11.70177
55	13	1.282854	6.130093
55	14	1.397587	7.778395
55	15	1.340546	6.873064
55	16	0.676229	12.47317
55	17	0.75585	15.19764
55	18	1.050102	9.27915
55	19	0.853967	13.82447
55	20	1.574452	2.966432
55	21	1.06817	9.548939
55	22	0.703567	16.30888
55	23	1.004829	11.09495

52	24	1.213729	6.2741
52	25	1.530167	2.653528
52	26	1.221009	5.266679
54	1	0.653219	7.54202
54	2	0.51363	11.5785
54	3	0.999237	5.17697
54	4	0.977152	5.096887
54	5	0.949279	4.79906
54	6	1.04921	3.920621
54	7	0.622916	8.234725
54	8	3.212236	1.940237
54	9	2.119345	2.097508
54	10	1.518248	3.840068
54	11	1.033734	5.067411
54	12	0.698687	8.004629
54	13	1.139862	5.099691
54	14	1.213316	6.062486
54	15	1.233712	5.359282
54	16	0.6008	9.126662
54	17	0.701122	10.58132
54	18	0.971219	6.960909
54	19	0.766552	9.357798
54	20	1.296991	2.340934
54	21	0.848875	6.729494
54	22	0.574312	10.52265
54	23	0.82095	8.065615
54	24	0.837442	8.409819
54	25	1.172722	2.787848
54	26	0.762767	6.783953
56	1	0.693952	8.5417
56	2	0.451521	14.38491
56	3	1.116342	5.740866
56	4	1.053057	5.759381
56	5	0.988385	5.519294
56	6	1.083522	4.484917
56	7	0.652847	9.715572
56	8	4.967155	1.816443
56	9	3.191073	1.949553
56	10	2.00124	3.898571
56	11	1.07317	5.788713
56	12	0.703686	9.838861
56	13	1.134653	5.635411
56	14	1.167083	6.99559
56	15	1.254525	6.316656
56	16	0.606571	10.80977
56	17	0.682712	13.12646
56	18	0.975336	8.338305
56	19	0.732675	11.80921
56	20	1.353396	2.671874
56	21	0.881524	8.439896
56	22	0.518087	14.08795
56	23	0.824249	9.862799

55	24	1.016319	11.6083
55	25	1.433669	3.624477
55	26	0.910863	10.02628
57	1	0.666735	8.819984
57	2	0.316326	19.24594
57	3	1.149155	5.740406
57	4	1.003383	6.074077
57	5	0.875874	6.128071
57	6	0.953741	4.99941
57	7	0.587316	10.80037
57	8	9.120158	1.331718
57	9	5.521266	1.432126
57	10	2.827371	3.240897
57	11	0.979804	6.275919
57	12	0.561169	12.09776
57	13	1.0393	6.533808
57	14	1.019138	8.669144
57	15	1.113666	7.296903
57	16	0.50577	12.7519
57	17	0.520189	17.38886
57	18	0.824612	9.980867
57	19	0.55313	15.80695
57	20	1.255441	2.854281
57	21	0.719288	10.60738
57	22	0.352356	20.15878
57	23	0.655929	12.70048
57	24	0.661919	13.34591
57	25	1.108211	3.420751
57	26	0.717507	8.927443
Sulfolane		0.415	6.61

56	24	0.835719	10.27825
56	25	1.206516	3.184706
56	26	0.791217	8.115534
58	1	0.375877	15.63309
58	2	0.485876	17.69107
58	3	0.485618	10.01746
58	4	0.545991	8.724804
58	5	0.651204	6.985245
58	6	0.857844	4.915581
58	7	0.417587	15.83923
58	8	0.696503	5.084008
58	9	0.517869	5.567076
58	10	0.473799	9.824704
58	11	0.632286	7.608987
58	12	0.507645	12.46856
58	13	1.250817	6.089281
58	14	1.340024	7.39046
58	15	1.188245	6.488621
58	16	0.471907	13.79588
58	17	0.680177	14.30773
58	18	0.858625	8.807996
58	19	0.725857	12.66586
58	20	1.08284	2.541235
58	21	0.783869	8.570362
58	22	0.617422	14.55522
58	23	0.807774	10.31346
58	24	0.822248	10.82296
58	25	0.858007	3.214751
58	26	0.439775	12.30087
Sulfolane		0.415	6.61

APPENDIX D: Experimental Data

Experimental Results for [dms][ms](1)+[moi][tfb](2)+Tolene(3)+Heptane(4)

Sample	FEED (gm)			
	1	2	3	4
P2	0	1	0.10	0.90
A1	0.16	0.844	0.10	0.90
A2	0.33	0.67	0.10	0.90
A3	0.4	0.6	0.10	0.90
A4	0.53	0.47	0.10	0.90
A5	0.75	0.25	0.10	0.90
P1	1	0	0.10	0.90

Sample	ORG-PHASE (MOLE %)				IL-PHASE (MOLE %)				C	S
	1	2	3	4	1	2	3	4		
P2	0	0	9.32	90.68	0.00	81.00	7.55	11.45	0.81	6.42
A1	0	0	7.00	93.00	15.58	72.50	4.68	7.25	0.67	8.57
A2	0	0	8.55	91.45	25.52	61.28	5.02	8.18	0.59	6.57
A3	0	0	9.04	90.96	35.25	55.09	5.02	4.64	0.56	10.90
A4	0	0	10.00	90.00	29.26	61.50	4.41	4.82	0.44	8.23
A5	0	0	9.33	90.67	57.12	35.48	4.73	2.67	0.51	17.24
P1	0	0	8.69	91.31	95.40	0.00	3.42	1.18	0.39	30.44

Experimental Results for [moi][tfb](1)+ [bmpy][tfb](2)+Tolene(3)+Heptane(4)

FEED (gm)				
Sample	1	2	3	4
P3	0.00	1.00	0.10	0.90
C1	0.10	0.88	0.10	0.90
C2	0.23	0.75	0.10	0.90
C3	0.33	0.66	0.10	0.90
C4	0.44	0.56	0.10	0.90
C5	0.64	0.36	0.10	0.90
C6	0.82	0.18	0.10	0.90
P2	1.00	0.00	0.10	0.90

Sample	ORG-PHASE (MOLE %)				IL-PHASE (MOLE %)					C	S
	1	2	3	4	1	2	3	4			
P3	0.00	0.00	9.31	90.69	0.00	93.38	3.88	2.74	0.42	13.80	
C1	0.00	0.00	7.35	92.65	7.13	88.16	2.88	1.83	0.39	19.79	
C2	0.00	0.00	8.97	91.03	19.07	74.74	4.35	1.83	0.49	24.15	
C3	0.00	0.00	10.08	89.92	27.12	64.62	5.16	3.10	0.51	14.85	
C4	0.00	0.00	9.56	90.44	35.71	53.13	5.31	5.84	0.56	8.60	
C5	0.00	0.00	7.61	92.39	51.23	35.56	5.32	7.89	0.70	8.18	
C6	0.00	0.00	9.07	90.93	68.93	15.66	7.52	7.89	0.83	9.55	
P2	0.00	0.00	9.32	90.68	81.00	0.00	7.55	11.45	0.81	6.42	

APPENDIX E: Sample NMR Spectra

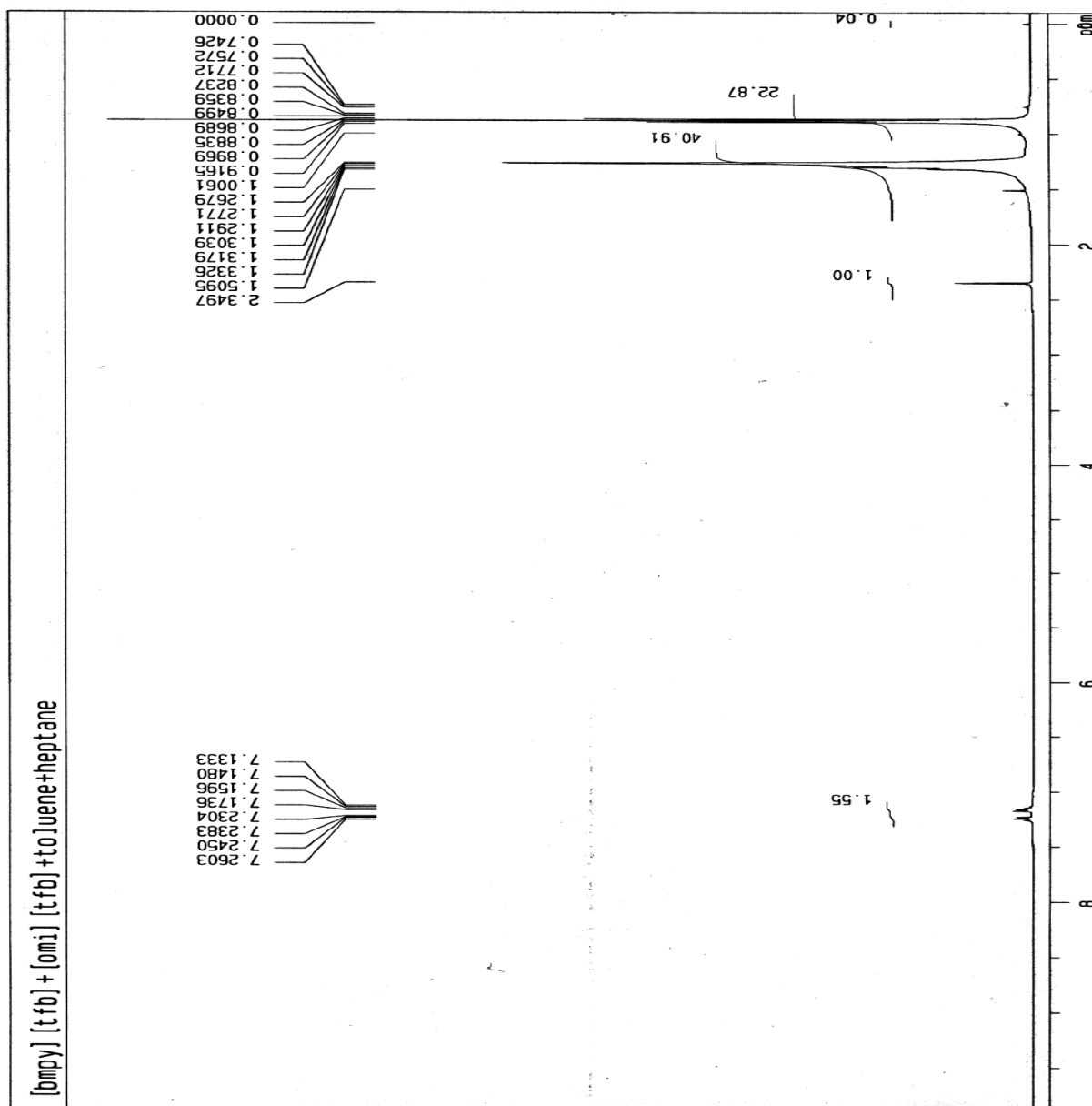


Figure E.1: NMR spectra of the organic phase of the mixture 1-butyl- 4-methyl pyridinium tetrafluoroborate+1-methyl-3-octylimidazolium tetrafluoroborate + toluene + heptane at 1 atm and 40°C. 1-methyl-3-octylimidazolium is 10 mol% of the solvent.

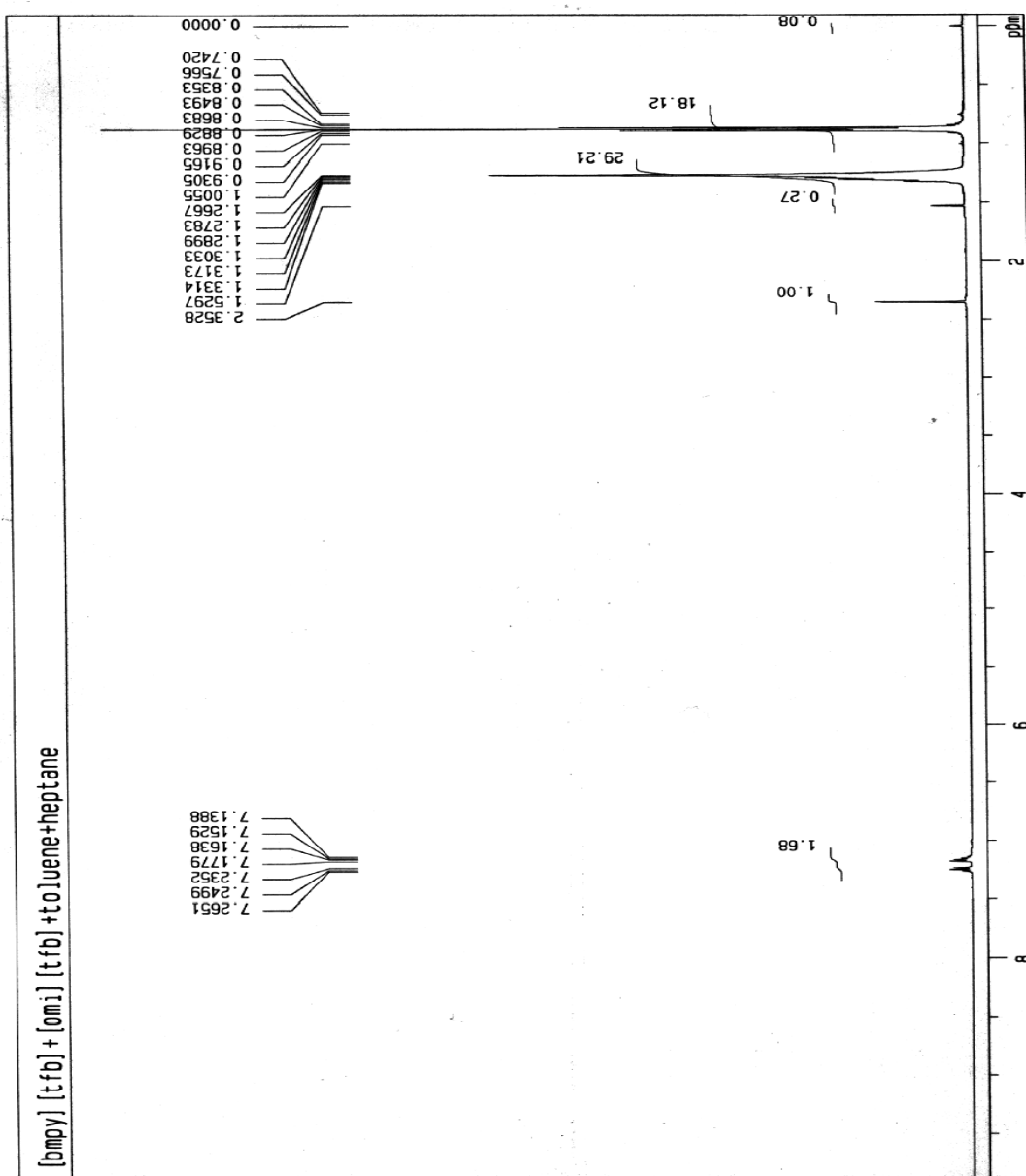


Figure E.3: NMR spectra of the organic phase of the mixture 1-butyl-4-methyl pyridinium tetrafluoroborate+1-methyl-3-octylimidazolium tetrafluoroborate + toluene + heptane at 1 atm and 40°C. 1-methyl-3-octylimidazolium is 30 mol% of the solvent.

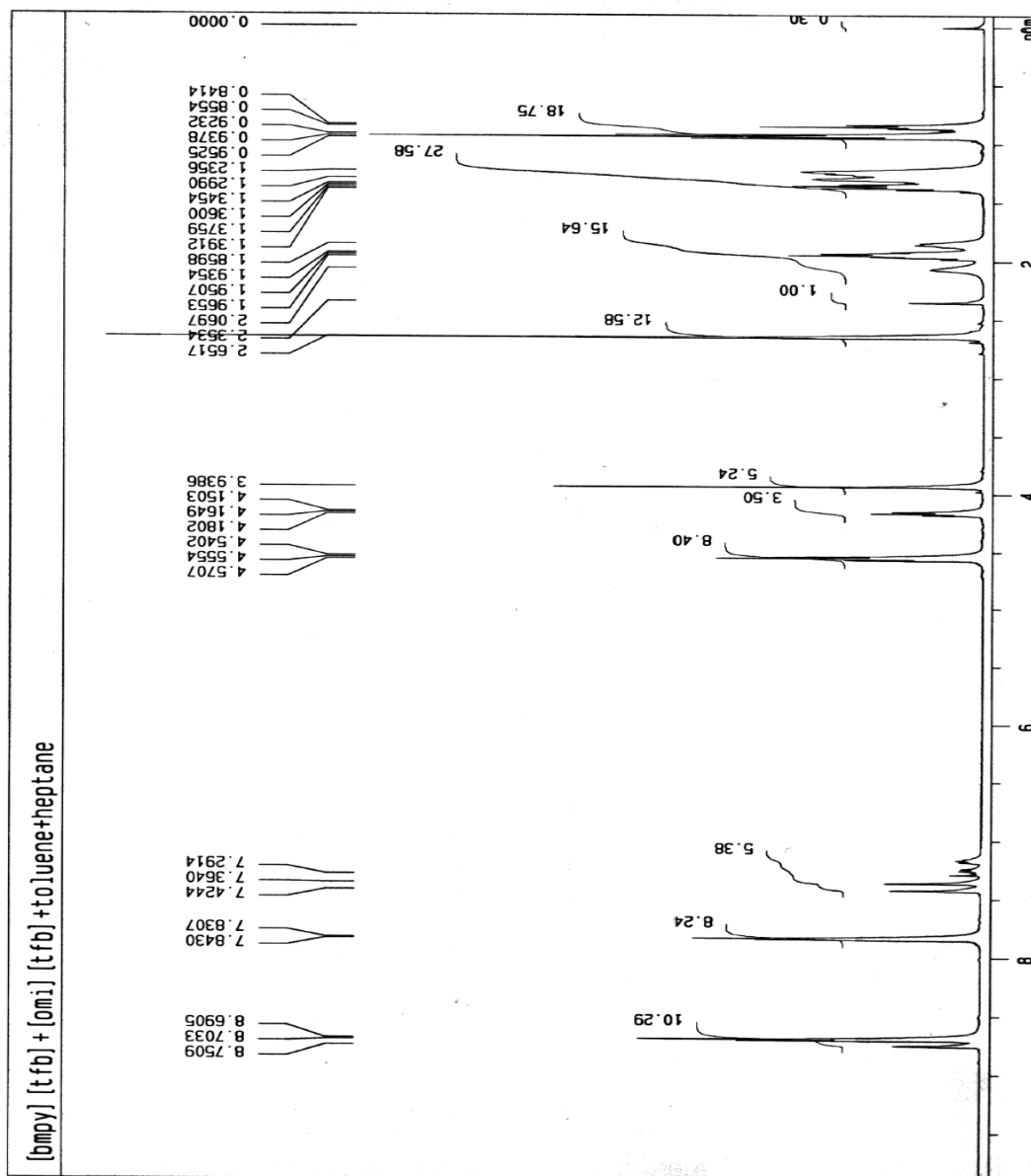


Figure E.4: NMR spectra of the IL phase of the mixture 1-butyl-4-methyl pyridinium tetrafluoroborate+1-methyl-3-octylimidazolium tetrafluoroborate + toluene + heptane at 1 atm and 40°C. 1-methyl-3-octylimidazolium is 30 mol% of the solvent.

NOMENCLATURE

am	Ammonium
att	Attractive
b*	Dimensionless temperature
bmpy	N-butyl-4-methylpyrrolidinium
dmi	dimethyl imidazolium
ϵ_m	Permittivity of the medium
ex	excess
η	Packing fraction
i/im	imidazolium
omi	Octyl methyl imidazolium
G	Gibbs free energy
g	Gram
h	Dimensionless variable
hs	Hard sphere
hb	Hard body
IL	Ionic liquid
ILs/ILS	Ionic liquids
k	Boltzman's constant
ml	Mililitre
ms	Methyl sulfate

P	Pressure
h	Phosphonium
p^*	Dimensionless pressure
p°	Defined variable
r	Radius of curvature
ρ	Number density of molecule
S_i	Geometric factor
T	Temperature
tfb	Tetrafluoroborate
t_{ij}	Depth of square well
v	Molecular volume
x	Mole fraction
z	Compressibility factor

REFERENCES

- Abraham M.H., Zissimos A.M., Huddleston J.G., Willauer H.D., Rogers R.D., Acree W.E., "Some novel liquid partitioning systems: water-ionic liquids and aqueous biphasic systems" , *Ind. Eng. Chem. Res.*, 42 413-418 (2003).
- Ahlich, R.; Bar, M.; Haser, M.; Horn, H.; Kolmel, C., "Electronic Structure Calculations on Workstation Computers: The Program System TURBOMOLE." *Chem. Phys. Lett.* , 162, 165 -169 (1989).
- Ali S.H., Lababidi H.M.S., Merchant S.Q., Fahim M.A., "Extraction of aromatics from naphtha reformat using propylene carbonate", *Fluid Phase Equilib.*, 214 25–38 (2003).
- Andersen H.C. and Chandler D., and Weeks J.D., "Roles of repulsive and attractive forces in liquids: the optimized random phase approximation", *J. Chem. Phys.* 56, 3812 (1972).
- Andersen H.C. and Chandler D., "Mode expansion in equilibrium statistical mechanics. III. Optimized convergence and application to ionic solution theory", *J. Chem. Phys.* 55, 1497 (1971).
- Anthony J.L., Maginn, E.J., Brennecke, J.F. "Solution thermodynamics of imidazolium-based ionic liquids and water," *J. Phys. Chem. B* 105 10942-10949 (2001).
- Arce A., Rodriguez O., Soto A., "Experimental determination of liquid– liquid equilibrium using ionic liquids: tert-amyl ethyl ether+ethanol+1- octyl-3-methylimidazolium chloride system at 298.15 K," *J. Chem. Eng. Data*, 49 (3) 514– 517 (2004).
- Arlt W., Seiler M., Jork C., Schneider T., "Ionic liquids as selective additives for the separation of close-boiling or azeotropic mixtures" *PCT Int. Appl.* WO 2002/074718 A2, 26-09-2002 (2002).
- AU Kosmulski M, Gustafsson J, Rosenholm JB. "Thermal stability of low temperature ionic liquids revisited", *Thermochimica Acta* 412 47–53 (2004).
- Blanchard L.A., Brennecke J.F., "Recovery of organic products from ionic liquids using supercritical carbon dioxide" ,*Ind. Eng. Chem.Res.* ,40 (1) 287– 292 (2001).

- Bosmann A., Datsevich L., Jess A., Lauter A., Schmitz C., Wasserscheid P., "Deep desulfurization of diesel fuel by extraction with ionic liquids", *Chem. Commun.*, 66(23) 2494–2495 (2001).
- Boublik T., "Equation of state of linear fused hard-sphere models", *Mol. Phys.*, 68, 191 (1989).
- Branco L.C., Joao G. C., Carlos A.M.A., "Highly selective transport of organic compounds by using supported liquid membranes based on ionic liquids," *Angew. Chem., Int.*, Ed. 41 (15) 2771–2773 (2002).
- Brennecke J.F., Maginn E.J., "Ionic liquids: innovative fluids for chemical processing". *AIChE J.* 47 (11) 2384–2389 (2001).
- Breure B., Bottini S.B., Brignole E. A., and Peters C. J., "Thermodynamic Modeling of the Phase Behavior of Binary Systems of Ionic Liquids and Carbon Dioxide with the Gc-Eos", AIChE Annual Meeting, 2005.
- Cadena C. and Maginn E. J., "Molecular Dynamics Study of Pyridinium- and Triazolium-Based Ionic Liquids" AIChE 2005 annual meeting conference, USA.
- Cammarata L, Kazarian SG, Salter PA, Welton T. "Molecular states of water in room temperature ionic liquids" *Phys. Chem. Chem. Phys.* 23 5192–5200 (2001).
- Carnahan N.F. and Starling K.E, "Equation of state for nonattracting rigid spheres", *J. Chem. Phys.* 51, 635 (1969).
- Chang J. and Sandler S. I., "The correlation functions of hard-sphere chain fluids: Comparison of the Wertheim integral equation theory with the Monte Carlo simulation", *J. Chem. Phys.*, 103, 3196 (1995).
- Chen, C. C.; Britt, H. I.; Boston, J. F.; Evans, L. B. Local Composition Model for Excess Gibbs Energy of Electrolyte Systems. " *AIChE J.* 28 588 (1982).
- David W., Letcher T.M., Ramjugernath D., Raal J.D., "Activity coefficients of hydrocarbon solutes at infinite dilution in the ionic liquid, 1-methyl-3-octyl-imidazolium chloride from gas–liquid chromatography", *J. Chem. Thermodyn.*, 35 (8) 1335–1341 (2003).
- Davis J.H., and Fox P.A., "From curiosities to commodities: ionic liquids begin the transition", *Chemical Communications*, 11 1209–1212 (2003).
- Dickman R. and Hall C. K., "Equation of state for chain molecules: Continuous-space analog of Flory theory", *J. Chem. Phys.*, 85, 4108 (1986).

- Diedenhofen M., Eckert F., and Klamt A., "Prediction of Infinite Dilution Activity Coefficients of Organic Compounds in Ionic Liquids Using COSMO-RS" *J. Chem. Eng. Data*, 48, 475-479 (2003).
- Dietz, M.L., Dzielawa, "Ion-exchange as a mode of cation transfer into room-temperature ionic liquids containing crown ethers: implications for the "greenness" of ionic liquids as diluents in liquid-liquid extraction", *J.A. Chem. Comm.*, 20 2124-2125 (2001).
- Domanska U., Marciniak A., "Solubility of 1-alkyl-3-methylimidazolium hexafluorophosphate in hydrocarbons", *J. Chem. Eng. Data*, 48 (3) 451-456 (2003).
- Dupont J., Consorti C.S., Spencer J., "Room temperature molten salts: neoteric green solvents for chemical reactions and processes", *J. Braz. Chem. Soc.*, 11 (4) 337-344 (2000).
- Earle M.J., Seddon K.R. : "Ionic liquids. Green solvents for the future", *Pure Appl. Chem.* 72 1391-1398 (2000).
- Eber J., Wasserscheid P., A. Jess, "Deep desulfurization of oil refinery systems by extraction with ionic liquids", *Green Chem.*, 6 (7) 316-322 (2004).
- Fadeev A.G., Micheal M. Meagher, "Opportunities for ionic liquids in recovery of biofuels," *Chem. Commun.* (3) 295-296 (2001).
- Fletcher K. A., Baker S. N., Baker G. A., Pandey S., "Probing solute and solvent interactions within binary ionic liquid mixtures", *New J. Chem.*, 12 1706-1712 (2003).
- Fry S.E., Pienta N.J.: "Effects of molten-salts on reactions nucleophilic aromatic-substitution by halide-ions in molten dodecyltributylphosphonium salts" *J. Am. Chem. Soc.* 107 6399-6400 (1986).
- Ghonasgi D. and Chapman W. G., "Prediction of the properties of model polymer solutions and blends", *AIChE J.*, 40, 878 (1994).
- Gutowski K. E., Broker G. A., Willauer H. D., Huddleston J. G., Swatloski R. P., Holbrey J. D., and Rogers R. D. "Controlling the Aqueous Miscibility of Ionic Liquids: Aqueous Biphasic Systems of Water-Miscible Ionic Liquids and Water-Structuring Salts for Recycle, Metathesis, and Separations", *J. Am. Chem. Soc.*, 125 (22) 6632-6633 (2003)
- Hamad E. Z., "Volume-explicit equation of state for hard spheres, hard disks, and mixtures of hard spheres", *Ind. Eng. Chem. Res.*, 36, 4385 (1997).
- Heintz A., Kulikov D.V., Verevkin S.P., "Thermodynamic properties of mixtures containing ionic liquids: 1. Activity coefficients at infinite dilution of alkanes, alkenes, and

- alkylbenzenes in 4-methyl-n-butylpyridinium tetrafluoroborate using gas– liquid chromatography”, *J. Chem.*
- Heinz A. , Kulikov D.V. , Verevkin S.P., “ Thermodynamic properties of mixtures containing ionic liquids: 2. Activity coefficients at infinite dilution of hydrocarbons and polar solutes in 1-methyl-3-ethyl-imidazolium bis(trifluoromethyl-sulfonyl) amide and in 1,2-dimethyl-3-ethylimidazolium bis(trifluoromethyl-sulfonyl) amide using gas– liquid chromatography ” *J. Chem. Eng. Data*, 47, 894– 899 (2002). *Eng. Data* ,46, 1526– 1529 (2001).
- Heintz A., Lehmann J. K. , Wertz C., “Thermodynamic properties of mixtures containing ionic liquids: 3. Liquid– liquid equilibria of binary mixtures of 1-ethyl-3-methylimidazolium bis(trifluoromethylsulfonyl)imide with propan-1-ol, butan-1-ol, and pentan-1-ol, ” *J. Chem. Eng. Data* 48 (3) 472– 474 (2003).
- Holbrey J.D. , Reichert W.M., Nieuwenhuyzen M., Sheppard O., Hardacre C., Rogers R.D., “ Liquid clathrate formation in ionic liquid– aromatic mixtures”, *Chem. Commun.* ,4 476–477 (2003).
- Huddleston J.G., Willauer H.D., Swatoski R.P., Visser A.E., Rogers R.D., “Room temperature ionic liquids as novel media for Fclean_ liquid–liquid extraction” *Chem. Commun.* ,16 1765– 1766 (1998).
- Huang J-F., Chen P-Y., Sun I-W., Wang S.P., “NMR Evidence of Hydrogen Bond in 1-Ethyl-3-Methylimidazolium-Tetrafluoroborate Room Temperature Ionic Liquid”, *Spectrosc. Lett.* , 34 591–603 (2001).
- Huddleston J.G., Visser A.E, Reichert W.M., Willauer H. D., Broker G. A., Rogers R. D. “Characterization and comparison of hydrophilic and hydrophobic room temperature ionic liquids incorporating the imidazolium cation”, *Green Chem.* 3 (2001) 156–164.
- Hurley F.N., Wier T. P. “Electrodeposition of Aluminum from Nonaqueous Solutions at Room Temperature” *J. Electrochem. Soc.* 98 207–212 (1951) .
- Jastorff B., Stormann R., Ranke J., Molter K., Stock,F., Oberheitmann B., Hoffmann J, Nuchter,M., Ondruschka B., and FILser J., “How hazardous are ionic liquids? Structure-activity relationships and biological testing as important elements for sustainability evaluation,” *Green Chemistry* 5 136-142 (2003).
- Jensen, M.P., Dzielawa, J.A., Rickert, P., Dietz, M.L., “EXAFS investigations of the mechanism of facilitated ion transfer into a room-temperature ionic liquid”, *J. Am. Chem. Soc.* 124(36), 10664 -10665 (2002).
- Kato R., Gmehling J., “Activity coefficients at infinite dilution of various solutes in the ionic liquids [MMIM][CH₃SO₄], [MMIM][CH₃OC₂ H₄SO₄], [MMIM][(CH₃)₂PO₄],

- $[\text{C}_2\text{H}_5\text{NC}_2\text{H}_5][(\text{CF}_3\text{SO}_2)_2\text{N}]$ and $[\text{C}_2\text{H}_5\text{NH}][\text{C}_2\text{H}_5\text{OC}_2\text{H}_4\text{OSO}_3]$, ”*Fluid Phase Equilib.*, 226 37–44 (2004).
- Kirk-Othmer: Encyclopedia of Chemical Technology, Fourth Edition, John Wiley & Sons, Law G, Watson PR. “Surface tension measurements of n-alkylimidazolium ionic liquids” *Langmuir* 17 6138-6141 (2001).
- Klamt A., “Conductor-like screening model for real solvents: a new approach to the quantitative calculation of solvation phenomena” , *J. Physical. Chem.* 99, 2224 (1995).
- Klamt, A.; Eckert, F., “COSMO-RS: a novel and efficient method for the a priori prediction of thermophysical data of liquids.” *Fluid Phase Equilib.*, 172, 43-72 (2000).
- Klamt, A.; Jonas, V.; Bürgler, T.; Lohrenz, J. C. W. “Refinement and Parametrization of COSMO-RS.” *J. Phys. Chem. A*, 102, 5074-5085 (1998).
- Klamt, A.; Schuurmann, G., “COSMO: A New Approach to Dielectric Screening in Solvents with Explicit Expression for the Screening Energy and its Gradient.” *J. Chem. Soc., Perkin Trans. 2*, 799-805 (1993).
- Krummen M., Wasserscheid P., Gmehling J., “ Measurement of activity coefficients at infinite dilution in ionic liquids using the dilutor technique” *J. Chem. Eng. Data* 47 1411– 1417 (2002).
- Larsen B., “Studies in statistical mechanics of coulombic systems. I. equation of state for the restricted primitive model” *J. Chem. Phys.*, 65(9), 3431 (1976).
- Letcher T.M., Deenadayalu N., Soko B. , Ramjugernath D., Naicker P.K., “Ternary liquid–liquid equilibria for mixtures of 1-methyl-3-octylimidazolium chloride+an alkanol+an alkane at 298.2 K and 1 bar,”*J. Chem. Eng. Data* 48 (4) 904–907 (2003).
- Letcher T.M., Reddy P., “Ternary liquid–liquid equilibria for mixtures of 1- hexyl-3-methylimidazolium (tetrafluoroborate or hexafluorophosphate)+ ethanol+an alkene at T=298.2 K” ,*Fluid Phase Equilib.* 219 (2) 107–112 (2004).
- Lieb E. H. and Mattis D. C. , “Mathematical Physics in One Dimension” Academic Press, New York, 1966.
- Liu J-F., Chi Y-G., Jiang G-B., “Screening the extractability of some typical environmental pollutants by ionic liquids in liquid-phase microextraction” *J. Sep. Sci.* 28 (1) 87–91 (2005).
- Matsumoto M., Inomoto Y., Kondo K., “Selective separation of aromatic hydrocarbons through supported liquid membranes based on ionic liquids ”, *J. Membr. Sci.*, 246 (1) 77– 81 (2005).

- McKetta, J.H., "Encyclopedia of Chemical Processes and Design", pp 78, Edited by
Published by Marcel Dekker, Inc (1984).
- Meindersma G. W., Anita (J.G.) Podt, Andre B. de Haan, "Fuel Processing Technology",
(2005) (In Press). P. Walden, "Molecular weights and electrical conductivity of
several fused salts". *Bull. Acad. Imper. Sci.* (St. Petersburg) 405–422 (1914).
- Mulero A., Galan C. and Cuadros F., "Simple modifications of the van der Waals and
Dieterici equations of state: vapour–liquid equilibrium properties", *Phys. Chem.
Chem. Phys.*, 3, 4991 (2001).
- Ngo HL, LeCompte K, Hargens L, McEwen AB., "Thermal properties of imidazolium ionic
liquids", *Thermochim. Acta*, 357 97–102 (2000).
- Okoturo O O, VanderNoot T J. "Temperature dependence of viscosity for room temperature
ionic liquids", *J. Electroanal. Chem.*, 568 167-181 (2004). Xu W, Wang L-M,
Nieman RA, Angell CA "Ionic Liquids of Chelated rthoborates as Model Ionic
Glassformers", *J. Phys. Chem. B* 107 11749–11756 (2003).
- Perdew, J. P., "Density-functional approximation for the correlation energy of the
inhomogeneous electron gas", *Phys. Rev. B*, 33, 8822-8824 (1986).
- Pringle J. M., Golding J., Baranyai K., Forsyth C.M., Deacon G.B., Scott JL, MacFarlane D.
R.: "The effect of anion fluorination in ionic liquids—physical properties of a range
of bis(methanesulfonyl)amide salts", *New J. Chem.* 27 (2003) 1504–1510.
- Raseev S. D., "Thermal and Catalytic Processes in Petroleum Refining", Chapter 13, p-836.
- Ruthven, D.M., "Zeolites as Seelctive Adsolrbents" *Chem. Eng. Prog.*, 84(2) 42-50 (1988) .
- Santiso E. and Mueller E. A., "Dense packing of binary and polydisperse hard spheres",
Mol. Phys., 100, 2461 (2002).
- Schafer, A.; Huber, C.; Ahlrichs, R. "Fully optimized contracted Gaussian basis sets of triple
valence quality for atoms Li to Kr", *J. Chem. Phys.*, 100, 5829-5835 (1994).
- Scurto, A.M., Aki, S.N.V.K., Brennecke J.F., "Carbon dioxide induced separation of ionic
liquids and water", *Chem. Comm.*, 572 (2003).
- Seddon K.R., Stark A., Torres M. "Influence of chloride, water, and organic olvents on the
physical properties of ionic liquids", *J. Pure Appl. Chem.* 72 2275–2287 (2000).
- Selvan M.S., McKinley M.D., Dubois R.H., Atwood J.L., "Liquid– liquid equilibria for
toluene+heptane+1-ethyl-3-methylimidazolium triiodide and toluene+heptane+1-
butyl-3-methylimidazolium triiodide", *J. Chem. Eng. Data*, 45 841– 845 (2000).

- Shah J. K., Brennecke J. F. and Maginn E. J., “ Thermodynamic properties of the ionic liquid 1-*n*-butyl-3-methylimidazolium hexafluorophosphate from Monte Carlo simulations” ,*Green Chemistry*, 4 112–118 (2002).
- Shyu L.-J., Zhang Z., Zhang Q., Nobel A., “Process for the extraction of an aromatic compound from an aliphatic phase using a non-neutral ionic liquid”, PCT Int. Appl. WO 2001/40150 A1, 07-06- 2001, (2001).
- Stewart A. Forsyth, Jennifer M. Pringle, and Douglas R. MacFarlane, “Ionic liquids-an overview”, *Aust. J. Chem*, 57, 113-119 (2004).
- Swatloski, R.P., Holbrey, J.D.,Rogers, R.D., “Ionic Liquids Are Not Always Green: Hydrolysis of 1-Butyl-3-Methylimidazolium Hexafluorophosphate”, *Green Chem.* , 5 361-363 (2003).
- Van de Broeke J, Stam M, Lutz M, Kooijman H, Spek AL, Deelman B-J, van Koten G.: “Designing Ionic Liquids: 1-Butyl-3-Methylimidazolium Cations with Substituted Tetraphenylborate Counterions”, *Eur. J. Inorg. Chem.*, 26 2798–2811 (2003).
- Visser A.E., “Metal ion separations in aqueous biphasic systems and room temperature ionic liquids”, *PhD thesis*, University of Alabama, Tuscaloosa, AL, USA, (2002).
- Visser A.E., Swatloski R.P., Griffin S.T., Hartman D.H., Rogers R.D., “Liquid/liquid extraction of metal ions in room temperature ionic liquids” , *Sep. Sci. Technol.* 36 (5&6) 785–804 (2001).
- Wei G-T., Yang Z., Chen C-J. , “Room temperature ionic liquid as a novel medium for liquid/liquid extraction of metal ions, *Anal. Chim. Acta* 488 (2) 183– 192 (2003).
- Weissermel K., Arpe H. J., *Industrial Organic Chemistry*, 4th Completely Revised Edition, Wiley-VCH, Weinheim D., pp 313-336, (2003).
- Wertheim M. S., “Fluids with highly directional attractive forces. IV. Equilibrium polymerization”, *J. Stat. Phys.*, 42, 477 (1986).
- Wertheim M. S., “Simulation Study of the Link between Molecular Association and Reentrant Miscibility for a Mixture of Molecules with Directional Interactions”, *J. Stat.Phys.*, 35, 19 (1984).
- Wu C-T., Marsh K. N., Deev A. V., Boxal J. A., “Liquid– liquid equilibria of room-temperature ionic liquids and butan-1-ol, ”*J. Chem. Eng. Data*, 48 (3) 486– 491 (2003).

- Yoshikawa, M.; Motoi, T; Tsubouchi, K., "Speicalty polymeric membranes, part 6, Pervaporation of benzene/cyclohexane mixtures through poly (vinyl chloride)-graft-poly (acrylic acid) membranes", *Angew. Makromol. Chem.*, 245, 193-202 (1997).
- Zhang S.G., Conrad Z., "Novel properties of ionic liquids in selective sulfur removal from fuels at room temperature," *Green Chem.* 4 (4) 376–379 (2002).
- Zhang S.G, Qinglin Z., Conrad Z., "Extractive desulfurization and denitrogenation of fuels using ionic liquids", *Ind. Eng. Chem. Res.* 43 (2) 614– 622 (2004).

VITAE

NAME: KAZI ZAMSHAD SUMON

PLACE OF BIRTH: Comilla, Bangladesh.

ADDRESS: 618/A, Middle Monipur,
Mirpur-2, Dhaka,
Bangladesh.

PHONE NO.: +880-28057476.

E-MAIL: kazizamshad@yahoo.com

EDUCATIONAL QUALIFICATION:

M.S. (Chemical Engineering)

December 2005

King Fahd University of Petroleum and Minerals

Dhahran, Saudi Arabia.

B.Sc. (Chemical Engineering)

August 2001

Bangladesh University of Engineering and Technology

Dhaka, Bangladesh.

PROFESSIONAL EXPERIENCE:

Research Assistant

June 2003-January 2006

Department of Chemical Engineering

KFUPM, Saudi Arabia.